



R_RRFM

Hamburg

02.3.-05.3.2008

R_RRFM
2008

Transactions



IAEA

International Atomic Energy Agency



2.3. -5.3. 2008

Hamburg, Germany

© 2008
European Nuclear Society
Rue de la Loi 57
1040 Brussels, Belgium
Phone + 32 2 505 30 54
Fax +32 2 502 39 02
E-mail info@euronuclear.org
Internet www.euronuclear.org

ISBN 978-92-95064-04-1

These transactions contain all contributions submitted by 29 February 2008.

The content of contributions published in this book reflects solely the opinions of the authors concerned. The European Nuclear Society is not responsible for details published and the accuracy of data presented.



Poster Gallery

DEVELOPMENT OF LEU SILICIDE FUEL ELEMENT FOR THE IPEN RESEARCH REACTOR

M. DURAZZO, E.F URANO DE CARVALHO, A.M. SALIBA-SILVA, J.A.B. SOUZA
*Centro do Combustível Nuclear, Instituto de Pesquisas Energéticas e Nucleares, IPEN-CNEN/SP
Av. Prof. Lineu Prestes 2242, 05508-000 São Paulo – Brazil*

H.G. RIELLA
*Departamento de Engenharia Química, Universidade Federal de Santa Catarina
P.O.Box 476, 88040-900 Florianópolis – Brazil*

ABSTRACT

IPEN has been increasing continuously its production of radiopharmaceutical medicines to come along with the expanding demand imposed by the Brazilian welfare. To reach its objectives, IPEN has been working in upgrading the IEAR1 research reactor to increase its power from 2 to 5 MW and its operational time from 64 to 120 hours by week. Since 1988 IPEN has been manufacturing its own fuel element. A program for autonomous serial fuel assembly production started in the 80's, motivated by the political constraint for buying these fuels abroad. The fuel was initially based on U_3O_8 -Al dispersion fuel plates with 2.3 gU/cm^3 . Based on previous experience with U_3O_8 fuel, a new higher uranium density fuel was developed to attend a more intense reactivity needs for continuous operation and to have a more compact core for better irradiation flux. This paper describes the developing path of silicide fuel at IPEN.

1. Introduction

The use of radioisotopes in medicine is certainly one of the most important social uses of nuclear energy and IPEN/CNEN-SP has a special place on the history of nuclear medicine in Brazil. Due to the federal monopoly, only the Institutes that belong to CNEN (Comissão Nacional de Energia Nuclear) can produce radioisotopes and radiopharmaceuticals for use in nuclear medicine. The production of IPEN represents nearly 98% of the total produced.

There has been a significant increase in the demand of radioisotopes over the years. Between 2002 and 2004 the increase in the demand was about 30%. Distributed to Brazilian hospitals and clinics, radiopharmaceutical products were used, in 2006, to attend more than 3 million patients, an increase of about 10% relative to the year before. To face this scenario, IPEN has been increasing continuously its production of radiopharmaceutical medicines to come along with the expanding demand imposed by the Brazilian welfare. One of the most important project aims at own production of Mo-99 in order to provide cheaper Tc-99 generators than the ones produced from imported raw materials. So, this medicine will be accessible to a bigger amount of patients. To reach the objective of this project, IPEN for years has been working on upgrading the IEA-R1 research reactor to increase its power (from 2 to 5 MW) and its operational time (from 64 to 120 hours by week). The reactor control board and ventilation system were upgraded and additional safety items were incorporated. Besides, CNEN is planning to build a new facility in order to expand and spread the use of radiopharmaceutical medicines all over the country.

Once the reactor power was planned to be raised from 2 to 5 MW, in 1997 IPEN started research activities aiming at the elevation of the uranium loading inside the fuel, in order to allow the reactor power increase. This was accomplished with the development of the silicide technology, which has been done under support of the IAEA. The Technical Cooperation Project BRA/4/047 "Fuel Improvement for the IPEN Research Reactor" was the objective to develop high-density fuel to improve the efficiency and applicability of the IPEN reactor. Until

this time, fourteen silicide fuel elements ($3.0\text{gU}/\text{cm}^3$) had been irradiated at the IEA-R1 research reactor. The irradiation was closely followed by visual inspections and sipping tests. After 40% burn up (average), no problems regarding to fuel performance was recorded. The enriched U_3Si_2 powder was imported from the international market until 2002, when IPEN started the development of the conversion technology to get de U_3Si_2 powder using national enriched UF_6 produced by CTMSP (Marine Technological Center in São Paulo). Nowadays, IPEN is able to fabricate the enriched U_3Si_2 powder, allowing the nationalization of all the fabrication cycle of dispersion fuel for research reactors. After mining and enrichment steps, IPEN is able to execute all the other fabrication steps. Recently, on 2007 June 26, the first fuel element fabricated with national materials and technology was put in operation at IEA-R1 reactor core. This work describes the journey of IPEN heading on to acquire uranium silicide technology.

2. Historical Background

The beginning of the development of the fuel element fabrication technology in IPEN is very old. The work started in 1960 aiming at fabrication of the fuel for the ARGONAUTA research reactor. Between 1964 and 1965 the fuel elements were manufactured with 20% enriched U_3O_8 powder provided by IAEA in the program Atoms for Peace. In spite of the low technological demand of the ARGONAUTA fuel (very low power), a seed was planted and would come to germinate 20 years later, in the decade of 80, and to bloom definitively in the decade of 90, when IPEN dominated the fabrication technology and began the production of the fuel for the IEA-R1 research reactor. The relative high power (2 MW) demanded a significant technological progress in the fabrication techniques.

Starting from 1980, IPEN intensified their efforts to develop the fabrication technology of dispersion fuel element, aiming at improving the technology for manufacturing fuels more advanced, substantially superior to the old ARGONAUTA fuel type. In that time, IPEN could not acquire fuel elements from the international market in order to supply the IEA-R1 research reactor. The growing difficulty to get fuel elements in the international market acted as an initial impelling force for IPEN to deflagrate their program for fuel element fabrication. The technology previously developed in the 60's was updated starting from 1985, with base in the recent technological advances in the area. Between 1985 and 1988, IPEN worked in assembling a small fuel fabrication facility as a laboratory level, with capacity to produce 6 fuel elements by year. This was enough to supply the IEA-R1 reactor operating at 2 MW and 40 hours a week.

On 1988 August 31, as part of the commemorations of their 32^o anniversary, IPEN provided the IEA-R1 reactor with the first fuel element fabricated in Brazil, only fifteen days before the exhaustion of the reactor fuel. The fissile material used was the same U_3O_8 powder previously used for the production of the ARGONAUTA fuel. There was a reserve of about 30kg of this material. Starting from 1988, after the production of the first fuel element, IPEN began a continuous production of fuel element, which continues until nowadays.

After the production of 26 fuel element, the enriched U_3O_8 powder finished in 1996. So, in 1994 IPEN started developing the processes for UF_6 conversion to U_3O_8 and for recovering the uranium scraps generated in fuel plate fabrication. In 1996, IPEN did the conversion of about 20kg of imported enriched UF_6 . IPEN was then prepared for the routine production of fuel elements starting from UF_6 as raw material. In 1997, IPEN raised the fuel production capacity from 6 annual fuel elements to 10, which was the maximum considering the infrastructure available.

As mentioned before, in order to increase the radioisotope production of IPEN, the IEA-R1 reactor power capacity was increased from 2 MW to 5 MW. In 1997, the development of a new higher uranium density fuel started, in order to attend the reactivity needs for continuous operation, to have a compact core for better irradiation flux and also to have a low number of irradiated fuel elements to be stored at the spent fuel pool. The new fuel was based on the

U₃Si₂-Al dispersion with uranium loading of 3.0 gU/cm³. In 1998, the fuel plate fabrication technology of the new silicide fuel was implanted. At that time, U₃Si₂ powder was imported from France. Between 1999 and 2000 sixteen silicide fuel elements were manufactured. Starting from 1998, the efforts to develop the U₃Si₂ powder production technology began, aiming at the nationalization of all the production process, starting from enriched UF₆ leading to the conversion to UF₄; its reduction to metallic uranium; U₃Si₂ powder fabrication and, finally, arriving at the fuel plate fabrication and fuel element assembly. At this time, IPEN participated in an international cooperation through IAEA under the Technical Cooperation Project TC BRA/4/047.

In 1999 IPEN get the technology for UF₄ production using SnCl₂ as reducing agent. In the area of metallic uranium, IPEN was a valuable previous experience in producing 150kg natural uranium ingots in 90's. Based on that experience, IPEN initiates efforts aiming at scaling down the size of the metallic uranium pieces, trying to produce pieces of about 3kg using 20% enriched material as raw material for the U₃Si₂ production. In 2002, the process for producing metallic uranium was dominated, which allowed the development of the U₃Si₂ intermetallic. In 2004, IPEN obtained the first lot of natural U₃Si₂ powder, manufactured with national technology, dominating then the "uranium silicide cycle". In 2006, IPEN consolidated the fabrication technology of the silicide fuel by manufacturing the first fuel element with fully national technology. This fuel element was put in the IEA-R1 reactor core last year, on June 26. Now, efforts have been made to produce and qualify high loaded fuel elements with 4.8 gU/cm³.

Due to the emergent increase in radiopharmaceuticals demand and the consequent increase in the IEA-R1 power, the reactor needed an increase of fuel, from 6 (U₃O₈-Al) to 18 elements (U₃Si₂-Al) a year. In addition, a new reactor for radioisotope production was cogitated to be constructed in the Northeast region of Brazil. This decision would be very significant in near future, since IEA-R1 reactor is quite aged (50 years) and this reactor is practically the only one producer of radioisotope in the country. The new reactor (probably 20 MW) would consume about 30 annual U₃Si₂-Al fuel elements. Therefore, a demand for about 50 annual fuel elements seems to be quite realistic.

Based on this forecast demand for fuel elements and the increasing need for fuel element production to supply IEA-R1 reactor in the near future, IPEN began a project in 2001 in order to adapt the production facilities seeking on improving the producing capacity. This project is nowadays under way aiming at replacing the current facilities by a fully new one, but with a researching laboratorial style. The new facility is planned to have nominal capacity for producing 30 fuel elements in yearly basis. That will attend wholly the fuel element demand in a short period. The producing capacity of the new facility should reach 80 annual fuel elements, which would supply also the new research reactor planned to be constructed. The conclusion of this project is foreseen for 2008-2009.

Looking at the future, in 2001, IPEN started working with the UMo fuel in contribution to RERTR program for developing high uranium loaded fuels. This fuel could eventually substitute with advantages the U₃Si₂ fuel. Nowadays this work is on course [1] and was also supported by the IAEA TC BRA/4/053 "Development of Alternative High-Density Fuel Based on Uranium-Molybdenum Alloys".

The production increased of fuel element will generate larger amount of waste (liquid, solids and gaseous) and pollutant, which has to be handled adequately. The higher fabrication scale of the new installation arise technical difficulties related to upgrading uranium recovery procedures and effluent treatment and waste disposal. As the facilities for fuel plates production are adequate to stand up the new production level, the main modifications and adjustments must be performed in the chemical processes for uranium recovery from scrap and for treatment on liquid waste and gaseous or aerosol-type pollutants, generated in fabrication plant. To face this new challenge, IPEN rely on the international skill in these subjects with support of the IAEA TC BRA/3/012 "Nuclear Fuel for Research Reactors: Improving Fabrication and Performance Evaluation in Brazil".

3. Silicide Fuel Development

The IEA-R1 Reactor of IPEN/CNEN-SP is a pool type reactor operating since 1957. This reactor uses MTR type dispersion fuel element in a 5 X 5 core arrangement. The Nuclear Fuel Center of IPEN is responsible for the production of the necessary nuclear fuel to keep the continuous operation of the reactor. Development of new fuel technologies is also a permanent concern. The Nuclear Fuel Center had produced 77 fuel elements until now, including 14 control fuel elements.

The fuel meat is fabricated according to conventional powder metallurgy techniques. The fuel element contains 18 fuel plates, each one 1.52 mm thick. Cladding and frame plates are made with the ASTM 6061 aluminum alloy. The fuel assembly is performed by a well-known picture-frame technique. The fuel element results from mechanical assembling of 18 fuel plates and other structural components.

As, in Brazil, we have not available hot cell laboratories to test irradiated fuels and as the irradiation tests abroad would be very expensive, IPEN decided to risk the testing and evaluating in pile for its own fuel, checking the performance under reactor operation. This was possible since IPEN fuel specification is conservative for dispersion fuel and the power of reactor is low. A program for fuel qualification was started with irradiation of some miniplates at the border of the reactor core just to identify any abnormal event. In July 1985 a partial fuel element with only two fuel plates (the external plates) and 16 aluminum plates was placed in the core to start fuel qualification. After this, other partial fuel element with 10 fuel plates and 8 aluminum plates was also placed in the core (November 1985). These two fuel element were identified as the precursor fuels. A periodic monitoring and evaluation was done upon them. After good results with these precursor fuels, it was decided to start loading standard fuel elements in the reactor core (August 1988), with $1.9 \text{ gU/cm}^3 \text{ U}_3\text{O}_8\text{-Al}$. The adopted criteria was that each IPEN fuel element had to start irradiation at peripheral positions of the core, with lower power densities, up to 4 % burnup (almost one year of irradiation) and then it could go to higher power density positions in the core. It was decided that the precursor fuels had to stay in the core up to the same time that a complete fuel element would stay. The last precursor fuel assembly was taken out of the reactor core without any operational problems. Previous paper presented details about the fuel qualification program [2]. To qualify the $\text{U}_3\text{Si}_2\text{-Al}$ fuel the same strategy was adopted. In this case, the volume fraction of the fissile material in the dispersion was kept the same, around 27 %, resulting in a uranium loading of 3.0 gU/cm^3 .

The program for silicide fuel development at IPEN had great impulse after the approval of the IAEA TC BRA/4/047 "Fuel Improvement for the IPEN Research Reactor" in 1999. The primary purpose of this program was to develop the whole fabrication process of $\text{U}_3\text{Si}_2\text{-Al}$ dispersion fuel plate (including 4.8 gU/cm^3), its irradiation test at the IEA-R1 reactor and post-irradiation analysis. This project gave the necessary background to IPEN to produce and qualify its own U_3Si_2 powder and silicide based dispersion fuel plates for the IEA-R1 fuel element fabrication. The project steps to achieve the objectives included the following steps:

- a) to develop the process for producing UF_4 starting from UF_6 ;
- b) to develop the process for producing metallic uranium starting from UF_4 ;
- c) to develop the process for producing U_3Si_2 powder;
- d) to produce miniplates with 20% enrichment for irradiation tests;
- e) to irradiate miniplates at the IEA-R1 reactor and to perform non-destructive analysis on the irradiated fuel miniplates inside the spent fuel pool.

3.1 UF₆ conversion towards UF₄

Essentially, the process to get UF₄ from UF₆ uses the reduction of hexavalent uranium present in aqueous solution to the tetravalent state and its precipitation as UF₄ by means of the HF solution. The preparation of UF₄ using chemical reduction has been carried out starting from UO₂F₂ solution resulting from UF₆ hydrolysis. The solution is heated under continuous stirring to reach a temperature set point and then the reducing agent is added. Next, the hydrofluoric acid HF precipitating agent solution is slowly added. Tests have been carried out using different reducing agents, such: SnCl₂, CuCl, FeCl₂, and Na₂S₂O₄. The reducing agent SnCl₂ was the one that showed the best results and achieved a level of UF₄ precipitation in the range of 98%. However, during the UF₄ preparation an amount of water is absorbed by the UF₄ crystal. This water could interfere in the other process steps, and to avoid problems it must be removed.

The elimination of crystallization water from the UF₄ is carried out in temperatures near 400°C, under a constant flow of argon over the surface of the powder, which avoid the UF₄ oxidation to UO₂F₂ or UO₂ and drag the water vapor released. The material, in a powder form, is placed in a small Monel boat and introduced inside the heating chamber. After purging with argon for 1 hour the system is heated to 400°C under flow of gas. The UF₄ powder remains in this temperature for 1 hour, which is a sufficient time to complete the water elimination. The subsequent cooling is carried out keeping the flow of argon till the temperature reaches 100°C. Details of the UF₄ precipitation procedures were presented in a previous work [6].

3.2 UF₄ Reduction to Metallic Uranium

The intermetallic U₃Si₂ is produced from metallic uranium. To produce metallic uranium in the required quantity (up 80 kg/year) IPEN has developed a process to produce small quantities of uranium (1000g) through magnesiothermic routine. The 1000g ingot of metallic uranium is rather small if compared to previous practice of IPEN. In 1980's, ingots of natural uranium ranged up to 100kg. The downscaling was difficult, since not only the reduced scale for the crucible was conceived, but also lower material amount to be reduced implied in difficulties to get reasonable metallic yields. The crucible itself has been planned several times to achieve the final format using a bottom extractable system to help removing the cast ingot from the crucible. The thermal profile of the furnace has already been achieved by experimentation and calculations, but to reach optimized yields it was necessary to identify the exact moment of the reaction. It was got by means of an accelerometer in order to recognize the sound waves perturbation during the reaction moment.

Optimization of this method was met only after 25 experiments with natural uranium simulations in the last 3 years. Once settled down this technology, IPEN started to produce the 20% LEU enriched uranium. The yield of this system is around 82-85% of metallic uranium. The enriched material was already produced with good operation and quality results.

3.3 U₃Si₂ fusion and powder fabrication

Since 2000, the Nuclear Fuel Center of IPEN has been dedicating great efforts to achieve expertise in production of intermetallic alloy U₃Si₂. After facing some difficulties, as reported previously [7], in 2004 IPEN has arrived to the full experimental route to produce, in production scale, the necessary alloy for nuclear fuel.

From the produced uranium ingot, the metal was melted inside an induction furnace with silicon addition, with an adequate vacuum instrumentation and facilities for handling and melting uranium and uranium alloys. The zirconia crucible was specially designed to reach temperatures higher than 1750°C and to support the aggressive environment created by uranium chemical attack. More than 20 trials were carried out, using natural uranium, before the first LEU U₃Si₂ were successfully made. It was produced 3 enriched U₃Si₂ melting in 2005,

which consisted the first own produced load of fuel plate fabrication in IPEN. In general terms, the quality of this intermetallic has fully met the needs postulated by the requirements for a routine nuclear material. The X-ray diffractogram attested the presence of the expected phases in the produced powder of this alloy.

3.4 Miniplate fabrication

As previously mentioned, IPEN started manufacturing its own fuel element by using U_3O_8 -Al dispersion fuel plates with 1.9 gU/cm^3 . This uranium loading represents a U_3O_8 volume fraction of 27 %. If this same volume fraction is used, the direct substitution of the U_3O_8 by U_3Si_2 would result in an increasing of uranium loading to 3.0 gU/cm^3 .

The increasing of U_3Si_2 volume fraction in the dispersion has a technological limit of 45 %, in order to allow fabrication of fuel plates. This means maximum uranium loading of 4.8 gU/cm^3 . This is the objective to be reached in the future. The increase in the volume fraction of both U_3O_8 and U_3Si_2 to 45 % implies in implementing modifications in the fabrication procedures in contrast to the currently adopted ones for LEU fuel. The necessary research work to adequate the fabrication procedures have been done under the IAEA TC BRA/4/047. It was fabricated 22 miniplates with approximately 120 mm length and 42 mm width fuel meats. The compacts were 20 X 40 mm. Aluminum alloy 6061 was used for the frames and dadding plates. The hot rolling temperature was 440°C . The cladding thickness over the defect zones (dog-boning) was 0.28 mm (specification states a minimum of 0.25 mm). All the fabricated miniplates showed good metallurgical bonding. In the first fabrication tests it could be observed some oxidation of U_3Si_2 particles located near the interface core/cladding. The volume fraction of the oxidized phase was quantified by means of image analysis and the results indicated that a volume fraction between 2 and 4 % of the U_3Si_2 particles has been oxidized. The presence of the measured volume fraction of this oxide phase, within the fuel core, was considered to be no deleterious to the fuel performance during irradiation. However, a study of the oxidation phenomenon was carried out to eliminate or minimize the oxide formation during the fabrication. The cause was determined to be the welding procedure. A modification in the welding device was done to minimize the air entrapment in the weld assembly. This was possible with the use of a glove-box with argon atmosphere. The oxidation problem was no more observed ever since.

3.5 Miniplate irradiation at IEA-R1 research reactor

The irradiation device was planned to be placed at the IEA-R1 core support plate. Its overall dimensions were similar to the fuel assembly dimensions. It was projected to contain miniplates for irradiation and also to allow their removal for post-irradiation NDT to be performed at the spent fuel pool. The project assumed the possibility to irradiate up to 10 fuel miniplates at once. It was designed an internal support for the miniplates, which could be assembled inside the irradiation box. The post irradiation examination includes miniplate thickness measurement, visual inspection and sipping. The fuel miniplate thickness measurement device will be used inside the reactor pool, in the spent fuel storage area. It will be operated from the reactor pool border and will be able to measure the fuel miniplate thickness variation along its surface. This device is based on a mechanical structure for positioning the miniplate and to perform the scanning along the miniplate surface. The thickness measurement will be performed by electronic probes (LVDT probes). The results are obtained by measurement instrumentation connected to the probes and the data are stored and processed by a laptop computer.

4. Conclusion

The developments involving fuel fabrication was satisfactorily completed. The next step is to fabricate full sized U_3Si_2 -Al fuel plates with 4.8 gU/cm^3 . This work was already started. The

experimental activities using the reactor have to be defined in written documents. Operational procedures was already written and analyzed by the reactor operational staff. The beginning of irradiation is waiting for a final approval of the Reactor Safety Review Committee for the experiment.

Acknowledgements

We want to express our gratitude to IAEA for the continuous support received along the years in developing the fuel fabrication in IPEN. This support certainly did the difference for the success of the fuel development program and helps us to follow the advances in the fuel technology.

5. References

- [1] F.B.V. Oliveira, M. Durazzo, E.U.F. Carvalho, A.M. Saliba Silva , H.G. Riella, "Powder Formation of γ -UMo Alloys Via Hidration-Dehydration". 2007 RERTR Meeting.
- [2] J.A. Perrota, A.M. Neto, M. Durazzo, J.A.B. Souza, R. Frajndlich, "Irradiation Experience of IPEN Fuel at IEA-R1 Research Reactor". Proceedings of the XXI International Meeting on Reduced Enrichment for Research and Test Reactors, São Paulo, Brazil, 18-23 October 1998.
- [3] M. Durazzo, J.A. Perrota, "Fuel Improvement for the IPEN Research Reactor". Semiannual Progress Report January-June 1999. IAEA Project Number BRA/4/047. IPEN, São Paulo, 1999.
- [4] M. Durazzo, J.A. Perrota, "Fuel Improvement for the IPEN Research Reactor". Semiannual Progress Report July-December 1999. IAEA Project Number BRA/4/047. IPEN, São Paulo, 1999.
- [5] M. Durazzo, J.A. Perrota, "Fuel Improvement for the IPEN Research Reactor". Semiannual Progress Report January-June 2000. IAEA Project Number BRA/4/047. IPEN, São Paulo, 2000.
- [6] E.U.C. Frajndlich, A.M. Saliba Silva, M.A Zorzetto, "Alternative Route For UF_6 Conversion Towards UF_4 to Produce metallic Uranium". Proceedings of the XXI International Meeting on Reduced Enrichment for Research and Test Reactors, São Paulo, Brazil, 18-23 October 1998.
- [7] A.M. Saliba Silva, J.A.B. Souza, E.U.C. Frajndlich, J.A. Perrota, M. Durazzo, "First Results of U_3Si_2 Production and its Relevance in the Power Scale-up of IPEN Research Reactor IEA-R1m". Proceedings of the XX International Meeting on Reduced Enrichment for Research and Test Reactors, Jackson Hole, Wyoming, 5-10 October 1997.

RESULTS OF PRE-REACTOR EXAMINATION OF THE U-9Mo-UO₂-Al FUEL ELEMENTS FABRICATED BY THE EXTRUSION METHOD

V.V. POPOV, G.A. BIRZHEVOY, A.D. KARPIN, V.N. SUGONYAEV
*RF State Scientific Centre IPPE
(Bondarenko Sq. 1, 249033, Obninsk, Kaluga Reg., Russia)*

ABSTRACT

Post-reactor tests of the (U-9Mo)-Al and (U-9Mo)-Al-12Si fuel compositions with the coatings (Nb, Zr-1%Nb alloy and UO₂) irradiated in the IVV-2M reactor to 60% ²³⁵U burn-up showed that the effect of their maximum radiation resistance increasing (more than two times) has been obtained using the oxidic layer coatings. But it is danger that fabricating the fuel elements using the extrusion method the integrity of the brittle UO₂ coating on the U-Mo fuel particles during the pressing out operation (pressing) can be broken. This paper presents the results of pre-reactor examination of the rate of interaction between the oxidized fuel particles and the Al matrix in the fuel elements fabricated using the extrusion method.

Introduction

Based on the literature data analysis we have concluded that it was possible to increase the (U-Mo)-Al fuel composition radiation resistance owing to creating the coatings of the necessary thickness on the fuel particles, reducing the fission fragments output into the matrix and the rate of interaction between the fuel particles and the matrix [1].

Reactor test was performed on the specially fabricated mini-elements with (U-9Mo)-Al and (U-9Mo)-Al-12Si fuel compositions irradiated in the IVV-2M reactor to 60% ²³⁵U burn-up. As the coatings Nb, Zr-1%Nb alloy and UO₂ have been used. Post-reactor tests showed that in all cases the coatings reduce the swelling rate of the fuel compositions. Moreover, the maximum effect (more than two times) has been obtained using the oxidic layer coatings [2].

It is necessary to confirm these results on the experimental fuel elements fabricated using the established technology by means of the extrusion method. At the same time it is necessary to decide some technological problems. As we see it, at this stage the basic problem is the preservation of the integrity of the brittle UO₂ coating on the U-Mo fuel particles during the pressing out operation (pressing).

The rate of interaction between the fuel particles and the matrix at the increased temperatures can testify the integrity of the coating. Our experiments have shown that the interaction between unoxidized U-9%Mo powder and Al began at 400°C and went on with the great rate at 550°C.

The given paper presents the results of pre-reactor examination of the fuel elements with the (U-9Mo-UO₂)-Al fuel composition fabricated using the extrusion method.

Materials and methods

As the fuel component the powder from the U-9%Mo alloy at 6.5% enrichment has been used. The particle size ~100-160 μm. Annealing of the U-9%Mo powder at 140°C at air during 8 hours has been used for fabricating the UO₂ layer. The matrix material – PA-4 alloy powder.

The intermediate products of cores (tablets) have been fabricated by the hot pressing method of the U-9Mo- UO₂ (30% volume) and PA-4 (70% volume) powder mixture in vacuum at 400°C.

Material of the fuel elements envelope – the CAB-1 alloy. The extrusion of the fuel elements has been produced at 400°C through the die holes of 3.5 mm and 2.8 mm size. The extraction coefficient is 9.7 and 15.2 respectively. For determining the presence and condition of the coating on the fuel particles after the pressing and extrusion technological operations in accordance with the earlier fabricated method the thermal processing of the samples has been carried out at 500, 530, 550 and 620°C during 3.5 and 6 hours.

Microhardness has been measured at the loading of 50 G.

Annealing of the samples has been carried out in vacuum with the residual pressure of $6.67 \div 9.3 \times 10^{-3}$ Pa.

The phase composition of the interaction layers has been determined by the X-ray microspectral analysis.

Results

The results of the present study of the rate of interaction between the U9Mo fuel particles without the coating and the Al matrix are shown in Table 1.

Table 1. Results of the rate of interaction between the U-9Mo powder without the coating and the Al matrix at different temperatures study

Test temperature, °C	Test duration, hour	Interaction zone width, μm	Interaction zone phase composition
200	650	-	-
400	21	10-15	UAl ₃ , UAl ₂ (traces)
500-530	1	4-8	UAl ₃ , UAl ₂ (traces)
	3.5	5-10	
	6.5	6-13	
	13.5	10-15	
	20	10-17	
600-620	4	10-15	UAl ₃ , UAl ₂ (traces)

Results presented show that the strong interaction between the fuel particles without the coating and the matrix begins at temperatures over 500°C.

The results of the tablets fabricated using the oxidized U9Mo fuel particles study show that the oxidic film thickness is $\approx 2 \mu\text{m}$ (Fig. 1).



Fig. 1. Microstructure of the (U-9Mo-UO₂)-Al tablets

The fuel particles interaction with the matrix after extrusion was not observed (Fig. 2).

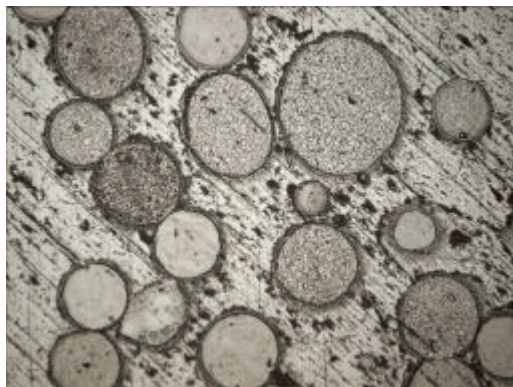


Fig. 2. Microstructure of the fuel composition after the fuel element fabrication

The U-9Mo-UO₂ fuel particles interaction with the matrix after the fuel elements annealing at 500 and 550°C during 3.5 hours was not observed. The fuel particles microhardness is equal to 3940 ÷ 4273 MPa, the matrix one – 560 ÷ 655 MPa.

The interaction traces were observed around the separate fragments after the annealing at 530°C during 6 hours (Fig. 3). The fuel and matrix microhardness was not changed.

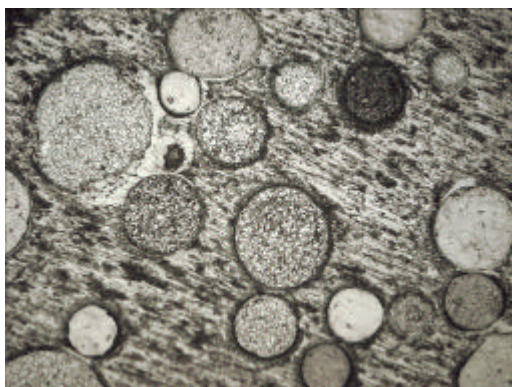


Fig. 3. Microstructure of the (U-9%Mo-UO₂)-Al fuel composition after the fuel elements annealing at 530°C during 6 hours

The appreciable interaction between the powder and the matrix was observed after the fuel elements annealing at 620°C during 6 hours. The interaction layer thickness in samples with fuel without the coating achieves to 5 ÷ 20 μm (Fig. 4). The fuel particles microhardness is equal to 3489÷3940 MPa, the matrix one – 420÷ 655 MPa, the interaction zone one – 6233÷7262 MPa.

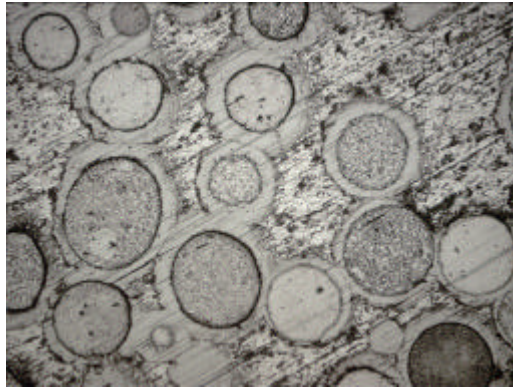


Fig. 4. Microstructure of the (U-9%Mo-UO₂)-Al fuel composition after the fuel elements annealing at 620°C during 6 hours

Conclusions

Based on the results obtained it is shown that in case of using the U-9%Mo-UO₂ powder the interaction with the Al matrix was practically absent up to 550°C. It shows that the oxide coatings have preserved their integrity in the process of the hot pressing of the tablets and fabrication of the fuel elements by the extrusion method.

At present time the fuel elements fabricated using given technology are irradiated in the MIR reactor (RIAR, Dimitrovgrad).

References

1 Birzhevoy G.A., Karpin A.D., Popov V.V., Sugonyaev V.N. «Some approaches to solving the problem of diminishing the interaction between UMo fuel particles - Al matrix». 10th International Topical Meeting Research Reactor Fuel Management, 30.04-3-05.06, Sofia, Bulgaria, Transaction European Nuclear Society, p.79-82.

2 Birzhevoy G.A., Popov V.V., Golosov O.A., Shushlebin V.V., Rychkov V.?, Lyutikova ?.S. «Results of post-irradiation examination of the (U-Mo)-aluminium matrix interaction rate» 11th International Topical Meeting Research Reactor Fuel Management (RRFM) and Meeting of the International Group on Reactor Research (IGORR). Lyon, France, 11-15.03.2007, p.468-472.

Radiation Effect on Microstructural Stability of RERTR Fuel

J. Gan¹, D. D. Keiser, Jr.¹, B. D. Miller², T. R. Allen², and D. M. Wachs¹

¹ Idaho National Laboratory, Idaho Falls, Idaho, USA

² University of Wisconsin, Madison, Wisconsin, USA

ABSTRACT

Three depleted uranium alloys are successfully cast for the radiation stability studies of the fuel-cladding interaction product using proton irradiation. Scanning electron microscopy (SEM) analysis indicates the presence of the phases of interest: $U(Si,Al)_3$, $(U,Mo)(Si,Al)_3$, and a mixture of UMo_2Al_{20} , $U_6Mo_4Al_{43}$, and UAl_4 . Irradiation with 2.6 MeV protons at 200°C to the doses of 0.1, 1.0, and 3.0 displacement per atom (dpa) are carried out.

1. Introduction

The RERTR Fuel Development Program is tasked with developing new low enrichment uranium (LEU) nuclear fuels that can be employed to replace existing high enrichment uranium (HEU) fuels currently used in some research reactors throughout the world. An important part of the fuel development program is an effort to conduct irradiation testing to better understand in-reactor fuel performance and to provide key data that can be incorporated into computer models that are used to model in-reactor fuel performance. For dispersion type fuels, radiation stability of the interaction layers at the interface of fuel particle and cladding matrix plays an important role in fuel performance. Proton irradiation studies of these interaction products will provide important insights on the microstructure stability under irradiation damage.

A variety of phases have the potential of forming in irradiated RERTR fuels as a result of fuel/matrix or fuel/cladding interactions. To study the radiation stability of these potential phases, three depleted uranium alloys are fabricated with compositions of 67U-5Si-28Al (alloy-A), 48U-5Mo-47Al (alloy-B), and 69U-4Mo-20Al-7Si (alloy-D). The first alloy composition selected is close to that of a $U(Si,Al)_3$ phase. This phase has been observed to form in uranium-silicide dispersion fuels and exhibit stable performance under irradiation [1]. The second composition is near that of $(U,Mo)Al_7$, a composition observed in interaction layers of the current version of U-Mo dispersion fuels that use Al as the matrix, which showed poor irradiation performance at very high burnup [2]. In order to improve the performance of U-Mo dispersion fuels, the RERTR program has been investigating the use of Si additions to the cladding matrix to influence fuel/matrix interaction such that a more stable interaction product will form. The idea is that by having Si participate in the inter diffusion process, then it is likely that a $(U,Mo)(Si,Al)_3$ phase will form and remain stable under irradiation, like the $U(Si,Al)_3$ phase did in the uranium-silicide fuels [3]. As a result, the third alloy has a composition near that of a $(U,Mo)(Si,Al)_3$ phase.

The first objective of this work was to verify that the microstructural response of $U(Si,Al)_3$ phase and the phase mixture that exist with a composition of $(U,Mo)Al_7$ under proton irradiation were consistent with the fuel performance reactor tests. The second was to investigate if the radiation stability of the interaction product, $(U,Mo)(Si,Al)_3$ phase was similar to $U(Si,Al)_3$ phase in the silicide fuel. Finally, phase stability, amorphization, and cavity formation and distribution as a function of irradiation dose were to be established.

2. Experiment

Three depleted uranium (DU) alloys were cast using arc melt. Ingot for each alloy weighs approximately 30 grams. High purity Mo, Al, and Si at 99.999% were used for alloy fabrication. These ingots were wrapped in Ta foil, sealed in a stainless steel tube, and homogenized at 500°C for 200 hours. Table 1 lists the material information for this proton irradiation study.

Table 1. DU alloys cast for proton irradiation studies.

Sample designation	A	B	D
Composition (wt%)	67U-5Si-28Al	48U-5Mo-47Al	69U-4Mo-20Al-7Si
Composition (at%)	$U_{19}Si_{12}Al_{69}$	$U_{10}Mo_3Al_{87}$	$U_{22}Mo_3Al_{56}Si_{19}$
To study F.C.I. product	$U(Si, Al)_3$	UMo_2Al_{20} , UAl_4 , $U_6Mo_4Al_{43}$ mixture	$(U, Mo)(Si, Al)_3$
Found in fuel type	H.E.U.	L.E.U. (U-Mo)	L.E.U./Al-Si Clad
Anticipated performance	Good	Not good	Good
Microstructure stability	Stable	Cavity + Swelling	Stable (?)

SEM analysis was performed to identify the phases of interest. Samples were mounted and polished through 1 μm polishing compound. The mounted samples were inserted into a ZEISS Model 960A scanning electron microscope that was equipped with an Oxford wavelength dispersive spectrometer (WDS) and energy dispersive spectrometer (EDS) that employed ISIS LINK software. Secondary electron images were generated to determine the alloy microstructures, and the WDS and EDS spectrometers were employed to generate X-ray maps and to perform point-to-point compositional analysis.

For proton irradiation, the ingots were cut into 300-400 μm thin slices with a low speed saw and core drilled to the disc samples of 3.0 mm diameter. The disc samples were mechanically wet polished to the 1200 grit finish. An average of 12-15 disc samples were loaded on the irradiation stage for each irradiation. A liquid metal interface was used between the back of the disc samples and the stage to improve the thermal conduction for improved temperature control. Proton irradiations were conducted using a tandem accelerator at the University of Wisconsin. The 2.6 MeV proton beam was rastering over an area of 10x16 mm² on the irradiation stage. The irradiation temperature was monitored through three thermocouples and controlled at 200 \pm 20°C. The rate of atomic displacement damage is estimated to be approximately 1.0 x10⁻⁵ dpa/s using STRIM2006 calculation with the default displacement energy of 25 eV[4]. The irradiation target

chamber and the irradiation stage are shown in Figure 1. Disc samples of three DU alloys were irradiated to doses of 0.1, 1.0 and 3.0 dpa. Microstructural analysis for both the unirradiated and the irradiated DU alloys will be performed using transmission electron microscopy (TEM). The results of TEM analysis are not available for this paper.

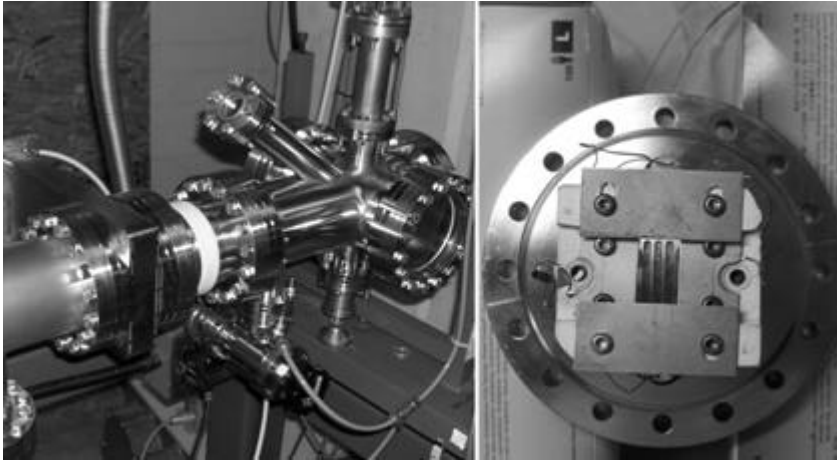


Figure 1. Irradiation chamber and stage for proton irradiation of DU alloys.

3. Results and Discussion

Secondary electron images of the Sample A microstructure are presented in Figure 2. Two phases comprise the alloy microstructure: a $U(Al,Si)_3$ phase and an Al phase. The $U(Al,Si)_3$ phase has an approximate composition in at% of: $U_{27}Al_{60}Si_{13}$ (± 1 at%).

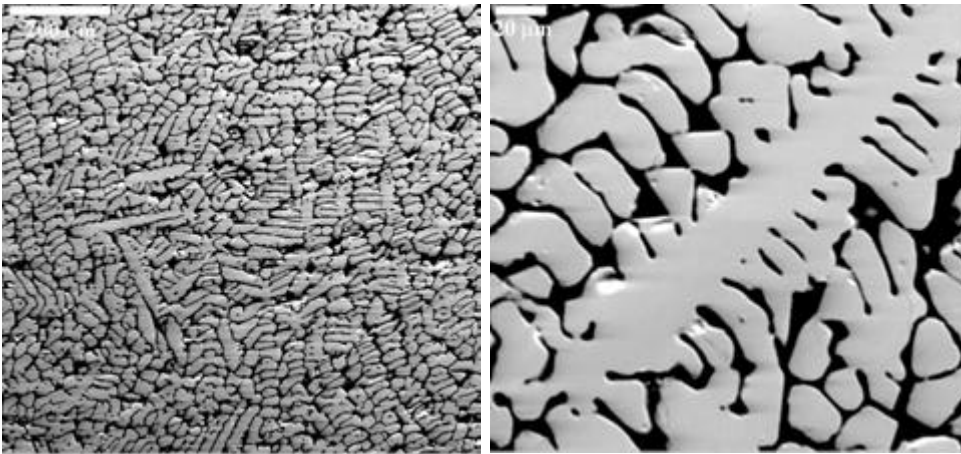


Figure 2. Secondary electron images at low (left) and high (right) magnification of the microstructure observed for alloy A. The black phase is Al, and the bright contrast phase is a $U(Si,Al)_3$ phase.

Secondary electron images of the Sample B microstructure are presented in Figure 3. Four phases comprise the alloy microstructure: UMo_2Al_{20} , $U_6Mo_4Al_{43}$, UAl_4 , and Al. The approximate compositions for the UMo_2Al_{20} , $U_6Mo_4Al_{43}$, and UAl_4 in at% are: Al₈₈-Mo₇-U₅, Al₇₉-Mo₉-U₁₂, and Al₇₈-U₂₂, respectively.

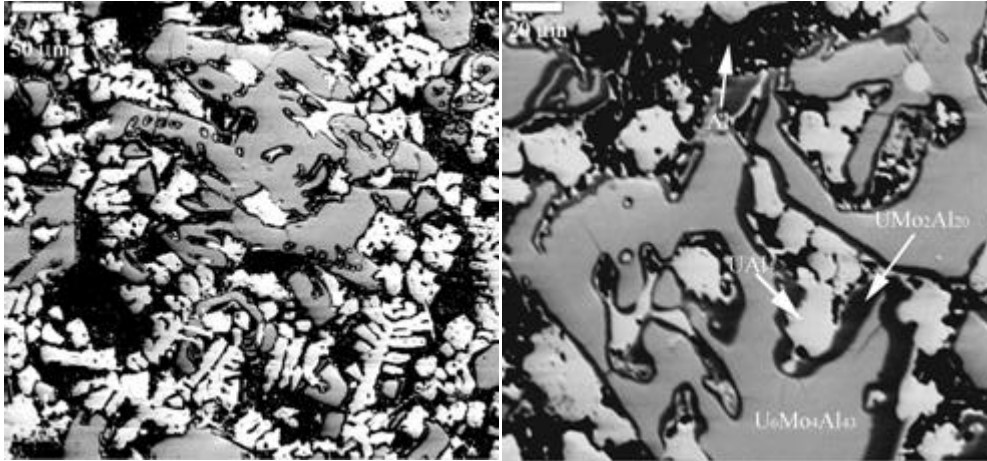


Figure 3. Secondary electron images at low (left) and high (right) magnification of the microstructure observed for Sample B

Secondary electron images of the Sample D microstructure are presented in Figure 4. Three phases comprise the alloy microstructure: $(U,Mo)(Si,Al)_3$, UMo_2Al_{20} , and Al. The approximate compositions for the $(U,Mo)(Si,Al)_3$ and UMo_2Al_{20} in at% are: Al₄₉-Si₁₉-Mo₃-U₂₇ and Al₈₆-Mo₈-U₆ respectively.

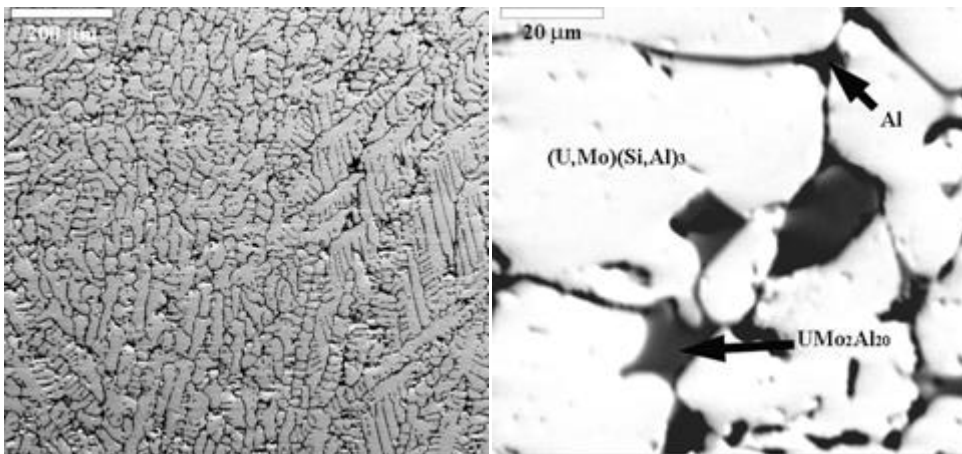


Figure 4. Secondary electron images at low (left) and high (right) magnification of the microstructure observed for Sample D.

For proton irradiation, the 0.1 dpa irradiation proceeded smoothly and was completed in approximately 3 hours. There is no problem for alloy "A" at 1 and 3 dpa. Some of the alloy "B" discs showed slight melting for 1 dpa and 3 dpa irradiation. The irradiation for alloy "D" discs at 1 dpa showed slight discoloration and crack development. The problem for alloy "D" discs becomes worse at 3 dpa. It is likely that the problem developed for the irradiated "D" alloy is associated with the microstructural changes which will be revealed through TEM analysis.

4. Conclusion

Three alloys have been successfully cast, homogenized, and characterized using SEM/EDS/WDS analysis. These alloys will work perfectly for their intended purpose as ion beam irradiation samples. Sample A contains only the $U(Al,Si)_3$ phase, besides some residual Al, which is the phase of interest to be studied. Sample B has U-Mo-Al phases that are assumed to influence the irradiation behaviour in the current versions of RERTR U-Mo dispersion fuels, and will be of interest as well. Finally, Sample D not only contains a quaternary phase that is of interest, i.e. the $(U,Mo)(Si,Al)_3$ phase, but it also contains one of the ternary U-Mo-Al phases (UMo_2Al_{20}) that is suspected to exhibit poor performance during irradiation. This will allow for a direct comparison, within one sample, of a phase that will hopefully exhibit favourable irradiation performance with a phase that is suspected to exhibit poor performance.

References

- [1] A. Leenaers, S. Van den Berghe, E. Koonen, P. Jacquet, C. Jarousse, B. Guigon, A. Ballangny and L. Sannen, *J. of Nucl. Mater.*, 327 (2004) 121.
- [2] A. Leenaers, S. Van den Berghe, E. Koonen, P. Jacquet, C. Jarousse, F. Huet, M. Trotabas, M. Boyard, S. Guillot, L. Sannen and M. Verwerft, *J. of Nucl. Mater.*, 335 (2004) 39.
- [3] Y. S. Kim, G. L. Hofman, H. J. Ryu and J. Rest, "Thermodynamic and Metallurgical Considerations to Stabilizing the Interaction Layers of U-Mo/Al Dispersion Fuel", Proceedings of the International Meeting on RERTR, Boston, USA, Nov. 6-10, 2005.
- [4] J.F. Ziegler, J.P. Biersack, U. Littmark, TRIM97 program, IBM Corp., Yorktown, New York, 1997.

THERMAL AND CHEMICAL STABILITY OF SOME HYPOEUTETOID γ -UMo ALLOYS

F. B. VAZ DE OLIVEIRA, E. F. U. CARVALHO
*Nuclear Fuel Center / Nuclear and Energy Research Institute / IPEN / CNEN
Av. Prof. Lineu Prestes 2242, 05508-000 São Paulo / SP / Brazil*

H. G. RIELLA
*Chemical Engineering Department - Federal University of Santa Catarina
/ Florianópolis / SC / Brazil*

ABSTRACT

To face the problem of the interaction layer in gamma-uranium-molybdenum based fuel alloys and the aluminium based matrix, in this work are presented some of the first results of differential thermal analysis DTA relating to the reactions between some γ -UMo fuel alloys with aluminium. Alloys were prepared by vacuum induction melting, and thermally treated at convenient temperatures and times, to the homogenization and obtention of full gamma structure, in the compositions of 5 to 10% wt. Mo, and a ternary with $\%(\text{MoSi})_{\text{wt}} = 8\%$ wt. Curves of heat flow as a function of time were obtained for each system. The temperatures of reaction were determined, and some graphs relating them with the Mo content were drawn. They lead to some important conclusions about the influence of Mo in the stability of the alloys, with those important materials found in the fuels environment inside the reactors.

1. Introduction

One of the most important problems of the γ UMo dispersion fuels is their reaction with aluminum. The formation of new compounds, mainly those with composition $(\text{UMo})\text{Al}_x$, exerts some effects in the fuel plates performance, due to changes in the thermal properties of the uranium phases, which causes changes in the plate's temperature profiles, among others. Thus, the obtention of thermally and chemically stable or non-reactive fuels are one of the main goals of the RERTR program.

Some important works are being carried out [1, 2, 3, 4] with the objective of the production of more gamma stable and non reactive fuel phases and, also, more chemically stable matrices. Studying the formation of the interaction layers in fuel-matrix thermocouples, they obtained that the additions of Zr, Ti and Si to the fuels, and Si to the matrix, are the most promising candidates to minimize the interaction layer problem, but they still present some problems, mainly those related to the reduction of the gamma stability. For example, it was shown that, in the conditions of the experiments carried out by PARK et al. [01, 02], some 5 of additions of Zr and Ti minimize the extent of the interaction layer, which is a good achievement. But both present the inconvenient of accelerate gamma decomposition.

In this paper the temperatures and energies of reactions with aluminium of the most important considered hypoeutetoid alloys, for use as nuclear dispersion fuels, are presented. Our main goal is to contribute with the study of the fuel-aluminium system reactions, and to evaluate

the compositions where the reaction occurs with less energy release. To have a term of comparison, and to contribute with the study of ternary additions to the phase fuel, a γ U(MoSi) alloy were prepared and also its behaviour studied.

2. Experimental procedure

Samples with approximately the same masses of uranium alloy and aluminum powder were assembled in alumina crucibles, inside the internal chamber of the DTA analyzer, in the form of small compacts. The thermal cycle was constituted by heating and cooling, with the goal to observe melting and solidification points of aluminum and, if it be the case, the reaction products. After a level of vacuum of 10^{-3} mbar, the temperature of the furnace was raised, at a rate of $10^{\circ}\text{C}/\text{min}$. up to 1000°C , where, at the same rate, the temperature was decreased. The choice for this temperature had the goal to verify possible interactions, even in the conditions far from the existent in the reactors environment.

The analysis of the curves was performed as follows. Differences of the melting points of aluminum and γ UMo alloys are of the order of 600°C . Thus, in the heating part, the first peak referred to the melting of aluminum. In the liquid state, the probability of the reaction between Al and γ UMo is greater than when aluminum is still in a more porous form, like its form in the compacts. If some reaction occurred, peaks will appear after the melting peak of aluminum, obviously with the consumption of some original aluminum.

Now, if the reaction formed stable products, they will have different properties when compared with the original fuels. In the cooling curve, according to the extent of the aluminum consumption, the peak of aluminum solidification, since it depends on the amount present in the system, will be different or will not keep the expected 1:1 proportion, in terms of area above it.

Our main strategy to determine the stability of the alloys is the comparison between the energies, obtained by integration of the area enclosed by both peaks. If the consumption by the reaction was low, the relation between the integrated areas of the cooling peak and heating peaks will be almost the same, normalized by the samples masses. The contrary will occur with the increasing in the reaction extent.

We are not concerned with the operational conditions of temperature in the reactors, plates or fuels inside the reactors, since stability criteria, as studied in this paper, are more general, and will serve also for these conditions.

3. Results and discussions

The graphs of heat flow, measured in the units given by the acquisition software, are given below. The first one refers to the melting of the aluminium, where the relation between the energies were almost 1,1, a 10% difference. So, it is reasonable to conclude that the intensities, in absolute values, are the same. What we are saying is that all the available mass to the melting, in the heating region, was also available for the solidification.

In the reaction curves are shown some small peaks, mainly in the heating curve, and in general, the solidification peaks and respective areas enclosed by them (energies) have less intensity. As observed by Kim [04], the temperatures for the reactions between γ UMo and aluminium are around 645°C . Since in all the experiments the melting temperatures of the aluminium were near 641°C , it is reasonable to suppose that the next peak represents the reaction, which is favoured in the presence of liquid aluminium. After integration, the energies for the melting and solidification of aluminium are, respectively, 441.89 and 492.35 (u.e.),

where u.e are the unities of energy adopted. Thus, we can measure the energies of the reaction by the difference between the aluminium energy of solidification and the equivalents for the alloys here studied. According to the following figures, this was the behaviour of the γ UMo binary alloys.

For the ternary γ UMoSi, this fact was not observed. Since the amount of aluminium in the crucibles was higher for silicon than for the other systems, and since that there was a slight excess of addition of silicon related to its solubility in the gamma structure, it was expected that some phases of uranium, with other compositions different from the gamma matrix, were also present in the material, with poor silicon and molybdenum contents.

Comparing the peaks of solidification of UMoSi and the binaries, we observed that in the ternary case the relation between the areas were the minimal. According to our stability criteria, it indicates that if some reaction occurred, a minimum amount of aluminium was consumed or, if this is not the case, the reacted aluminium was promptly returned to its original phase after solidification. had the less intense energy released.

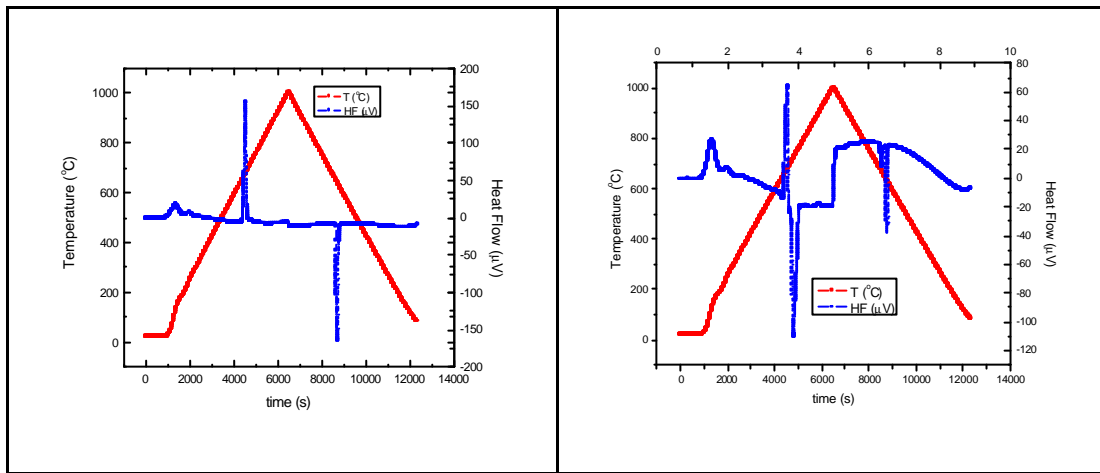


Figure 1 – Aluminium melting and solidification (left); reaction with γ U5Mo (right).

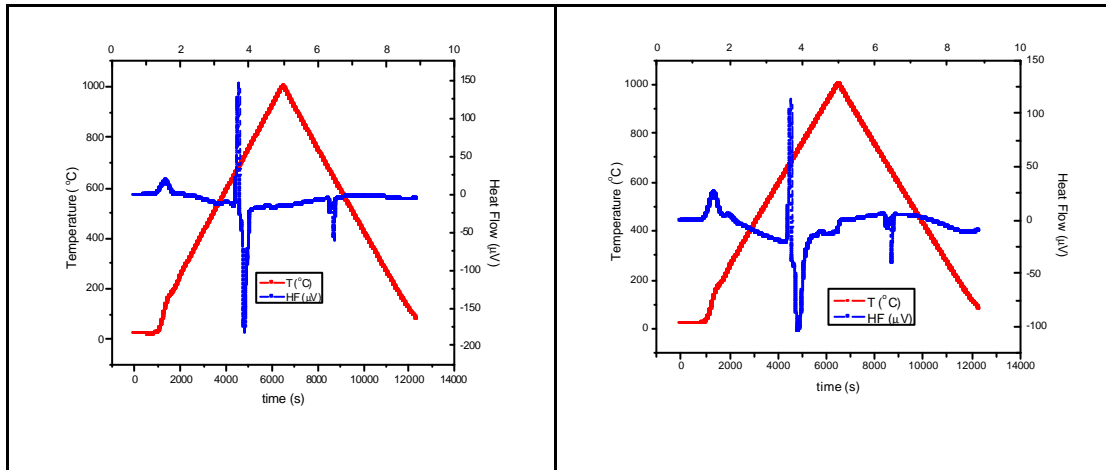


Figure 2 – Reaction with γ U6Mo (left); reaction with γ U7Mo (right).

In the table 01 are shown the results of the energies per unity of mass. The strong evidence for the stability increase due to the addition of silicon is given by the fact that there are almost

equality between the values of the aluminum solidification and the aluminum solidification after reaction with γ UMoSi. The small difference obtained, 15.31 u.e., corresponds to the initial fraction of the aluminum which reacted with this alloy. Comparing with the binaries, this value is too small.

Event	γ U5Mo	γ U6Mo*	γ U6Mo	γ U7Mo	γ U8Mo	γ U9Mo	γ U10Mo	γ UMoSi
E	458,03	507,82	722,89	728,70	732,28	880,16	574,39	169,00
<i>E (g)</i>	33,6	37,9	57,8	55,3	61,4	65,4	45,1	11,4

Tab 1: Energies, absolute and normalized values.

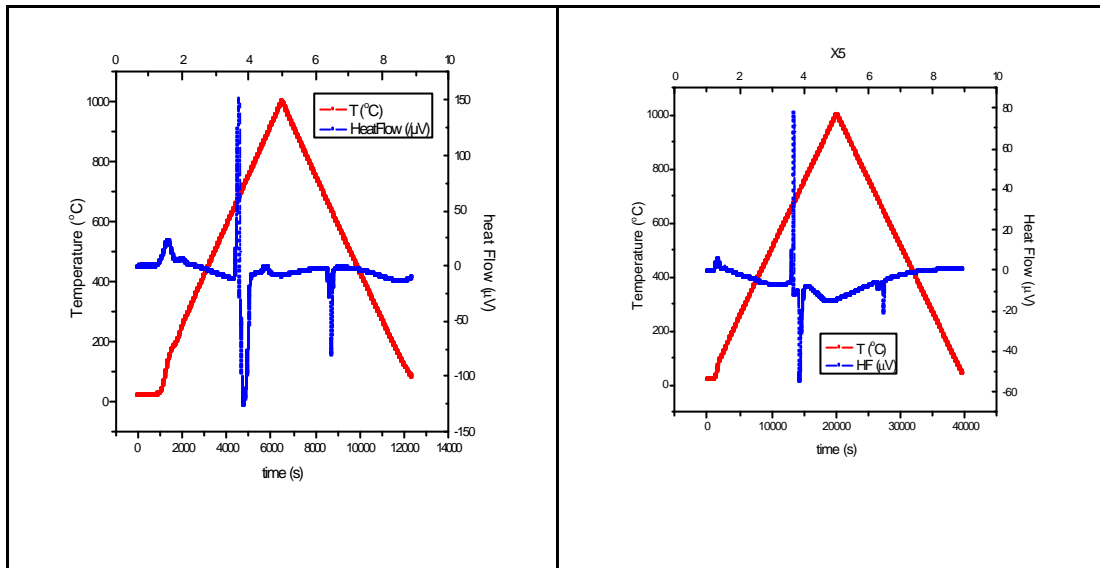


Figure 3 – Reaction with γ U8Mo (left); reaction with γ U9Mo (right).

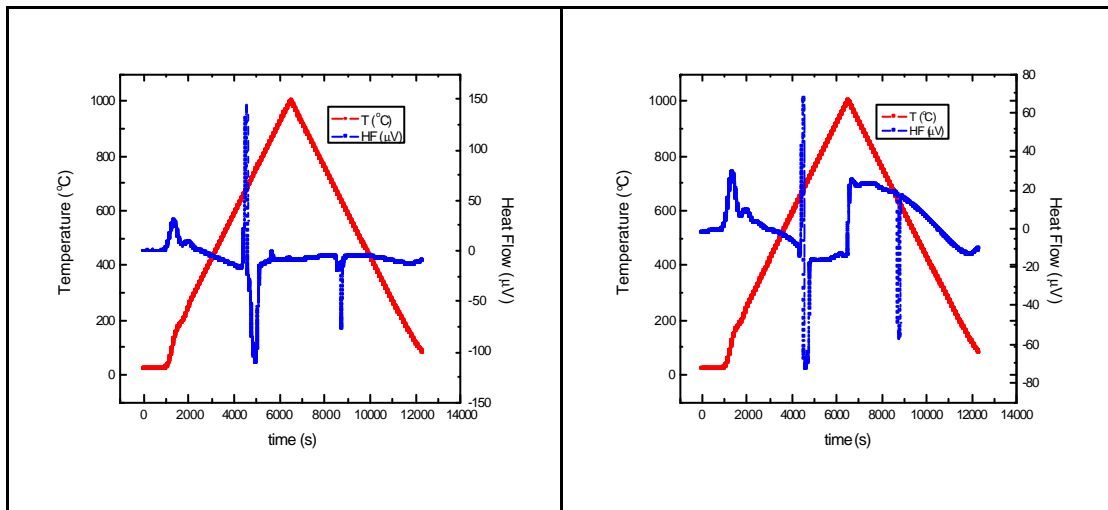


Figure 4 – Reaction with γ U10Mo (left); reaction with γ UMoSi (right).

In the figure 5 the points corresponding to the energies relating to the reaction phenomenon for each Mo addition are displayed. They show a tendency to increase with the Mo content, which confirms the fact that Mo is a layer former. The fall in the 10% addition has some relation with the internal structure of those alloys, more porous and therefore less dense than the others, which can interfere in the contact between the reaction phases.

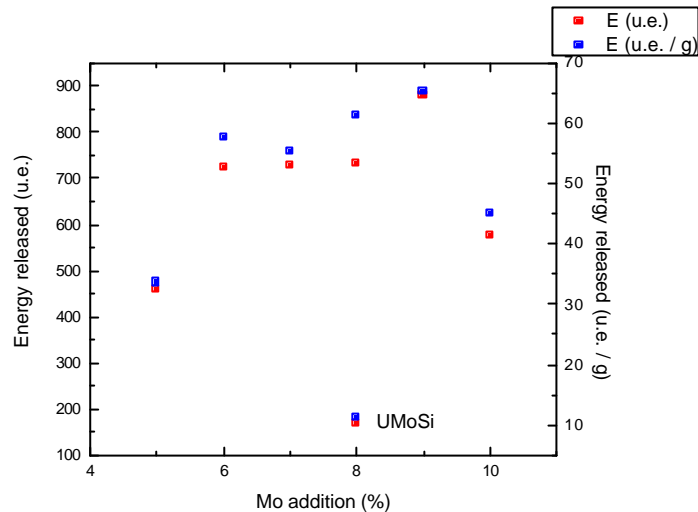


Figure 5 – Reaction with γ U10Mo (left); reaction with γ UMoSi (right).

4. Conclusions

For the RERTR experiments, we know that one of the main problems with γ UMo fuels is its high tendency to react with the matrix. Thus, additions of some ternary elements were considered along the time. Silicon, at least for the IPEN current needs, is the candidate to improve gamma stability and minimize the reaction extent with aluminum or improve its stability. Comparison between the results confirmed also the fact that Mo is a layer former, but a more complete analysis, which must deal with the binaries microstructures, must still be carried out.

Also, it was demonstrated here, by thermal analysis, that silicon, in small additions, can improve the behaviour of γ UMo alloys, at least in the experimental conditions here used, by the minimization of the energies and the differences between the energies of the aluminium melting and solidification.

5. References

- [01] PARK, J.M., et al., Interdiffusion Behaviors of. U-Mo-Zr / Al-Si, *Proceedings of the XXVIII RERTR Meeting*, Cape Town, South Africa, 2006.
- [02] PARK, J.M., et al., Interdiffusion Behaviors of. U-Mo-Ti / Al-Si, *Proceedings of the XXIX RERTR Meeting*, Prague, Czech Republic, 2007.

[03] VARELA, C. L. K., et al., Identification of Phases in the Interaction Layer Between U Mo-Zr / Al and U-Mo-Zr / Al-Si, ***Proceedings of the XXIX RERTR Meeting***, Prague, Czech Republic, 2007.

[04] KIM, Y.S., et al., Interaction-Layer Growth Correlation for (U-Mo) / Al and Si added (U-Mo) / al Dispersion Fuels, ***Proceedings of the XXVIII RERTR Meeting***, Cape Town, South Africa, 2006.

Distinctive Features of Interaction of the U-Mo Fuel Composition Fission Products and the ?I Matrix with Barrier Coating

D.P. SHORNIKOV

Department of material science Moscow engineering physical institute (State University)
Kashirskoe st.31, Moscow, Russian Federation

ABSTRACT

Based on the thermodynamic analysis of stability of a number of compounds used as barrier layers at the "U-Mo dispersed nuclear fuel – Al matrix" boundary, it was proposed to use pure Mo as a perspective coating. Interaction in the Mo-Al system at 600-700 °C was examined. The results obtained demonstrate attenuation of Al matrix-Mo interaction when Mo purity increases.

1. Introduction

At present, fuel of U^{235} reduced enrichment (from 90% to 20%) is proposed to be used as fuel for research reactors for the purpose of non-proliferation efforts. In this case, the decrease of burnup depth is observed due to the decrease of volume content of fissionable nuclide ^{235}U . To minimize some negative consequences of transition to low-enriched fuel, it was proposed to use materials based on high-density compositions as fuel particles, for example U-9wt.%Mo (density 17,2g/cm³). Alongside with using new fuel type, Al alloys continue to be used in research reactors as fuel claddings. They are characterized by good nuclear physical features, high heat conductivity and mechanical properties. Al alloys demonstrate operational strength at a water flow rate of 4–10 m/s and a cladding temperature of up to 260°C.

Operation experience of fuel elements with high-density fissionable phase U-9wt.%Mo of low ^{235}U enrichment (20 %) showed that at a burnup of 80-90 MWd/kgU fuel-cladding interaction is observed, resulting in local form changes, such as swellings, and finally, in fuel failure [1].

Intensive interaction of fuel and matrix material, i.e. their insufficient compatibility, is the main factor limiting fuel element performance in energy-stressed high-flux research reactors.

Decrease of fuel-Al matrix interaction could allow to increase considerably radiation stability of dispersed fuel elements with the specified fuel and to extend service life of fuel elements, respectively. In this context, work on increasing stability of dispersed fuel is conducted and several ways to increase fuel element reliability are proposed.

1) Introduction into the U-Mo-Al system of component(s) which considerably decreases the interaction rate. Specifically, alloying of U-Mo fuel with Si additions was proposed because they decrease the interaction rate in the U-Al system.

2) Application of barrier coating to the surface of fuel particles, which prevents the interaction of the U-Mo alloy and the Al matrix. This method is considered to be perspective and, therefore, a search for the barrier coating material is underway now.

2. Thermodynamic analysis of stability of prospective barrier layers

Based on the reference data, several types of prospective materials, such as uranium dioxide and nitride; Nb, Ti and Zr nitrides, as well as Mo, were investigated. Moreover, Mo is of special interest due to the fact that it is chemically less active if compared to U and it can supposedly be more competitive with Al matrix than the material of fissionable phase U-Mo.

Thermodynamic calculations were conducted for the purpose of selection of the most chemically stable barrier layer compositions at the fuel-matrix boundary. Preliminary calculations of interaction of the UO_2 , UN, UC, AlN, SiC barrier layers with Al and U-Mo were conducted using existing programs and database on the properties of specific substances [2]. The calculation results showed that these materials can not serve as reliable barrier layers. Uranium compounds interact with Al, while Al compounds – with uranium. Silicon carbide interacts with both metals, as well as with Mo. It can be explained by the affinity of U and Al chemical properties. Due to high chemical activity of these metals, it should not be expected that there is a compound that is resistant to their simultaneous influence.

The calculations showed that Mo, being a considerably less active metal, doesn't interact with UO_2 , UN, AlN, Al_2O_3 . The latter two high-temperature compounds don't interact with Al as well. Therefore, it is proposed to make at least double barrier layer to solve the problem technically: a granule is primarily coated with pure Mo, and only then with AlN or Al_2O_3 layer. The material of the second layer is planned to be specified by additional calculations.

3. Investigation of interaction in Mo-Al system

The calculation results confirmed a possibility to use Mo as a barrier coating material. Therefore, at the first stage, the Mo-Al system was subjected to corrosion testing within a range of 300-700° without addition of chemically active fission products and I and with addition of the above-mentioned FP.

To check Mo and Al compatibility at 660 and 700°, the testing was performed in vacuum, under a layer of the degassing flux of Mo chloride (99,99% purity) and Mo of vacuum melting (99,97% purity), respectively. The objective of testing was to determine the interaction rate at the barrier coating-matrix boundary at a short-term temperature increase and melting of Al layers adjacent to fuel.

A number of Mo specimens were placed into a crucible, free space was filled with Al granules and heated in vacuum up to 700°. The photo of microstructure is presented in Fig. 1a.

In the second case, Al was subjected to melting under a layer of the degassing flux (50wt.%NaCl+50wt.%KCl). The Mo plate and Al granules were placed into the preliminary melted flux. The melt was held up at 700° for an hour. The photo of microstructure is presented in Fig. 1b.

In the third case, polished surfaces of 99,97% purity Mo and Al were coated with alcoholic solution of CsI. In this case, accumulation of chemically active FP was simulated and the effect on the Mo-Al interaction nature was revealed. CsI saturation of surface was conducted in the argon atmosphere at 2atm at 550° for 5 hours.

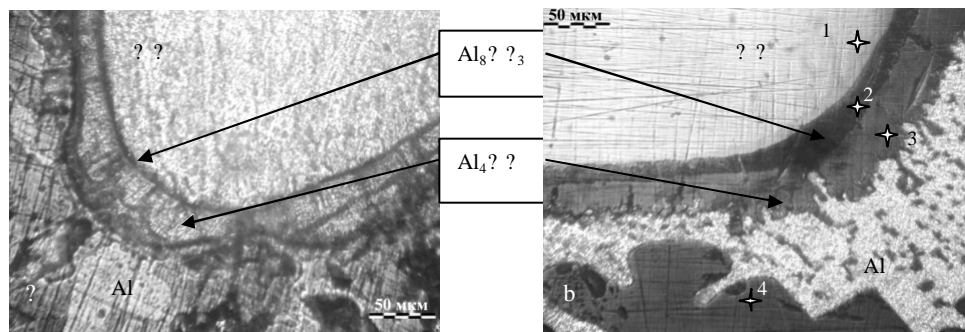


Fig.1. Mo-Al boundary. a- Mo chloride of 99,99% purity, vacuum melting, b- Mo chloride of 99,99% purity, flux melting, section is etched,x400.

The microstructure of specimens presented in Fig. 1a, b, as well as the results of the X-ray spectrum microanalysis given in Table 1, show the interaction of liquid Al with Mo.

Table 1: Results of X-ray spectrum microanalysis of Al-Mo specimen, flux melting.

Phase, point in Fig. 1 b	Element	Content, wt. %	Error, %	Atomic %
1	Mo	99,93	0,19	99,95
2	Al	40,99	0,31	71,18
	Mo	59,01	0,98	28,82
3	Al	52,72	0,33	79,86
	Mo	47,28	1,4	20,14
4	Al	45,08	0,33	64,1
	Ni	54,92	0,69	35,9

The inter-metallic compound Al_8Mo_3 (72-75at.% Al) the layer thickness of which makes up 8-10 μm is observed to form directly on the surface of the Mo specimen. Then the Al_4Mo layer (homogeneity area 80,0-80,4at.%Al) is observed to form. Its thickness makes up 20-50 μm . After an hour the total area of Al-Mo interaction makes up 30 μm at 660°?, while at 700°? it is equal to 50-60 μm .

After that, Knoop (H_k) and Vickers microhardness (H_v) of the Mo-Al specimens produced under different conditions was measured. The results are presented in Table 2

Table 2: Microhardness values for different Mo specimens in the Al matrix. H_k – loading mass= 100g, indentation period = 10s; H_v – loading mass = 100g, indentation period = 15s.

Specimen	Phase	H_k , GPa	Specimen	Phase	H_v , GPa
??-?I, 700°?, t=1h, vacuum	99,99%Mo	1,5	??-?I +CsI, 550°?, t=5h, argon P=2atm	99,97%Mo	3,2
	99,97%Mo	3,2		Al	0,2
	Al_4 ??	5,9			
??-?I, 700°?, t=1h, flux	99,99%Mo	2,7	??-?I+(Cs, I), 630°?, t=5h, vacuum	99,98%Mo	2,3
	Al_8 ? ? ₃	6,3		Al	0,2
	Al_4 ??	5,9		?? at the Mo-Al boundary	0,2
	Al	0,2		Al at the Al-?? boundary	0,45

The obtained microhardness values allow to conclude that at vacuum melting the hardness of Mo chloride is by 2.2 times lower than H_k of Mo (MChVP), while at flux melting of Al, H_k of Mo chloride increases by 2 times and achieves H_k values of 99,97% Mo. This effect can be explained by the fact that Mo chloride absorbs oxygen, nitrogen and carbon in the process of flux melting. Values H_k of the Al – Mo interaction boundary made up 6 GPa that is the result of inter-metallic compounds formation.

Measurement of microhardness of the CsI-saturated ??-?I specimen didn't reveal any considerable differences in H_k if compared to other specimens.

Further, Mo and Al (earlier saturated with CsI) were examined for compatibility at 630°? and a hold-up period of 5 hours. Mo (99,98% ??) and Al pellets were pressed tightly to each other from polished sides and annealed at 630°? for 5 hours in vacuum. The microstructure photos are given in Fig.2.

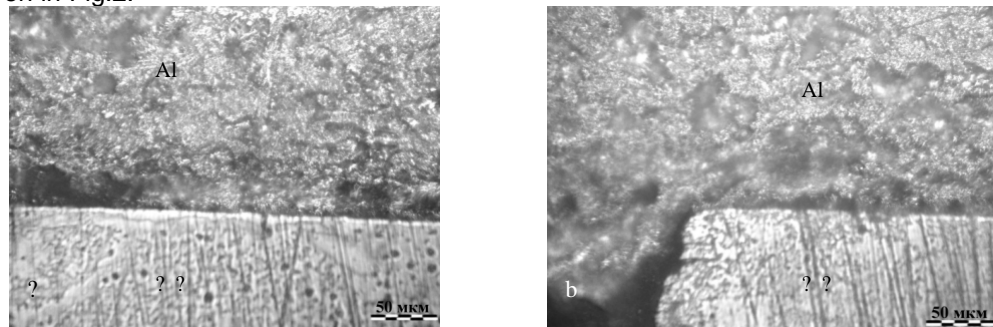


Fig.2. a, b – Microstructure of Mo-Al specimen - (CsI). Annealing at $T=630^\circ C$, $t=5h$ in vacuum, section is etched, $\times 400$.

The presented microstructure allows to conclude that the Al-Mo interaction doesn't occur. The Vickers microhardness (Table 2) of 4 areas (Mo area, Mo-Al boundary from the Mo side, Mo-Al boundary from the Al side and Al area) was measured. For Mo, average value H_v makes up 2,3GPa; at the Mo-Al boundary from the Mo side it amounts to 2.2 GPa that is equal to the microhardness value in the Mo area removed from the area conjugating with Al. At the Al-Mo boundary from the Al side, H_v makes up 0,45GPa, and for Al, H_v is equal to 0,2GPa. The

obtained results show that at a temperature close to the melting point the inter-metallic compounds are observed to be formed.

4. Conclusion

Based on the thermodynamic analysis of stability of a number of compounds and elements, several types of prospective materials, which are supposed to be used as barrier coating of U-Mo fissionable phase of dispersed nuclear fuel, were considered. Among such types of materials are uranium dioxide, carbide and nitride; niobium, titanium, zirconium nitrides and pure metals – Zr, Nb, Mo. It was demonstrated that all the above-listed coatings can not provide reliable protection of U-Mo particles from interaction with Al matrix.

Based on the results of thermodynamic analysis and chemical properties of Mo, it was proposed to use the latter as a material for barrier coating.

The corrosion testing conducted in the Mo-Al system at 300-700° showed that at a temperature exceeding 660°, intense liquid Al-Mo interaction is observed. Testing performed at 630° revealed short-term Mo-Al compatibility at a holding-up period of 5 hours.

The testing conducted in the Mo-Al system demonstrated interaction at a different purity of Mo (Mo chloride - 99,99% ??, MChVP – 99,97%? ?, arc vacuum melting - 99,97%? ?). Dependence of the inter-metallic compounds area on the content of impurities in the initial Mo is not revealed.

The results obtained showed that Mo can serve as a barrier coating of U-Mo particles of disperse fuel provided that the temperature is lower than 630°. However, it is needed to exclude the possibility of local overheating of Al matrix layers adjacent to the fuel particle over 660°. In its turn, it can result in the melting of the Al matrix and interaction of barrier coating with Al.

5. References

1. Lukichev V.A., Aden V.G., Kartashev Ye. F., Golosov O.A. et al. In-pile Tests and Post-Reactor Examination of Fuel Elements with Uranium-Molybdenum Fuel of reduced Enrichment // 8th Intern. Topical Meeting on Research Reactor Fuel Management, Munich, Germany, March 21-24 2004.
2. Internet site Outokumpu HSC Chemistry (www.outokumpu.com/hsc).

PROGRESS IN HEAVY-ION BOMBARDMENT OF U-MO/AL DISPERSION FUEL

R. JUNGWIRTH, W. PETRY, W. SCHMID

*Technische Universität München
Forschungsneutronenquelle Heinz Maier-Leibnitz (FRM II)
Lichtenbergstr. 1, 85747 Garching, Germany*

L. BECK

*Maier-Leibnitz-Laboratorium (MLL)
Am Coulombwall 6, 85748 Garching, Germany*

ABSTRACT

It was shown, that heavy ion bombardment of U-Mo/Al dispersion fuel allows to simulate the effects of radiation damage during in-pile irradiation. Heavy ion bombardment avoids (strong) activation of the specimens. They may therefore be readily examined in simple laboratory experiments. We report further progress in refinement and application of this technique. The behaviour of U-Mo/Al dispersion fuel during heavy ion bombardment under temperatures below 100°C was investigated. In contrast to irradiation experiments with heavy ions, which were conducted under temperatures of ~200°C some time before, the sample broke apart. SEM pictures show a large interdiffusion layer around every UMo particle. EDX data of the examined sample will be given.

1. Introduction

For the conversion of research reactors operating with highly enriched Uranium to fuel of lower enrichment a high density fuel is required. One option for conversion is the development of UMo/Al dispersion fuel with a Uranium density of at least 8g/cc [1,2]. However, during in-pile irradiation of this fuel, growth of an undesired interdiffusion layer (IDL) was observed [3,4]. It was shown that bombardment of nuclear fuel specimens with heavy ions produces effects comparable to those after in-pile irradiation [5]. Especially the growth of an IDL around UMo particles inside an aluminium matrix was observed after bombardment with I-127. It was shown that this IDL is comparable to the one observed after in-pile irradiation [6]. We continued bombardment of UMo/Al dispersion fuel at MLL in Garching. The most recent results are presented in this paper.

2. Experimental setup

The samples contains atomized U10Mo inside a pure aluminium matrix. All samples were cut out of miniplates provided by Argonne National Lab and polished before irradiation. Sample size was 3x7.6mm²x300µm.

The samples were irradiated at the tandem accelerator of the Maier-Leibnitz Laboratory (MLL) in Garching, Germany. We used I-127 at 80MeV for irradiation. The incident angle between the ion beam and the sample surface was 60°. The size of the beam spot was ~3x3mm². The sample temperature was monitored during irradiation by a thermocouple and did not exceed 100°C. The irradiations were carried out under a vacuum of ~1x10⁻⁷mbar. The total integral fluency was ~1x10¹⁷ ions/cm². The penetration depth of 80MeV I-127 ions in UMo is ~6.5µm respectively ~16.5µm in Al. This results in an ion density of at least 1.6 10²¹ ions/cm³ in UMo and 6 10²⁰ ions/cm³ in Al. Due to the high kurtosis of the range of heavy ions in matter, the ion density is even larger in certain depths. This means, that at least the final fission density of FRM II (2.1 10²¹ fissions/cm³) was reached [7].

After the irradiation light microscope and scanning electron microscope pictures were taken. Also a qualitative and quantitative analysis of the isotope distribution at certain points of the sample was performed using EDX technique.

3. Results

After irradiation the sample was very brittle and deformed. It broke apart during handling (Fig. 1). Optical inspection revealed that a large IDL grew around the UMo particles inside the area hit by the ion beam (Fig. 2). Electron microscopy shows a large, asymmetric IDL around every UMo particle hit by the ion beam (Fig. 3,4). Smaller grains were completely consumed (Fig. 5). No IDL was found around UMo particles which had not been hit by the ion beam. (Fig. 6).

EDX data were taken on the marked points on Fig.3-6. Results are given in Tab.1-4. It was found, that the composition of the IDL is aluminium rich and approximately the same in all examined positions (~20at%U, ~3at%Mo, ~77at%Al). The composition of the unaffected UMo core (Fig.3,4) respectively the unirradiated UMo grain did not change.

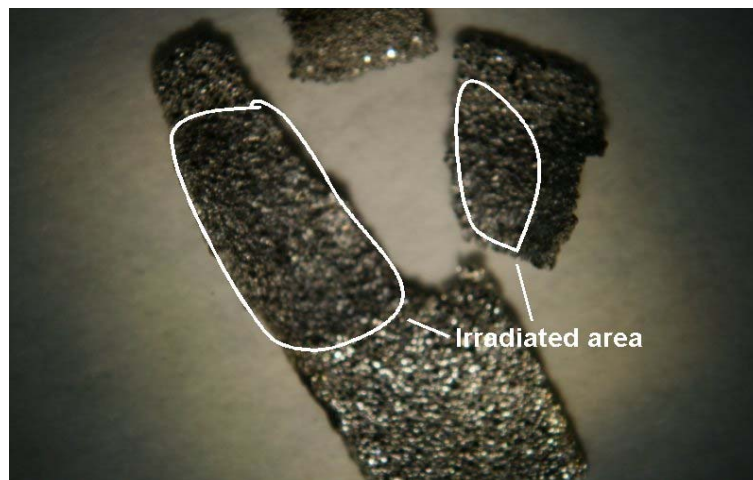


Fig. 1: Optical image of the examined sample. It is very brittle and broke apart after irradiation. The irradiated area is marked white.

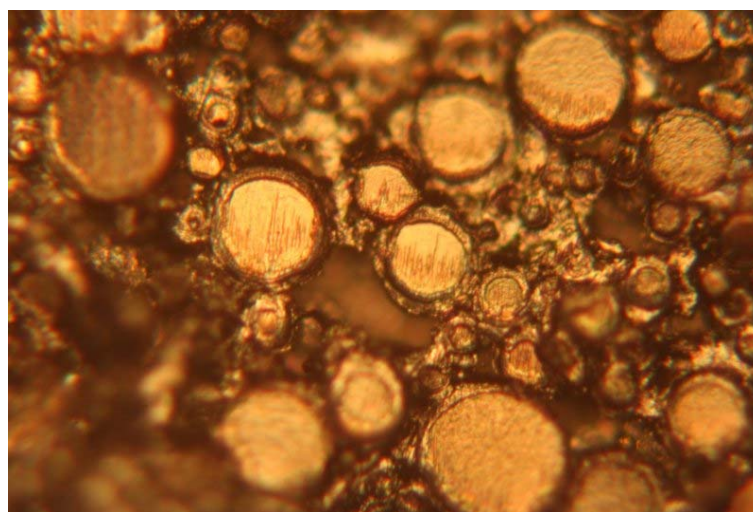


Fig. 2: Optical microscopy of the irradiated area. An IDL around the UMo grains is visible.

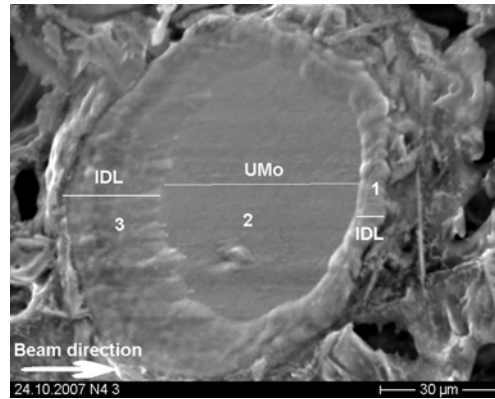
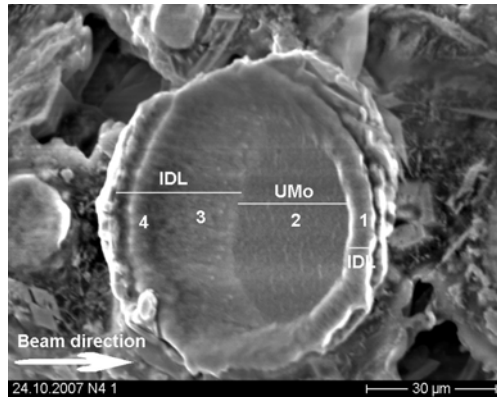


Fig 3 (left) Fig 4 (right): SEM image of UMo grains which were directly hit by the ion beam.

The incident beam direction is marked in the pictures. A large, asymmetric IDL around a remaining UMo core is visible. The asymmetry of the IDL is associated to the direction of the incident beam. EDX measurements were taken at the marked positions. Figures are given in Tab. 1 and Tab. 2.

Position	U [at%]	Mo [at%]	Al[at%]
1	20.9	2.8	76.3
2	88.3	11.7	0
3	24.3	3	72.7
4	20.5	0.8	78.8

Tab. 1

Position	U [at%]	Mo [at%]	Al[at%]
1	17.8	3.1	79.1
2	87.7	12.33	0
3	18.92	3.1	78

Tab. 2

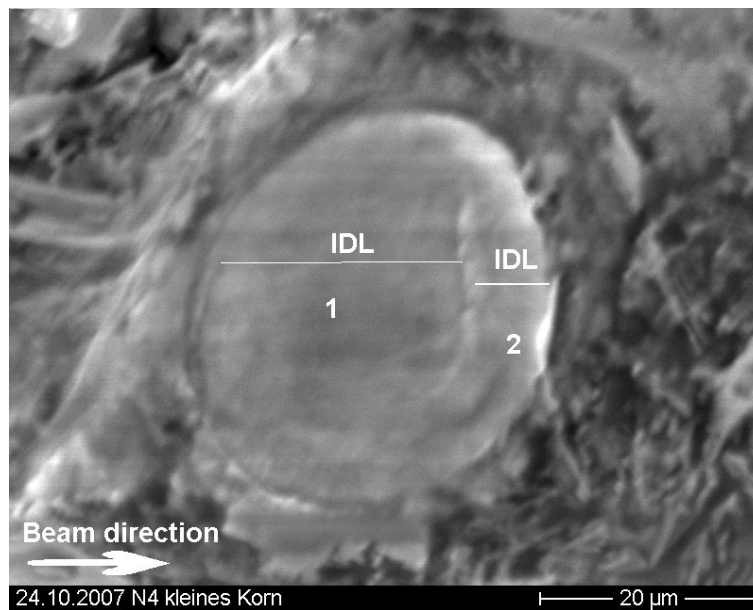


Fig. 5: SEM image of a small grain. It has been completely consumed by an asymmetric IDL.

EDX data were taken on positions 1 and 2, see Tab. 3.



Fig. 6: SEM image of a not irradiated UMo grain. No IDL is visible. EDX data was taken on position 1, see Tab. 4.

Position	U [at%]	Mo [at%]	Al[at%]
1	18.6	3	78.4
2	17.7	2.1	80.1

Tab. 3

Position	U [at%]	Mo [at%]	Al[at%]
1	87.7	12.3	0

Tab. 4

4. Conclusion and Outlook

For the first time UMo/Al samples were irradiated by heavy ions up to a fluency which corresponds to fission densities typically reached during the burn up of such fuel in research reactors. SEM pictures and EDX data were taken on several points on the sample. It was found, that the composition of the IDL (~20at%U, ~3at%Mo, ~77at%Al) does not change significantly on different positions on the irradiated area. The composition of the IDL is in good agreement with values found after in-pile irradiation tests [8].

It is planned to examine the crystal phases contained in the IDL using XRD. Further heavy-ion bombardment experiments are scheduled.

5. Acknowledgments

We would like to thank G.L. Hofman and J.L. Snelgrove from ANL for provision with samples.

6. References

- [1] A. Röhrmoser, W. Petry, K. Böning, N. Wieschalla, *Reduced Enrichment Program for the FRM II*, RERTR Vienna, Austria, 2004
- [2] A. Röhrmoser, W. Petry, K. Böning, N. Wieschalla, *Increasing Depletion*, Nuclear Engineering - International Magazine, 10. December 2004
- [3] G.L. Hofman, M.R. Finlay, Y.S. Kim, *Post-irradiation analysis of low enriched U-Mo/Al dispersion fuel miniplate tests*, RERTR 4&5, RERTR Vienna, Austria, 2004
- [4] P. Lemoine, J.L. Snelgrove, N. Arkhangelsky, L. Alvarez, *UMo dispersion fuel results and status of qualification programs*, 8th RRFM Meeting, Munich, Germany, 2004
- [5] D.G. Walker, *The simulation of fission damage in U₃Si*, Journal of nuclear materials 37, p. 48-58, 1970

- [6] **N. Wieschalla, A. Bergmaier, P. Böni, K. Böning, G. Dollinger, R. Grossmann, W. Petry, A. Röhrmoser, J. Schneider**, *Heavy ion irradiation of UMo/Al dispersion fuel*, Journal of nuclear materials 357, p. 191-197, 2006
- [7] **N. Wieschalla**, *Out-of-pile examination of the high density U-Mo/Al dispersion fuel*, Dissertation at TUM, Munich, Germany, 2006
- [8] **A. Leenars, S. Van den Berghe, E. Koonen, C. Jarousse, F. Huet, M. Troabas, M. Boyard, S. Guillot, L. Sannen, M. Verwerft**, *Post-irradiation examination of uranium-7wt% molybdenum atomized dispersion fuel*, Journal of nuclear materials 335, p. 39-47, 2004

MANUFACTURING OF THICK MONOLITHIC LAYERS BY DC-MAGNETRON SPUTTERING

W. SCHMID, R. JUNGWIRTH, W. PETRY
*Forschungsneutronenquelle Heinz Maier-Leibnitz, Technische Universität München
Lichtenbergstrasse 1, 85747 Garching – Germany*

P. BÖNI
*Physik Department E21, Technische Universität München
James-Franck-Strasse, 85747 Garching – Germany*

L. BECK
*Maier-Leibnitz-Laboratorium (MLL)
Am Coulombwall, 85748 Garching – Germany*

ABSTRACT

Magnetron sputtering is a well-known and widely used process in microelectronics to grow thin layers of sub-micrometer scale on different substrates. We want to use this process to manufacture U-Mo foils and U-Mo fuel plates with Al cladding.

In first attempts we demonstrate, that growing mono and multilayer structures with a thickness of several hundred micrometers from different metals and alloys is possible without difficulty. In further experiments we successfully manufactured full size test foils and plates with copper as meat replacement and Al cladding. At the moment we prepare the manufacturing of first U-Mo / Al structures.

1. Motivation

Over the next years many research reactors, which currently use Highly Enriched Uranium (HEU), are supposed to be converted to Low Enriched Uranium (LEU). Monolithic LEU U-Mo fuel is a most promising fuel material to convert several of these research reactors [1]. Unfortunately it was not possible so far to produce full size fuel plates from monolithic U-Mo, because the demanding mechanical and metallurgical properties of the materials to be used make common processing techniques hardly applicable [2,3].

A new approach to solve this problem is the use of DC-magnetron sputtering [4]. Sputtering is a commonly used process for growing metal layers on a micrometer or sub-micrometer scale on different substrates. The sputter deposited layers provide excellent substrate adhesion and high density [5]. In contrast to thermal vacuum deposition methods the sputtering process will not change the composition of the deposited materials, because it is independent of the vapour pressure of the materials being used.

We intend using this technique in a first step to grow a massive full size meat layer of U-Mo. In a second step, sputtering will be used to surround the meat layer with several ten micrometers of Al as pre-cladding. The resulting U-Mo / Al sandwich structure will then be further processed by common and more economic welding, rolling or hot pressing techniques to finalize the Al cladding and thus to produce a full size fuel plate.

2. Setup

For this purpose a DC magnetron sputtering plant was built (figure 1). The dimensions of the apparatus were chosen to enable the production of samples with a size of 700 x 65 mm², which corresponds to the size requirements of the currently used FRM II fuel plates [6,7]. A 15 kW self-adjusting DC-power supply provides up to 800 V and 30 A for maintaining the plasma for the sputtering process. The racetrack on the target to be sputtered is defined by means of more than 300 magnets providing a magnetic field of 1.43 T at the surface. The magnets are mounted closely-above the target inside the copper block that acts as the cathode. The base pressure in the vacuum chamber is 510⁻⁶ mbar. The argon working pressure during the sputtering process can be regulated by a flow controller to within typically 1·10⁻³ to 110⁻¹ mbar. The substrate carrier and the sputtering target are water cooled and their temperature is monitored. The whole process volume is surrounded by an aluminum shield to prevent a coating of the vacuum vessel.

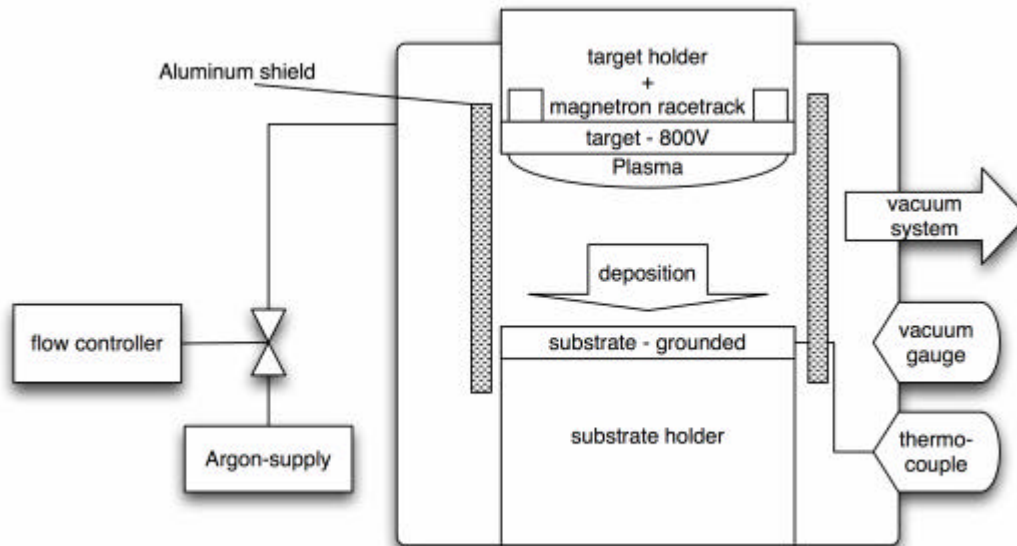


figure 1: Scheme of the used DC magnetron sputtering plant.

3. Test of the sputtering plant

In preliminary tests the deposition of different metals (Cu, Al, Zn) and alloys (brass, stainless steel) on Al and stainless steel substrates for process pressures between 110⁻³ and 1 mbar was studied. Achievable plasma current and deposition rate were determined for each material in the given pressure range. The temperature evolution of target, substrate, shield, magnets and cooling water was monitored. As a result we succeeded to obtain the useful range of each parameter defining the sputtering process providing a guideline for further deposition experiments. As most important limiting factors for the deposition rate and therefore for the process speed we identified the heat removal from the target and the maximum voltage provided by the DC- power supply.

Based on these efforts we tried to deposit very thick layers of size 700 x 65 mm² to examine the general feasibility of depositing metal foils and blank sheets. We were able to produce monolayers of 50 – 150 μm thickness (foils) from stainless steel (Fe + Co) and Al, which have

a sputtering yield similar to that of U and Mo [5], as well as from Cu and brass (Cu + Zn). For thicker deposits (blank sheets) we decided to use Cu as target material exclusively to speed up the deposition process and to have a better optical contrast between substrate and deposited material during examination. In about 40 hours we succeeded to deposit Cu layers with a thickness of up to 1300 μm (figure 2(a)).

The deposits had an elasticity and strength that was similar to industrial bulk material. However, the layers showed a gradient in thickness from centre to the edges of up to 50% of the maximum in length and of up to 20% in width. Therefore all thickness values given are maximum thickness values at the centre region.

The reason for the thickness gradient in width is the shape of the magnetron racetrack, which forces both the process plasma and the target erosion zone into an elongated toroidal geometry. As the magnetron racetrack is immobile, superposition of material fluxes from opposite sides of the erosion zone leads to a cosine shaped deposition profile along the width of the substrate with a maximum at the centre of the film. The gradient along the long dimension of the film is caused by gaps in the racetrack of the magnetron, which are necessary to mount the magnetron plate within the cathode. Each gap is equivalent to a missing magnet in the racetrack and causes inhomogeneities in the magnetic field, which decreases locally the confinement of the plasma and the erosion at the short sides of the target significantly. The superposition of the flux of material is, however, negligible here.

Finally we produced multilayer structures to show the feasibility of our two step production procedure mentioned in the first paragraph. For the inner layer again Cu was chosen, as the material will not influence the layer growth or the adhesion. For the outer cladding layer we have chosen Al. We were able to produce a multilayer structure of 300 μm thick Cu surrounded by 40 μm of Al (figures 2(b), (c)). Again the deposits were as stable as industrial foils made from bulk material. The Al cladding showed a good adhesion to the Cu layer. Thickness gradients occurred as expected.

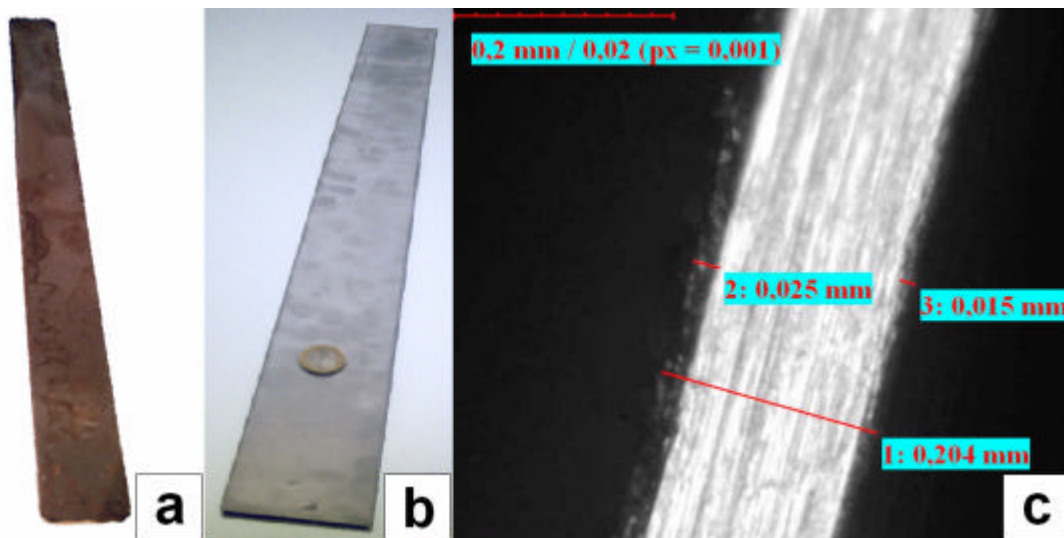


figure 2:

(a) Sputtered blank sheet of Cu with a thickness of 1300 μm and a size of 700 x 65 mm^2 .

(b) Sputtered multilayer foil from Cu with Al cladding, size 700 x 65 mm^2 .

(c) Microscopy image of a cross section of the multilayer structure shown in figure b. The examined intersecting plane is about 10 cm from the short side of the sputtered foil. Here the inner Cu layer has a thickness of 200 μm , the Al cladding has on one side a thickness of 15 μm and on the other side a thickness of 25 μm .

4. Conclusion

Our tests demonstrate that it is possible to deposit different metals and alloys as blank sheets and foils of 700 x 65 mm² size and several hundred micrometers thickness by DC-magnetron sputtering. We also showed, that it is possible to clad these structures in a second step with several tens of micrometers of Al using sputtering.

We plan to repeat the sputter process to fabricate blank sheets of depleted UMo and clad them with AlFeNi. Therefore sputter targets of each of these materials were ordered and obtained in winter 2007. The sputtering plant was installed inside a glove box and is right now prepared for the use of UMo. We expect the first UMo deposition tests to begin in April 2008.

5. References

- [1] A. Travelli, *Status and Progress of the RERTR Program in the year 2004*, RERTR Vienna (2004)
- [2] C. Jarousse, *AREVA-CERCA's UMo fuel plates developments*, RRFM Hamburg (2008)
- [3] C. R. Clark, *Monolithic fuel plate development*, RERTR Chicago (2003)
- [4] N. Wieschalla, P. Böni, *New manufacturing technique for U-Mo monolithic*, patent reference no. DE 10 2005 055 692 (2005)
- [5] H. Frey, G. Kienel, *Dünnschichttechnologie*, VDI Verlag (1987)
- [6] K. Böning, W. Petry *FRM II Test irradiations of full sized U₃Si₂-Al fuel plates up to very high fission densities*, to be published (2008)
- [7] A. Röhrmoser, W. Petry, N. Wieschalla, *Reduced Enrichment Program for the FRM II*, RERTR Vienna (2004)

THE EFFECT OF FUEL BURN-UP FOLLOWED BY ANNEALING ON CHANGES IN STRUCTURE AND STRUCTURAL PARAMETERS OF U-9% Mo DISPERSION FUEL

?.?. GOLOSOV, ?.S. LYUTIKOVA, V.B. SEMERIKOV, ?.?. TEPLYKH
Institute of Nuclear Materials
Zarechny, Sverdlovsk region, Russia, 624250

ABSTRACT

A performance capability of the U-Mo/Al dispersion fuel depends on a stability of fuel composition and a condition of its components. It was found that the structure of the fuel particles and matrix were changing during a fuel operation life and new phases were observed to form in the fuel. In order to predict the safe operation life-time of fuel elements with the U-Mo/Al dispersion fuel under irradiation the relationships of the changes in the structure-and-phase condition of the components of the dispersion fuel as dependent of burn-up and temperature were studied.

This paper presents the results of the study on the effect of fuel burn- up of 33 to 97 % and the following annealing in the range of 150 to 580 °C on the changes in the structure and structural parameters of the phases of the U-9%Mo/Al dispersion fuel after its operation life in the full-size fuel elements of the IVV-2M reactor.

1. Introduction

A performance capability of the fuel elements with the U-Mo/Al dispersion fuel depends on a stability of fuel composition and a condition of its components. It was found from the experimental studies that the structure of the fuel particles and that of the Al matrix were changing under irradiation and new phases, including gas pores, were observed to form. These changes are a complex function of temperature, fission rate and burn-up of the fuel. Therefore in order to predict a safe-operation life-time of the fuel elements with the dispersion U-Mo/Al fuel one needs to know the relationships of the changes in the structure-phase condition and structure parameters of the dispersion fuel components as dependant on burn-up and temperature. The results of the study on the effect of fuel burn-up and that of the temperature of the following annealing on the changes in the phase composition of the U-9% Mo/Al dispersion fuel are presented in ref. [1].

This paper presents the results of the study on the changes in the structure parameters of the components of the U9% Mo/Al dispersion fuel as irradiated to different burn-ups from 33 to 97 % and after annealing during 1 hour within the temperature range from 150 to 550-580 °C in the IVV-2M reactor (Zarechny), for the study the neutron diffraction method was used.

2. Materials and methodology of the experiments

For the experiments the plates of the size 40x8x1.3 mm were cut out of the fuel elements at different positions in the core; the fuel elements were taken from the combined fuel assemblies designated as G93 and G94, which had been irradiated in the IVV-2M reactor to reach a mean equivalent burn up of 40 and 80 % [2], respectively. The specimens are characterized by the data in Table 1. The specimen G98 was taken from the area directly adjacent to the place of bulging formation in the claddings. In the fuel meat of specimen G98 there were both individual gas pores and their coalescences as well as small cracks up to 1.5-2 mm long.

The neutron diffraction experiments were carried out at the IVV-2M reactor, Zarechny. The experimental data were obtained for an angle interval from 5° to 105° by 2θ with a spacing of 0.1° . The experiments were performed in two stages. At the first stage the spectra were obtained for all the specimens. At the second stage three specimens (G96, G98 and G99) underwent stepwise annealings within temperatures T_{an} from 150 to 550-580 °C with a step of 50 °C, annealing time was 1 hour. Neutron diffraction patterns were obtained after each annealing.

Table 1: Specimens data

specimen #	Assembly #	Bu ¹⁾ , %	f, 10 ¹⁴ f·m ⁻³ ·s ⁻¹	?, 10 ²¹ f.cm ⁻³	? _{BOL} , %	q _{BOL} , W·cm ⁻²	IL ²⁾ , μm	Volume fraction of phases in a specimen, %			
								Al	U-Mo	IL	Al _{FP} ³⁾
G13	?? 003	32.9	2.6	2.1	43.5	48	1.2	87.0	12.1	0.9	13.4
G100	?? 003	51.1	4.5	3.8	61.4	80	3.6	85.6	11.6	2.8	14.2
G96	?? 004	55.1	3.1	4.1	48.6	66	3.5	85.7	11.6	2.7	14.2
G97	?? 004	96.3	5.5	7.2	77.2	115	11.3	80.7	10.1	9.2	16.9
G98	?? 004	96.9	5.7	7.3	85.3	118	11.2	80.8	10.1	9.1	16.8
G99	?? 004	78.4	4.6	5.9	86.4	95	9.0	82.3	10.5	7.2	16.0

¹⁾ equivalent burn-up;
²⁾ a thickness of the layer (U,Mo)Al_k;
³⁾ an aluminum matrix damaged by fission fragments.

3. Results and discussion

3.1. Effect of burn-up

A change in a λ (U,Mo) lattice parameter against fuel burn-up is plotted and the structure of fuel particles corresponding to the conditions of the specimens is shown in Figure 1.

According to data in Fig.1. there are three regions, where the λ (U,Mo) lattice parameter changes with burn-up but a manner of parameter changing is different. In the first region this parameter increases with the burn-up changing from 0 to 50 %; the burn-up being within 33 to ~55 % the parameter increases with a rate of $\sim 3.9 \cdot 10^{-4}$ Å per 1% of the burn-up. In the second region, where burn-up is from 50 to 75 %, the lattice parameter practically does not change. In the third region, where burn-up is higher than 75 %, the parameter decreases reaching the values relevant to an unirradiated condition of the specimens.

The change in the λ (U,Mo) lattice parameter correlates with the change in the fuel structure. At Bu= ~ 50 % gas pores are practically absent in the fuel structure (specimens G13 and G96). An increase of burn-up to ~ 75 % leads to a formation of gas pores (G99). A further increase of burn-up to ~ 95 to 97 % results in an increase of both the quantity and the sizes of pores (specimens G97 and G98).

The analysis of the above data shows that:

- the λ (U,Mo) lattice parameter increases when there are no gas pores in the fuel structure,
- the λ (U,Mo) lattice parameter practically does not change with burn-up when gas pores are forming in the fuel particles,
- the λ (U,Mo) lattice parameter decreases dramatically with burn-up $>75\%$ when the gas pore sizes increase and the pores are forming in large quantities in the fuel particles.

The changes in the Al lattice parameter against burn-up are plotted in Fig. 2. Similar to the dependence of the λ (U,Mo) lattice parameter changes there are also three regions where the Al lattice parameter changes proceed in a different manner. However, in this case the first region, which corresponds to the increasing Al lattice parameter, has a larger range and extends up to the region corresponding to ~ 75 % burn-up and in the range of 33 to ~ 75 % the parameter changing rate for the specimens is $(2-2.7) \cdot 10^{-4}$ Å per 1% burn-up. In this burn-up range a formation of gas pores in the Al matrix structure was not detected as well as in the matrix layer around the fuel particles, which was damaged by fission products (Fig. 2*b-d*).

In the second region in the burn-up range of ~ 75 to ~ 95 % the Al lattice parameter does not practically change and individual gas pores are formed at the interface «IL-Al matrix» (Fig. 2*e*) in the Al matrix structure.

When burn-up is more than ~ 95 % the Al lattice parameter starts to decrease; and in the fuel meat along with the individual gas pores the coalescences of these pores and small cracks of 1.5 to 2 mm (Fig.2*f*) are present.

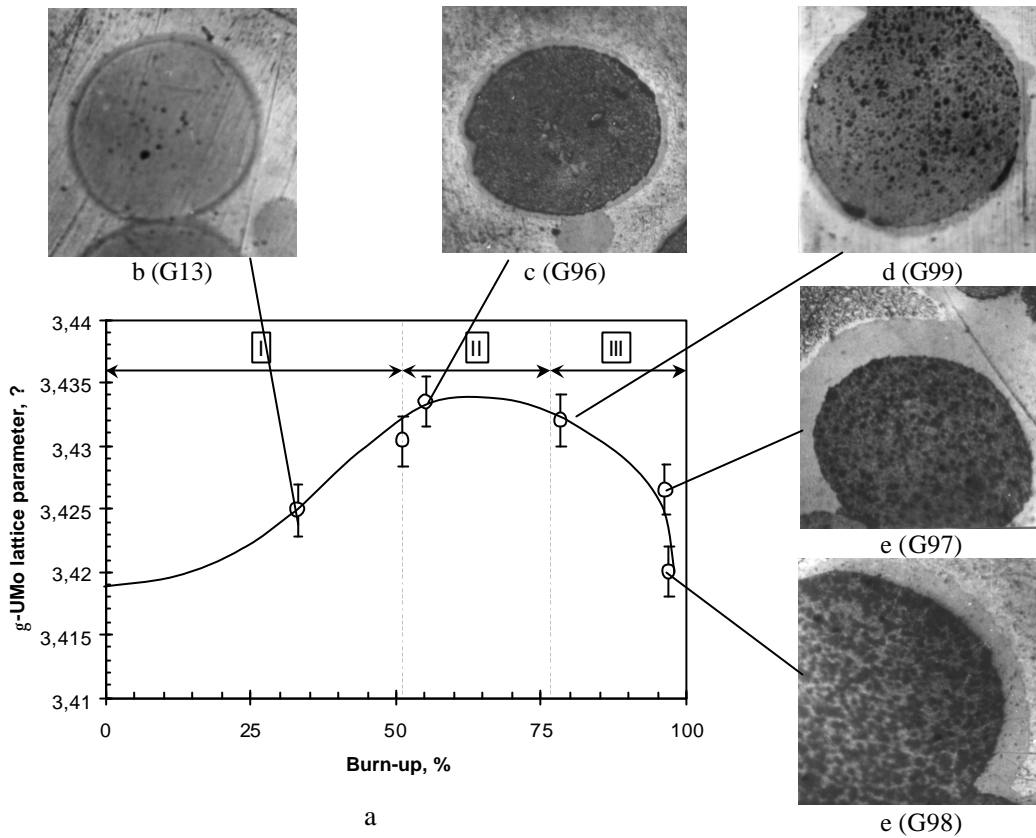


Figure 1: Changes in the U-Mo alloy lattice parameter against fuel burn-up (a); the fuel structure of the specimens G13 (b), G96 (c), G99 (d), G97 (e) and G98 (f) as irradiated.

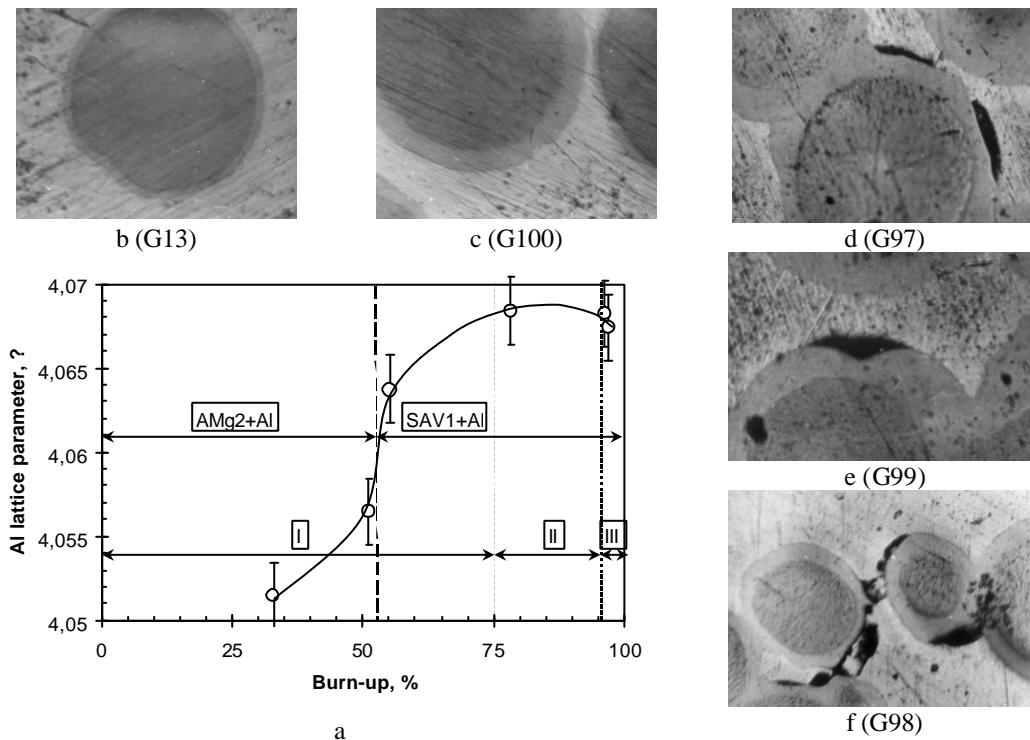


Figure 2: Changes in the Al lattice parameter against fuel burn-up (a); the structure of the fuel meat of the specimens G13 (b), G100 (c), G96 (d), G97 (e) and G98 (f) as irradiated.

3.2. Effect of annealing temperature

In Fig.3 the annealing temperature dependence of the changes in the lattice parameter of both γ -(U,Mo) and Al are shown for the specimens G96, G98 and G99, which have different fuel burn-ups. In all these specimens the lattice parameter of both γ -(U,Mo) and Al is decreasing monotonously within the whole range of the annealing temperature changes. However, the manner of the parameter changing of both phases against the annealing temperature was different in these specimens due to the difference in their burn-up values.

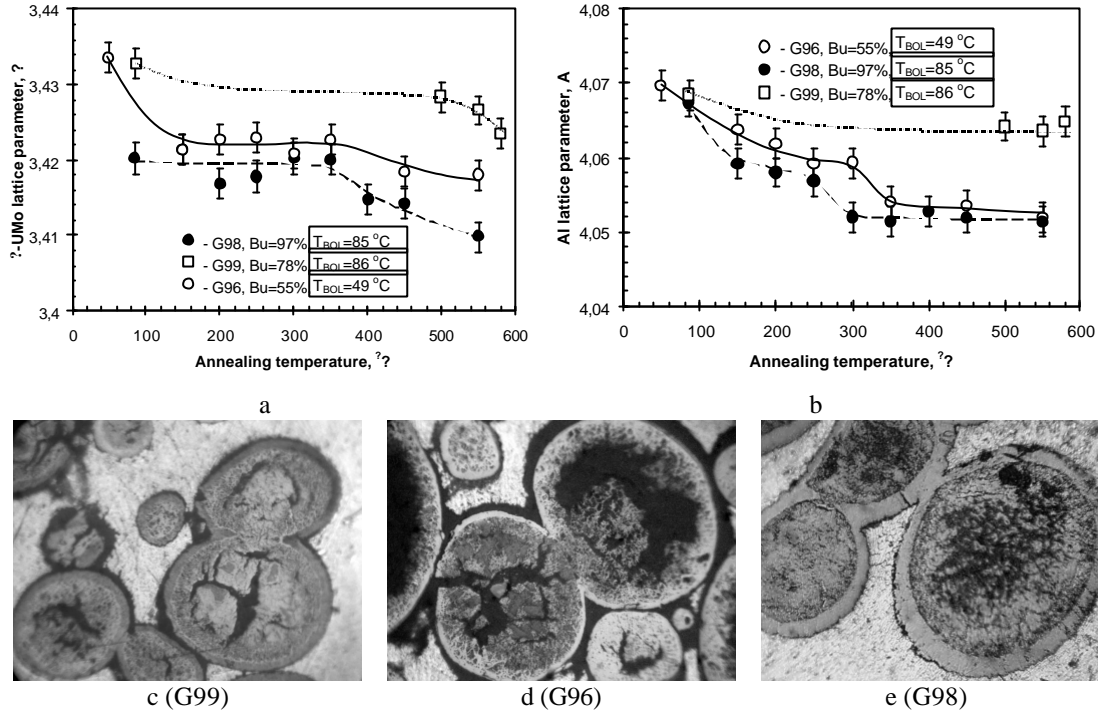


Figure 3: Influence of annealing temperature on changes in the lattice parameter of both γ -(U,Mo) (γ) and Al (β) and in the fuel meat structure of the specimens G99 (c), G96 (d) and G98 (e)

The highest decrease of the γ -(U,Mo) lattice parameter is observed in G96, whose burn-up is lower (Bu=55 %). This decrease proceeds in two stages (Fig. 3.a): first after the annealing of the specimen at 150 °C and then after the annealing at 400 °C. The first stage of the decrease in the γ -(U,Mo) lattice parameter is probably due to the annealing of radiation defects in the material of the fuel particles and the second stage is due to the precipitation of gas fission products from a solid solution and the formation of large gas pores (Fig. 3.d).

The specimen G98 with the highest fuel burn-up (Bu=97 %) reveals only one stage of the γ -(U,Mo) lattice parameter decrease, this stage begins at ~400 °C. The first stage was absent seemingly because the annealing of radiation defects in the fuel particles had taken place under irradiation conditions. This decrease of the γ -(U,Mo) lattice parameter of G98 at annealing temperature higher than 400 °C is also due to the formation of larger gas pores in the structure of the fuel particles (Fig. 3.e).

The annealing of G99 with Bu=78 % started at temperature 500 °C, which was higher than the T_{an} of G96 and G98, and the decrease of the γ -(U,Mo) lattice parameter in G99 was less, which was probably because the effect of the total temperature on G99 was less than that on G96 and G98. However, in this case large gas pores also formed and initiated cracking (Fig. 3.c) in the fuel particles.

Contrary to the changes in the γ -(U,Mo) lattice parameter the Al lattice parameter decrease in all the specimens (except G99, whose annealing began at higher temperature) proceeded in two stages (Fig. 3.b). The peculiar feature observed for the 97% burn-up G98 were the temperatures of the beginning and end of both stages which were less by ~50 °C than those observed for the 55% burn-up G96. This difference is probably due to a higher concentration of fission products in the Al matrix of G98 as

compared to G96. The decrease in the Al lattice parameter at the first stage for these specimens was caused not only by the radiation defects annealing but, probably, also by a gas pores nucleation as Genie-Preston zones, which were revealed in [3]. The decrease of the lattice parameter at the second stage (as is the case with the fuel particles) is explained by the precipitation of gas fission products from the solid solution and formation of gas pores. However, in this case the formation of gas pores is localized at the interface «(U,Mo)Al_x layer - Al matrix» (Fig.3c-e).

4. Conclusions

The effect of irradiation at fuel burn-ups from 33 to 97 % followed by annealing at temperatures from 150 to 550 °C on the changes in the structure and lattice parameter of the phases γ -(U,Mo) and Al of the U-Mo/Al dispersion fuel in the assemblies “003” and “004”, irradiated in the IVV-2M reactor at initial temperatures of the fuel cladding ~44 to 86 °C and average fuel fission rates within $2.6 \cdot 10^{14}$ to $5.7 \cdot 10^{14}$ f·cm⁻³·s⁻¹ was investigated.

The investigation revealed three regions, where the lattice parameters of γ -(U,Mo) and Al were changing with fuel burn-up. They are as follows:

- In the first region of the fuel burn-up the lattice parameter increases, the interval of the change in the γ -(U,Mo) lattice parameter is within 0 to ~50 % fuel burn-up and that of the Al lattice parameter is within 0 to ~78 % burn-up. The rate of changing in γ -(U,Mo) lattice parameter is $(3.9) \cdot 10^{-4}$ Å per 1% burn-up and that of Al lattice parameter is $(2-2.7) \cdot 10^{-4}$ Å per 1% burn-up.
- In the second region of the fuel burn where the intervals are from 50 to 75 % for γ -(U,Mo) and from ~75 to 95 % for Al the lattice parameters of both phases do not practically change.
- In the third region of the fuel burn-up being > ~75 % for γ -(U,Mo) and > ~95% for Al the decrease of the lattice parameter of both phases is observed.

It was found that the change in the lattice parameter of both phases was due to the changes in their structure, accumulation of the radiation defects and fission products. It was assumed that the increase of the lattice parameter in the first region of burn-up is due to the accumulation of radiation defects and fission products in the solid solution of both phases. A stability of the lattice parameters of both phases is attributed to the precipitation of the gas fission products from the solid solution and the formation of gas porosity in the fuel particles and Al matrix. The decrease of the lattice parameter of both phases in the third region is attributed to the intensive formation of gas pores and their coalescences as compared to the accumulation of the fission products in these phases.

It was revealed that the irradiated U-Mo/Al dispersion fuel annealed within the range 150 to 550 °C resulted in the decrease of the lattice parameter of both γ -(U,Mo) and Al. The decrease of the γ -(U,Mo) lattice parameter depends on burn-up value; and the decrease in the specimen with ~55 % burn-up proceeds in two phases, the decrease in the specimen with ~97 % has only one phase. The Al lattice parameter decreases with the annealing temperature in two stages irrespective of the burn-up value. The decrease of the lattice parameters of both phases at the first stage of the annealing is attributed to the annealing of the radiation defects in the material of the fuel particles, the Al claddings of the fuel elements and matrix, and specially for the Al phase it is attributed to the formation of gas pores nucleation, i.e. Genie-Preston zones. The decrease of the lattice parameter of both phases at the second stage of the annealing is due to the precipitation of the gas fission products from the solid solution in the material of the fuel particles and Al matrix with the gas porosity to form in them.

5. References

- [1] Golosov O.A., Semerikov V.B., Teplykh A.Ye. et al. Investigation of the U-Mo dispersion fuel structure after irradiation and isochronal annealing in the temperature range of 150-580 °C using the neutron diffraction method // 11th Int. Mtg. RRFM'2007, Lyon (France), 11-14 March, 2007.
- [2] Golosov O.A., Lyutikova M.S., Semerikov V.B. et al. The results of studying uranium molybdenum fuel elements irradiated in the IVV-2M reactor to high burn-up values // 9th Int. Mtg. RRFM'2005, Budapest (Hungary), 10-13 April, 2005.
- [3] Golosov O.A., Semerikov V.B., Bogdanov S.G. et al. Small angle neutron scattering by U-9%Mo/Al dispersion fuel irradiated to high burn-ups // 29th Int. Mtg. RERTR'2007, Prague (Czech Republic), 23-27 September, 2007.

Zircalloy effect on the LEU fuel enrichment of the Syrian MNSR

M. Albarhoum

Department of Nuclear Engineering, Atomic Energy Commission, P. O. Box, 6091,
Damascus- Syria

Abstract:

The use of Zircalloy instead of Aluminum alloys in MNSRs would improve the initial excess reactivity of the reactor and lower the enrichment required for the core conversion. Different components in the core may be made of Zircalloy. The upper and lower fuel grids would save about 0.13% enrichment. Other savings can be obtained supposing the shim tray and the frames to be made of Zircalloy. The total savings of the major components of the reactor would be about 0.60% of the fuel enrichment.

KEYWORDS

Reactor, MNSR, Comparison, LEU, HEU, Fuel, Core.

1. Introduction

Some studies have been performed on the conversion of the core of the Syrian MNSR [1-4]. These studies considered some fuel types like the dispersion ones in general (U-Al_x-Al) [2-4], besides to UO₂ fuels [1]. The general conclusion for the dispersion fuel types was that these fuels had low densities so that special configurations of the core should be used (the reflector characteristics are essential to the adjustment of the initial excess reactivity). Another configuration has been considered [4] in which a mixed fuel (some rods contain HEU fuel, and others containing LEU fuel) was employed. In the case of the UO₂ fuel, different results were obtained [1,5]. In a previous work of some colleagues [1] a UO₂ fuel with 5.45 g content of ²³⁵U/fuel element was used. The paper indicated a configuration in which only 199 fuel elements were necessary to have about 4.579 mk for the initial excess reactivity. In other works [5] two types of UO₂ were considered: the UO₂ as a dispersed fuel, and a ceramic pellet fuel fabricated by Zircatec (CANADA). These works considered the use of zircalloy only as a clad material. In the RERTR-2007 it has been suggested to consider the effect of the other components of the reactor when are made of zircalloy instead of aluminum. In the following this option will be considered in detail.

2. Methodology

Since the approach to the calculations of a new fuel would require principally the quantity of uranium and the total number of fuel elements it would be convenient to adopt a model of the reactor (and in particular of the core) that considers the conservation of matter in the core rather than a very detailed model in which the single pins are described.

A rather complete model of the reactor has been constructed (see Fig. 1). The reactor is formed of the core (central gray zone), the annulus reflector (side purple

zone), the bottom reflector(bottom purple zone), the tank wall(external blue zone), the internal irradiation sites (two parts: the yellow zones inside the annulus reflector and the underlying dark purple zones), the upper grid (brown zone at the upper end level of the annulus reflector), the shim tray base (dark purple zone lying above the upper grid with a thin layer of water in between, and the control rod (the black zone in Fig.1).

Other, but less important components like the upper, bottom, and lateral frames are considered too. The Codes WIMSD4 [6] and CITATION [7] are both used here as a cell and core-calculation codes, respectively. The same number of neutron groups and the same limits of these groups, which pertain to the previous models [9], are adopted here.

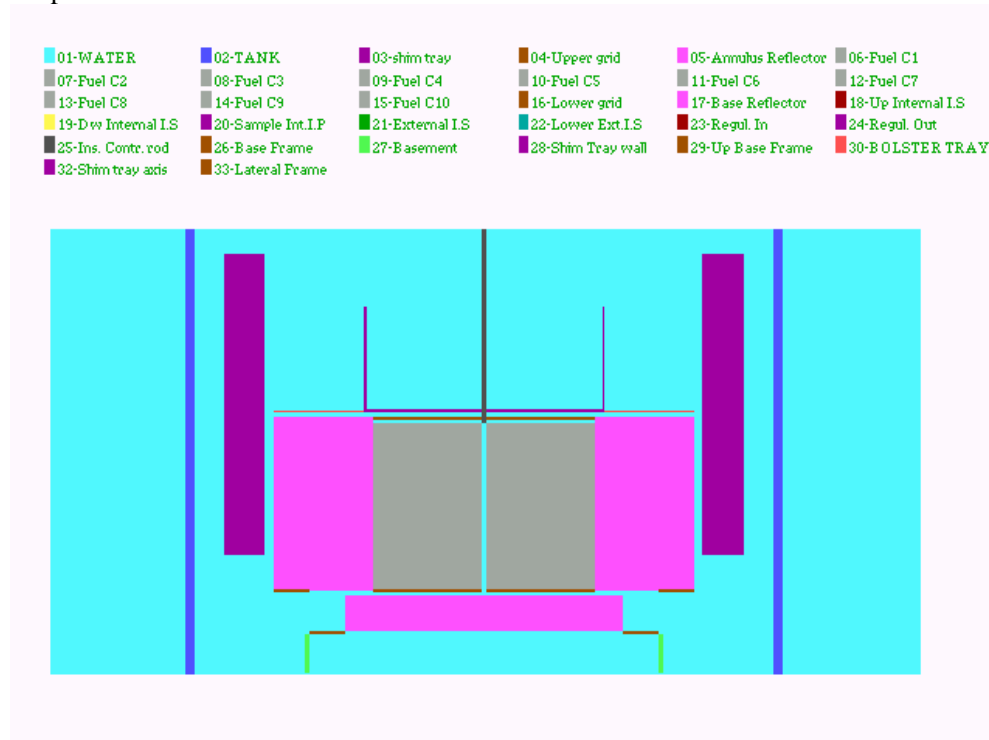


Fig. 1 . The model of the Syrian MNSR used for the core calculations.

3. Results and Discussion

Using the above-described model for the Syrian MNSR the following parameters would be found (see Tab. 1) for the actual reactor using HEU fuel.

There are 3 dummy elements made of aluminum having the same external diameter of the fuel rods plus other 4 tie rods connecting the upper and lower grids. They are made of aluminum too.

This model produces data which have a fairly good agreement with the experimental ones [8] (the thermal flux in the internal irradiation site is $\sim 1.10^{12}$ n/cm².s, and the initial excess reactivity of the reactor is ~ 3.94 mk). The type of fuel is obviously a dispersion one.

Table 1. The reactor parameters resulting from the above-mentioned model.

Flux in the Internal Irradiation Sites (*10 ¹²)				Initial Excess reactivity (mk)	Fuel Type	No. of Fuel rods	No. of Dummy elements	No. of Tie Rods
Group 1	Group 2	Group 3	Group 4					
0.195	0.328	0.467	1.05	3.9206	U-Al ₄ -Al	347	3	4

When the UO₂ fuel pellets (with Zircalloy cladding) are used instead, the results contained in Tab. 3 would be found.

Table 3. The reactor characteristics resulting from the use of the only UO₂ pellets clad with Zirconium.

Flux in the Internal Irradiation Sites (*10 ¹²)				Initial Excess reactivity (mk)	Fuel Type	No. of Fuel rods	No. of Dummy elements	No. of Tie Rods
Group 1	Group 2	Group 3	Group 4					
0.0202	.0407	.0827	.4358	4.3500	UO ₂ ceramic	347	3	4

Fluxes in the case of LEU fuel are smaller with respect to the case of HEU fuel by about 5% in the inner and outer irradiation sites. This would imply that the reactor power be raised by the same percent at least.

The use of zirconium alloys for some reactor components of the Syrian MNSR is shown in table 4.

Table 4. The cumulative worth of some components of the Syria MNSR.

Component name	Component material	Excess reactivity(mk)	Fuel enrichment(%)	Remarks
Clad	Zircalloy-4	4.35	13.00	Cumulative
Shim tray	Zircalloy-4	5.4422	13.00	“
Upper Grid	Zircalloy-4	6.7265	13.00	“
Lower Grid	Zircalloy-4	7.9178	13.00	“
Shim Tray Axis	Zircalloy-4	7.9552	13.00	“
Shim Tray Wall	Zircalloy-4	8.9020	13.00	“
Bolster Tray	Zircalloy-4	9.3802	13.00	“
Lateral frame	Zircalloy-4	9.6843	13.00	“
Base Frame Part 1	Zircalloy-4	9.9834	13.00	“
Base Frame Part 2	Zircalloy-4	10.431	13.00	“

In Tab. 4 the cumulative worth of the different components is shown. The cumulative excess reactivity reaches about 10.431 mk when all the components mentioned in Tab. 4 are made of zircalloy-4.

If a fuel of 12.4% enrichment is used instead of the UO₂ pellets (which are 13.00% enriched) , the cumulative excess reactivity of this reactor configuration would be 4.3857 mk, which is very near to the initial excess reactivity of the reactor (4.3500 mk).

This means that the use of zircalloy for this components in the Syrian MNSR would save about 13.00%-12.4%=0.6%

The use of zirconium for the only upper and lower grid would save about 0.13% enrichment as stated in the abstract.

More savings will be obtained when additional components (parts) of the reactor, which actually are made of aluminum alloy, are substituted by identical parts made of zircalloy.

Acknowledgment

The author thanks Professor I. Othman, Director General of the Atomic Energy Commission of Syria for his encouragement and continued support.

References

- [1] I. Khamis, K. Khattab. Lowering the enrichment of the Syrian miniature neutron source reactor. *Annals of Nuclear Energy* 26, 1999, P. 1031-1036.
- [2] Albarhoum M., **Core Configuration of the Syrian reduced enrichment fuel MNSR**. Proceedings of the 2004 International Meeting on Reduced Enrichment for Research and Test Reactors, Vienna, Austria, November 7-12, 2004. Enrichment for Research and Test Reactors, Boston, USA, November 6-11, 2005.
- [3] Albarhoum M., **The use of UAl_x-Al reduced enrichment fuel in a well reflected MNSR**. Proceedings of the 2005 International Meeting on Reduced Enrichment for Research and Test Reactors, Boston, USA, November 6-11, 2005.
- [4] Albarhoum M., **Mixed Fuel versus Low Enriched Fuel in the Syrian MNSR**. Proceedings of the 2006 International Meeting on Reduced Enrichment for Research and Test Reactors, Cape Town, South Africa, October 29- November 2, 2006.
- [5] J. Matos, R.M. Lell. **Feasibility study of Potential LEU Fuels for a Generic MNSR Reactor**. Proceedings of the 2005 International Meeting on Reduced
- [6] **A General Description of Lattice Code WIMSD**. Askew J.R, Fayer F.J. and Kemshell P.B. (1966)*Journal of the British Nuclear Energy Society*.
- [7] **Nuclear Reactor Core Analysis Code: CITATION** Fowler T.B, Vondy D.R, and Cunningham G.W. (1971)ORNL-TM-2496, Rev. 2, July.
- [8] **Safety Analysis Report (SAR) for the Syrian Miniature Neutron Source Reactor**, China Institute of Atomic Energy, 1993, China.
- [9] Albarhoum M. **A 3-D Neutronics Model for the Calibration of the Control Rod of the Syrian MNSR**. *Progress in Nuclear Energy*, 46, No. 2, pp. 159-164 (2005).

STUDY OF Al FUEL PLATE OXIDATION

R. HADDAD, A. BURKART

*Materials Department, Comisión Nacional de Energía Atómica
Av. Gral Paz 1499, B1650KNA – Buenos Aires, Argentina*

R. AMORUSO

*Nuclear Fuel Department, Comisión Nacional de Energía Atómica
Av. Gral Paz 1499, B1650KNA – Buenos Aires, Argentina*

ABSTRACT

An experimental approach is presented, which intends to provide a way of measuring oxide growth in aluminium MTR fuel plates during operation in Research Reactors, in order to predict fuel performance in a variety of situations. It essentially consists in a coolant channel formed between two parallel aluminium plates, which are heated by means of a hot fluid. Experimental conditions try to simulate the situation between two fuel plates in a MTR fuel. Preliminary results indicate a consistent dependence of oxide growth with variables temperature and time.

1. Introduction.

Aluminium clad MTR fuel undergoes oxidation during operation in Research Reactors. Aluminium oxides are poor heat conductors; hence, heat transfer between fuel and coolant could be disturbed by the growth of a thick layer. If this should happen, fuel plate temperature will increase, even at constant coolant temperature, due to the temperature drop across the oxide layer, thus accelerating the oxidation process, generating a vicious circle. Aluminium and its alloys may suffer corrosion in water at temperatures above 150-200 °C (which could conceivably be attained in the fuel plate if the oxide film exceeds certain thickness), with penetrating intergranular attack, blistering and oxide exfoliation. As oxide growth is a function of plate temperature, water condition, coolant flow and other reactor parameters, the heat transfer situation will vary from reactor to reactor, depending on thermal power and other specific characteristics. A reliable performance prediction may then be relevant to fuel design. There is no predictive model taking into account all these parameters. Only empirical regressions are available, which are just valid for the conditions of the experiments used to develop them. It can be mentioned, among them, those by Griess [1], Kritz [2], the so called "Correlation II" [3], and a recent one by Soo Kim et al [4]. Some are shown in Figure 1, which also includes a recalculation of the Griess correlation using data obtained only at pH=7.

An experimental approach is presented, which intends to supply a way of measuring oxide growth in different conditions, in order to foresee fuel performance in a variety of situations. These may include variations in inlet and outlet coolant temperature, heat transfer, coolant flow and/or speed, coolant chemistry conditions, plate metallurgical conditions, etc.

2. Experimental

In order to reproduce the heat transfer conditions which are present in the interface between fuel plates and flowing coolant, a double loop device was built, which simulates a fuel channel segment. The heart of the system is composed by two parallel aluminium alloy plates separated by a channel distance (2.5 to 2.7 mm). A water flow passes between them,

which takes out the heat supplied by a hot fluid which circulates on the two external sides of the channel, as depicted in the schematic diagram displayed in Figure 2.

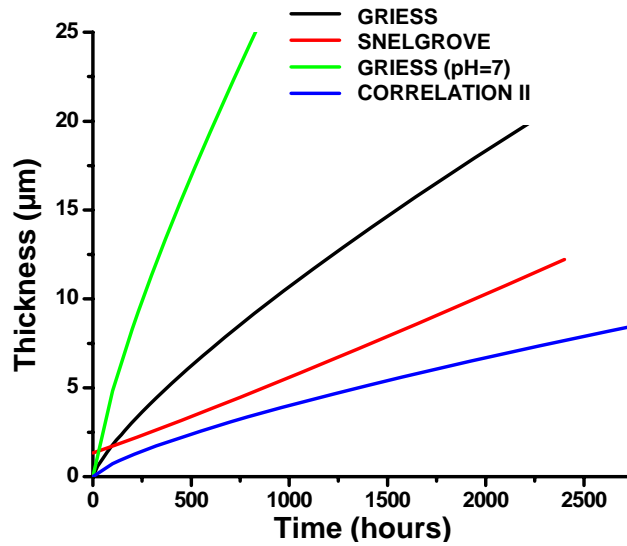


Figure 1: Oxide thickness prediction by different authors. In green, a modification of the Griess correlation, based on data obtained at pH=7.

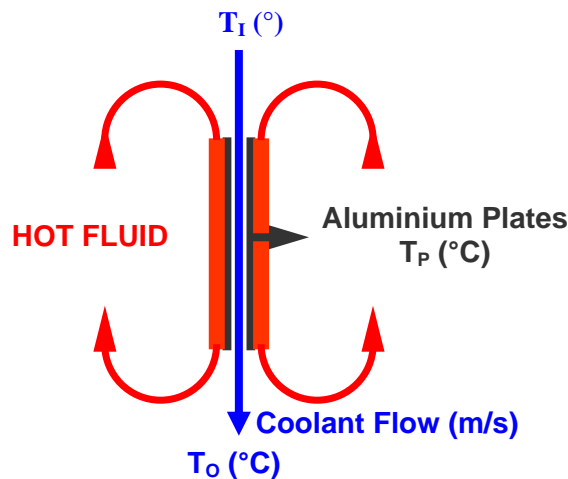


Figure 2: Schematic Diagram of the test device. T_I Inlet Temperature, T_O Outlet Temperature, T_P Plate Temperature

Figure 3 shows a simplified layout of the full experimental disposition. The hot fluid is pumped through an electric heater before being flushed on to the external sides of the aluminium channel. Fluid temperature is regulated by a P&D temperature controller. A proper supplier insures an adequate feeding pressure (not shown). The coolant circuit comprises a pump which pushes the water into the fuel channel at a controlled flow rate. Temperatures at the channel entrance and exit are continuously monitored and provisions are made to have part of the flow to circulate through a purifying system, in order to maintain water quality in nuclear grade standards (conductivity below $1 \mu\text{S/cm}$, pH between 5 and 7 and no detectable amounts of dissolved ions).

Knowing the Inlet and Outlet temperatures and the flow rate, it is easy to calculate the heat transfer rate. All these parameters can be adjusted to reproduce the values corresponding to any specific condition of a fuel in operation. The experiment does not reproduce the operation of a full fuel plate, but that of a smaller window, 8 cm long and 4 cm wide. This is the size of the exposed region of the channel which is heated from the outer sides. After a

cycle completion, the device can be disassembled, the plates removed and the oxide thickness measured using an Eddy Current Probe.

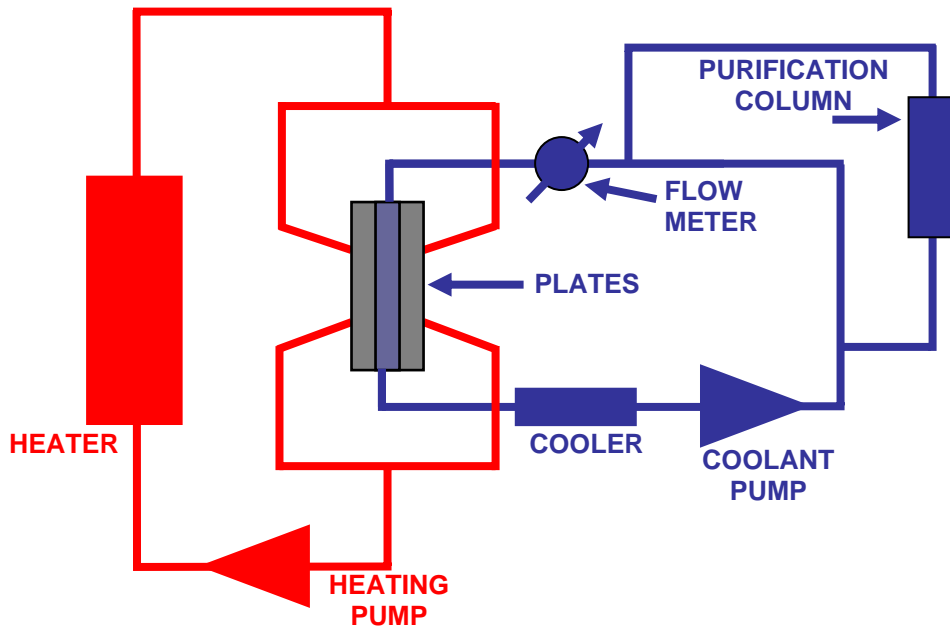


Figure 3: Double Loop Layout: hot branch in red, cooling branch in dark blue.

Cycles of various lengths can be performed, thus obtaining oxide growth data for different exposure times. This way, a correlation could be derived for the oxide thickness as a function of the main variables: inlet temperature, outlet temperature, coolant flow, coolant velocity, heat transfer rate, plate temperature, linear power, etc. This could be done for different coolant and plate conditions (chemical conditions, metallurgical conditions, etc.). Figure 4 depicts the main part of the experimental arrangement, the sample holder. Parts of the heat insulation have been removed in order to permit a better view. Plate's temperatures can also be monitored using thin thermocouples inserted along the plate's thickness.

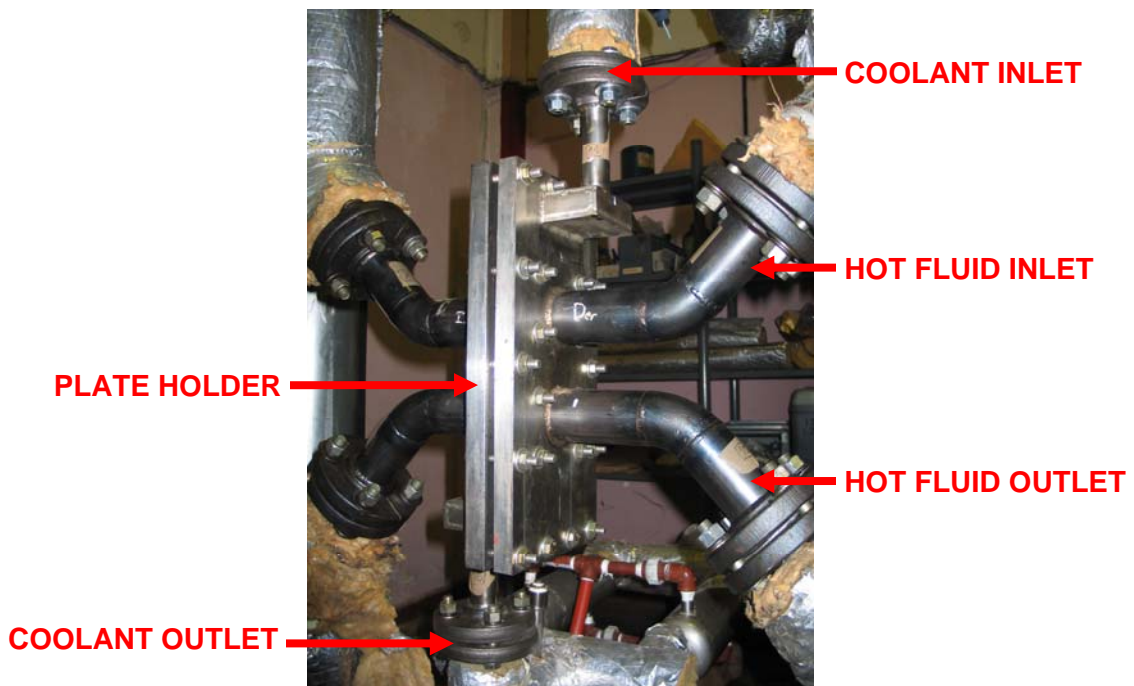


Figure 4: View of the assembled plate holder (T_p thermocouples not shown).

Coolant chemical conditions can be altered to reproduce different situations, like variation in coolant pH, conductivity or even chemical composition. The device admits the insertion of plates with various surface conditions, as pre-oxidation, coatings, etc.

For the first experiments conducted with the described arrangement, test conditions were chosen to be similar to those of the hottest part of the fuel plates developing highest linear power in a production-experimental reactor, aiming to study the oxidation behaviour in the limit of the design capacity.

Four preliminary tests have been performed so far, using four different sets of plates with the main purpose of testing the system ability to consistently produce a controlled heat transfer; two experiments were carried out with a coolant inlet temperature of 50 °C and two with 52 °C. In both cases the experiments were left to last for 5 days and 20 days. The heat transfer conditions were adjusted in all cases to produce a coolant temperature increment ($T_O - T_I$) of 5.3 °C.

3. Results.

Table 1 shows the results of the measured oxide growth in the four tested plates. They show a strong dependence with variables temperature and time. For the higher temperature case, the obtained correlation is almost linear (1 $\mu\text{m}/\text{day}$), but in the other case tends to be more parabolic.

		OXIDE THICKNESS (μm)	
		Inlet Temperature (T_I)	
TEST TIME	5 days	3	5
	20 days	7	20

Table 1: Oxide thicknesses measured on aluminium plates in different conditions.

Figure 5 shows a metallographic cross section of the oxide grown in 5 days in the most exigent condition. These pictures served to validate the Eddy Current measurements, so as to demonstrate this non destructive method could be used to determine the oxide thickness, thus permitting to perform successive tests with the same samples.

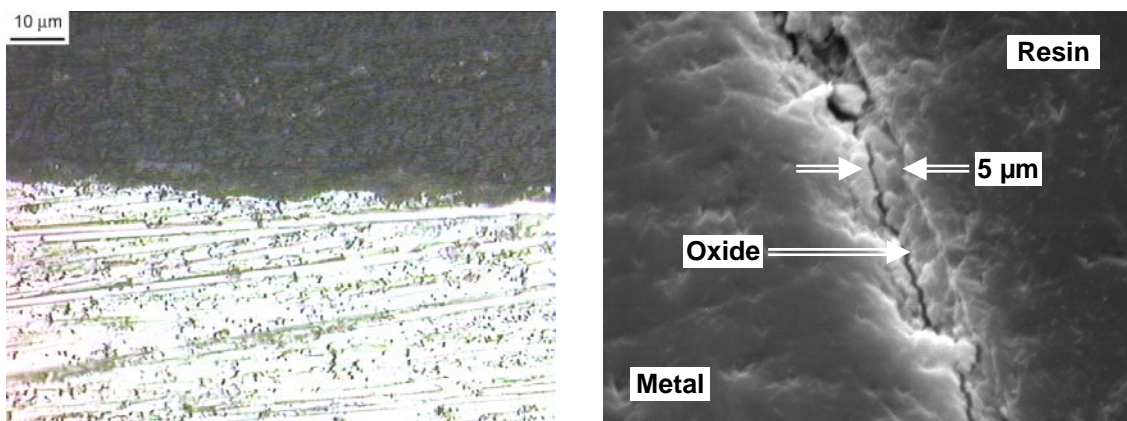


Figure 5: Oxide grown on an aluminium plate. Left: optical microscope image. Right: SEM image.

Figure 6 shows a typical histogram obtained with the Eddy Current probe. The film thickness increases from the inlet to a maximum in the centre of the exposed window.

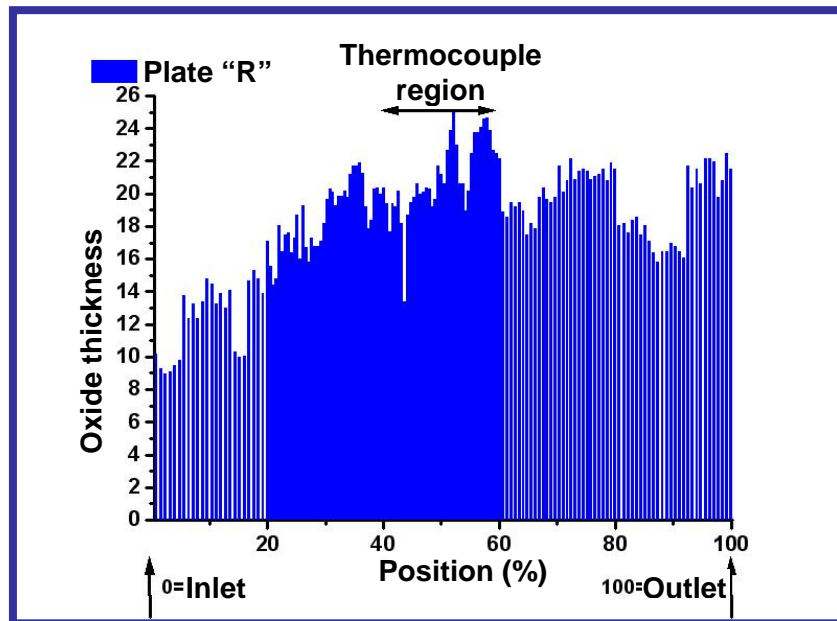


Figure 6: Typical histogram obtained with an Eddy Current Probe, showing Oxide Thickness Distribution along the length of the tested window.

4. Discussions and conclusions

The described experimental disposition has shown to be capable to reproduce the situation in a MTR fuel channel. The preliminary results indicate that the grown oxides thicknesses bear a relation with the experimental settings. A systematic study should comprise a full series of tests with specific heat transfer conditions at different times, to derive a correlation which may permit to predict the fuel performance in an operating Research Reactor. Different correlations could then be extracted for the various possible Reactors's operating situations (coolant chemistry, plate metallurgical state).

5. Acknowledgments

The authors wish to acknowledge the strong support of the INVAP Company, which supplied most of the engineering to build the facility. Also, to thank Dr. A. Denis from CNEA, for her collaboration with valuable theoretical information on heat transfer and to the Nuclear Fuel Dept. of CNEA, for the help in installing the device and providing the shift attendance.

6. References

- [1] J. C. Griess et al., "Effect of heat flux on the corrosion of Aluminium by water. Part IV", ORNL-3541 (1964).
- [2] R. S. Ondrejcin, "Evaluation of Mark 22 cladding", Savannah River Laboratory DPST-83-324 (1983).
- [3] S. J. Pawel et al., "Influence of coolant pH on corrosion of 6061 Aluminium under reactor heat transfer conditions", report ORNL/TM-13083 (1995).
- [4] Yeon Soo Kin et al, "Prediction Model for Oxide Thickness on Aluminium Alloy Cladding During Irradiation.", 25th Int. Meeting on RERTR, Chicago (Illinois), October 5-10 (2003).

STUDY OF NUCLEAR FUEL BURN-UP IN A LOW POWER REACTOR

L. HERALTOVÁ, A. KOLROS

heraltoval1@troja.fifi.cvut.cz, antonin.kolros@fifi.cvut.cz

*Department of Nuclear Reactors, Faculty of Nuclear Sciences and Physical Engineering,
Czech Technical University,
V Holešovickách 2, 180 00 Prague 8, Czech Republic*

ABSTRACT

The insertion of fresh IRT-4M fuel elements into the core of VR-1 Sparrow enabled to initiate long-term monitoring of isotopic changes in the fuel and experimentally determine the burn-up of the fuel in a low power reactor by gamma spectrometry measurements.

The principle of this method is to determine the activity of properly selected fission products generated in the fuel. From these activities, the number of ^{235}U fissions necessary for generation of these fission products in the examined parts of the fuel can be determined. Using the known dependence of the fission yield on the mass number, it is possible to evaluate the total mass of the ^{235}U spent in the sample. Based on neutron flux distribution in radial and axial directions, the total burn-up in the reactor core of the VR-1 reactor in 1 year can be determined.

Key words: gamma spectrometry, burn-up, ^{137}Cs , low power reactor, reactor VR-1

1. Reactor VR-1 Sparrow

Reactor VR-1 Sparrow is an experimental reactor used for the training and education of students. The plant operator of the reactor is the Faculty of Nuclear Sciences and Physical Engineering, Czech Technical University in Prague.

Reactor VR-1 is a light water pool-type reactor with low-level enriched uranium. Demineralised water is used as a moderator, coolant, and biologic shielding. Pool type settlement of the reactor enables quick access to the reactor core, simple insertion of experimental channels, and safe manipulation with fuel elements

1.1. Engineering characteristic of VR-1

The nominal power of the reactor is 1 kW; for a short time is possible to operate the reactor on the power of 5 kW. The reactor vessel is made of stainless steel. The biological shielding is provided by light water and heavy concrete. Operational conditions of the reactor– the temperature is approximately 20°C (it depends on the temperature in the reactor hall) and atmospheric pressure. Regulation of the reactor is supported by 5 – 7 absorbing rods (depending on configuration of the reactor core)

1.2. Nuclear fuel of VR-1

Nuclear fuel IRT-4M is Russian fuel for experimental reactors. It is provided in three types: four, six and eight tube. The fuel elements consist of concentric tubes of square cut, where one is inserted in another. The top and bottom of the tubes are set into a distant head to define space between tubes and for fixation in the reactor core. These fuel elements were designed with respect to simple interchanges and minimal requirements on modification during change of configuration. Inside the six-tube fuel element it is possible to insert the absorption parts of control rods or experimental channels. The amount of ^{235}U is from 200 g up to 300 g (it depends on the type of fuel – number of tubes).

In current configuration of the reactor core (see Fig. 1) there are 9 six-tube and 8 eight-tube fuel elements. The total content of ^{235}U is 4774.2 g.

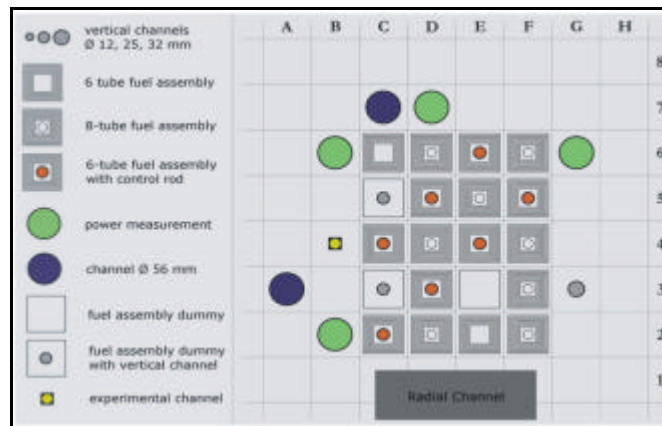


Fig 1 – Configuration of reactor core

2. Gamma spectrometric measurements

Due to irradiation of nuclear fuels during operation, isotopes ^{235}U and ^{238}U are changed into a number of various radionuclides. Most of them are radioactive and their decay - α or β , is followed by the emission of a certain number of gamma quanta. By gamma spectrometry it is possible to detect this gamma and uniquely determine the isotopes included in the fuel and specify the relative distribution of the fission products in the fuel. Gamma spectrometry used a semiconductor HPGe detector, High Purity Germanium detector, (GC2518, FWHM 1.8 keV, efficiency 25 %) by Canberra and primary analysis of experimental data was made by Genie 2000 v.3.0 software by Canberra.

3. Theoretical part

3.1 Methodology

The calculations were performed for three groups of isotopes. The first group consisted of ^{95}Zr , ^{137}Cs and ^{141}Ce , the second group of ^{95}Zr and the third one was represented by ^{137}Cs . Especially ^{137}Cs is a very suitable isotope from the viewpoint of long-term kinetics of origin thanks to its long half-life of 30.07 years.

At first, the measured data were corrected by correction factors (see chapter 3.2). Based on the measured number of gamma of certain energy, the activities of appropriately chosen isotopes were evaluated. In the next step, the amount of split nuclei of ^{235}U was determined. This number characterizes the amount of ^{235}U , which has to be split to generate measured activity of the monitored isotope in surveyed part of the fuel element. All fission products were included, using the known dependence of the fission yield on the mass number. At this point, it was supposed that two different fission products originate per one split nucleus of ^{235}U . This value of fissioned nuclei of ^{235}U identifies the mass of ^{235}U , which has to be split in the surveyed part of fuel element (geometry of experiment – see chapter 4.). The value of the burn-up is changing along the fuel element, and also the value of burn-up will be different in various positions of the fuel elements in the reactor core. To evaluate the burn-up of the whole fuel element, it is required to know the axial distribution of thermal neutron flux. Burn-up of the operational reactor core depends on radial distribution of thermal neutron flux as well. Three approximations of spatial distribution of the neutron flux (see 3.3) – the constant distribution, the sinus curve and the distribution obtained from the MCNP calculation – were used for evaluation of the total burn-up per 1 year.

3.2 Correction factors

Before evaluation, it is necessary to correct the obtained experimental value to eliminate imperfections of the measurement.

The data were corrected on geometry. By reference emitter ^{152}Eu the attenuation of gamma beam in the air and parasite absorption in the lead shielding was taken into account. During evaluation of the measurements point geometry was assumed. This postulate was verified by reference emitter ^{137}Cs and calculation code MCNP-4C. In the time between two operational periods and the time from end of irradiation up to beginning of the measurement part of the amount of generated fission product is lost due to radiation decay. For correct interpretation of the experimental results and for obtaining the proper value of burn-up it is necessary to include all atoms, which originate in the fuel. Finally, the self-attenuation coefficient of uranium was specified. This correction factor was quantified by the calculation code MCNP-4C, which allows us to count the response of HPGe detector to the defined activity. Comparison of the calculated value of activity and value obtained from measurements gives the self-attenuation factor.

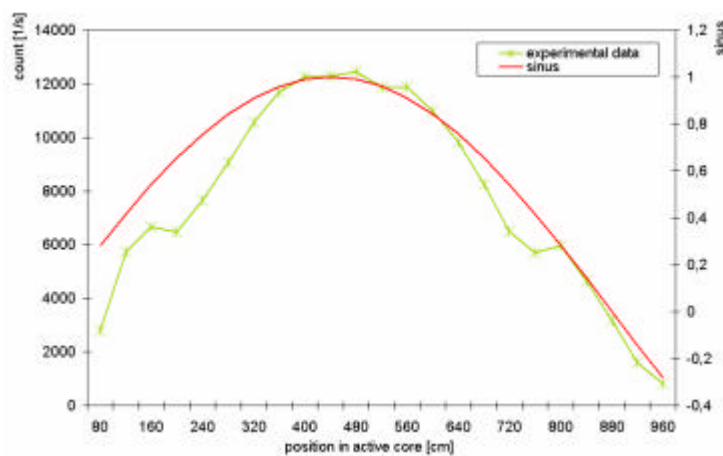


Fig 2 – Thermal neutron flux in axial direction

3.3 Spatial distribution of neutron flux

The maximum value of neutron flux is approximately in the middle of the reactor core and it decrease towards periphery of the reactor core. Initial guess of the burn-up was based on the assumption of constant production of fission products. However, the real distribution of neutron flux is more complicated. Better results were obtained by calculation with sinus distribution. The axial distribution of thermal neutron flux inside the fuel element was measured by the small corona detector SNM 13 (^{10}B). Based on experiments carried out at the reactor VR-1, the approximation by sinus function in axial direction is very acceptable (Fig. 2). The heterogeneity of the reactor core is more obvious in radial direction. In this case this approximation is not very precise. The sinus describes the distribution of the neutron flux for the neutrons of all energies and fission of the ^{235}U is caused by thermal neutron. Most exact radial distribution is obtained by MCNP. Distribution of the thermal neuron flux in radial direction was calculated in imaginary channels in the reactor core and standardised to the maximal value (Fig. 3).

4. Experimental part

For this experiment two eight-tube fuel elements were chosen from the operational reactor core of reactor VR-1, positions F4 and F6 (Fig. 1). Six-tube fuel elements were omitted from

the experiment, because the absorption parts of the control rods are inserted in them. This caused difficulty during manipulation with fuel elements.

The whole fuel element is too long for gamma spectrometry, so the lead shielding was built to shade the fuel element, and only an 80 mm gap was kept in the middle of the fuel element (see Fig. 4).

The first measurement – 8/11/2005 was carried out approximately 14 days after the refuelling. Before this measurement there was minimum load of the reactor. The second measurement was realized in 1/6/2006 after several months of operation. These measurements were performed 2 days after shut-down. The third measurement – on 16/8/2006 - was made during holiday an availability time. The cooling time of the fuel elements in this case was almost two months. Due to that, the short-time radionuclides were decayed and only the long-term nuclides such as ^{137}Cs - which is the most suitable nuclide for calculating the burn-up - remained. The last measurement ran on 25/9/2007; the cooling time was than approximately three months. The time of measurement was 20 minutes for the first and second measurements; and 30 minutes for the remaining ones.

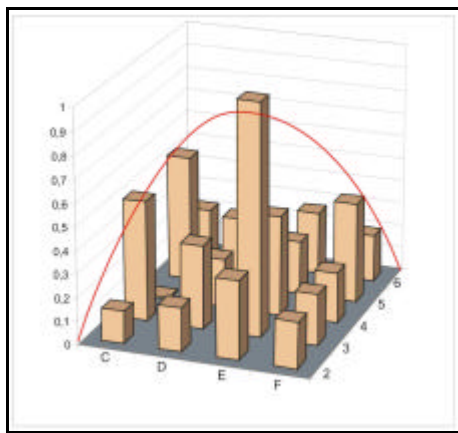


Fig 3 - Ratio of neutron flux in singular positions of reactor core

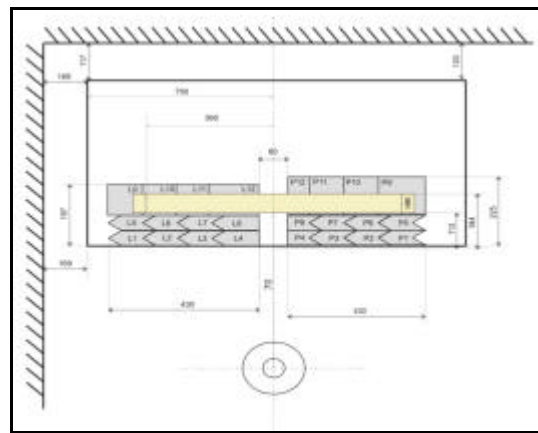


Fig 4 - Geometry of experiment

5. Conclusion

The measured data show the expected trend. Due to irradiation, the number of ^{235}U nuclei decreases and a large amount of fission products is generated. Isotopes originating in the fuel correspond to the dependence of the fission yield on the mass number, and the highest representation corresponds to products with mass numbers 95 and 140 (e.g. ^{95}Zr , ^{95}Nb , ^{140}Ba , ^{140}La). Between the second and third measurement is possible to observe degradation of peaks due to radiation decay of short-time radionuclides. Because of this fall of detected counts, the background is lower, and it is possible to measure long-time fission products that are more interesting for experimental evaluation of burn-up (e.g. ^{137}Cs). See Fig. 5.

Three groups of fission products were considered to determination of burn-up. The best results were obtained by ^{137}Cs due to its long half-life and its standard deviation is lowest.

The calculation code MCNP-4C was used to asses the self-attenuation coefficient. This correction improves the results by approximately 30 %. Also the assumed point geometry was verified by MCNP calculation. The error caused by ignoring the no-point geometry is below 4.5 %.

During the evaluation of the burn-up three approximations of the spatial distribution of the neutron flux were used – the constant production of fission products, the sinus distribution, and the MCNP calculation. The constant production of fission products without the respecting the spatial distribution is only a rough guess. In fact, the maximum of fission products concentration is in the middle of the fuel element and towards the boundary of the fuel elements it decreases. The results obtained by approximation by the sinus give almost the same values, but the description of the neutron flux in the reactor core is more suitable. Moreover, characterization by sinus in axial direction causes the error lower than 3 %. This was verified by measurements carried out at the VR-1 reactor (see Fig. 2) and also by MCNP code. In radial direction the sinus is useful to describe the distribution of neutrons of all energies, but not the thermal neutrons. In third approximation the axial direction was described by the sinus and for the radial direction the MCNP calculation was used.

So far, the burn-up of fuel elements IRT-4M in the VR-1 reactor at a level of 10 – 100 mg of ^{235}U was assumed. The value gained by evaluation of the experimental data is approximately 0.5 mg of ^{235}U per 1 year of operation. This value is roughly by about two orders lower.

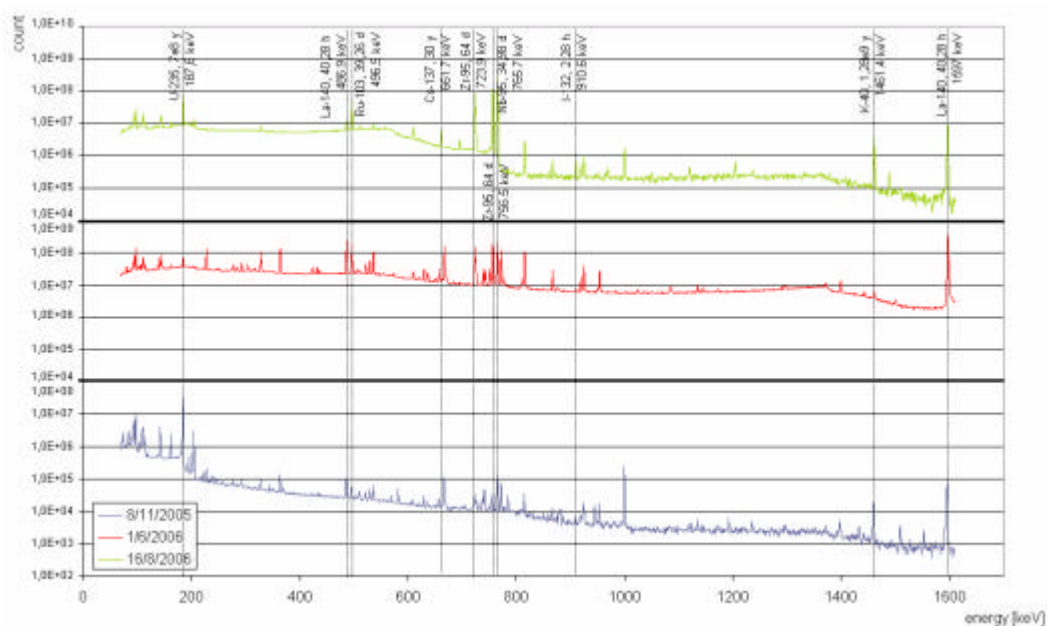


Fig 5 – Measured gamm spectra for one of the fuel elements

References

- [1] Heraltová, L. - Nuclear fuel burn-up determination in low power reactor, Master thesis, Department of Nuclear Reactors, Faculty of Nuclear Science and Physical Engineering, Czech Technical University, Prague 2007 (in Czech)
- [2] Heraltová, L.; Kolros, A. - Study of Nuclear Fuel Burn-up in a Low Power Reactor, Workshop Czech Technical University, Prague 2007
- [3] IAEA – TECDOC – 633, Determination of Research Reactor Fuel Burn-up, January 1992
- [4] Kolros, A.; Bílý, T.; Heraltová, L.; Huml, O.; Katovský, K.; Klupák, V.; Rataj, J.; Soucek, I.; Vinš, M.; - Školní reaktor VR-1 Vrabec: Experimentální stanovení vybraných parametru, Faculty of Nuclear Science and Physical Engineering, Czech Technical University, Prague, 2007, (in Czech)

This project was supported by MŠMT grant No. MSM6840770040.

RESULTS OF THE REACTOR CONTROL SYSTEM REPLACEMENT AND REACTOR CORE CONVERSION AT THE DALAT NUCLEAR RESEARCH REACTOR

PHAM VAN LAM, NGUYEN NHI DIEN, TRINH DINH HAI, LUONG BA VIEN,
LE VINH VINH, HUYNH TON NGHIEM, NGUYEN MINH TUAN
AND NGUYEN KIEN CUONG
Nuclear Research Institute
01 Nguyen Tu Luc Street, Dalat, Vietnam

ABSTRACT

We started to realize project to replace the reactor control system of The Dalat Nuclear Research Reactor (DNRR) by new one on 9 December 2006. This project was supported by International Atomic Energy Agency and Vietnam Government. Equipments were supplied by company SNIIP-SYSTEMATOM, Russia. The project was fulfilled in April 2007.

Contracts for reactor core conversion between Russia, Vietnam, USA and the International Atomic Energy Agency for Nuclear fuel manufacture and supply for DNRR and Return of Russian-origin non-irradiated highly enriched uranium fuel to the Russian Federation have been realized. The 35 fresh HEU fuel assemblies (FA) (34 standard and 1 instrumented) were sent back to Russian Federation. We have received 36 new LEU FAs from Russian Federation. Fuel reloading has been executed by using LEU FAs on 12 September, 2007. Now DNRR core consists of 98 HEU FAs and 6 LEU FAs. This paper presents results of the reactor control system replacement and reactor core conversion at the DNRR.

1. Results of the reactor control system replacement

The DNRR is a pool type research reactor which was reconstructed from the 250 kW TRIGA-MARK II reactor. The reactor core, the control and instrumentation system, the primary and secondary cooling systems as well as other associated systems were newly designed and installed [1]. The core was loaded with WWR-M2 fuel assemblies with 36% enrichment. The reconstructed reactor reached its initial criticality in November 1983 and attained its nominal power of 500 kW in February 1984. The reactor control and instrumentation system was upgraded in 1994. We started to realize project to replace the reactor control system by new one on 9 December 2006. This project was supported by International Atomic Energy Agency and Vietnam Government. Equipments were supplied by company SNIIP-SYSTEMATOM, Russia. The incoming inspection, assembling and mounting works, autonomous tests, complex tests and reactor operation tests at minimum control level and energy levels of the power were performed. The project was fulfilled in April 2007. New reactor control system ensures the safety, control, check and monitoring of the reactor facility by means of the following channels and equipment: channels for monitoring of reactor power and period by thermal neutrons flux density (NFME channels); channel for monitoring of process parameters; channels for logical processing of signals from NFME channels, from technological and supporting systems and for generation of control signals for protection safety system and for normal operation system; channel for automatic power regulation; channels for reactivity monitoring; channel for monitoring of control rods position; information channels for displaying operative information at control panel; buttons and keys of control

panel and equipment for archiving, diagnostic and recording. On 3 October 2007 licence for use of new control system has been issued. Figure 1 shows operation of DNRR with new control system.



Fig 1. Operation of DNRR with new control system

2. Results of the reactor core conversion

Contracts for reactor core conversion between Russia, Vietnam, USA and the International Atomic Energy Agency for Nuclear fuel manufacture and supply for DNRR and Return of Russian-origin non-irradiated highly enriched uranium fuel to the Russian Federation have been realized. The 35 fresh HEU FAs were sent back to Russian Federation. We have received 36 new LEU FAs from Russian Federation. Each HEU (enrichment of 36%) FA contains about 40.2 g of U-235 with U-Al alloy dispersion fuel meat. Each LEU (enrichment of 19.75%) FA contains an average of 49.7 g ²³⁵U with UO₂-Al dispersion fuel meat. They have the same geometry. Each of the fuel elements in the HEU and LEU FA has the same thickness of 2.50 mm, but the fuel meat and cladding thickness are different [2]. Fuel reloading has been executed by using LEU FAs on 12 September, 2007 [3]. The 8 HEU FAs with highest burnup were removed from the core periphery positions (P 1-3, P 1-5, P 1-2, P 2-1, P 13-3, P 13-1, P 13-4 and P 12-8). The 8 HEU FAs from second ring counted from neutron trap (P 6-9, P 5-8, P 5-4, P 6-4, P 8-4, P 9-4, P 9-8 and P 8-9) were moved to previous FA positions. The 2 HEU FAs from the core periphery positions (P 1-4 and P 13-2) were moved to 2 positions in second ring (P 6-9 and P 8-4). The 6 new LEU FAs were added in 6 positions in second ring (P 5-8, P 5-4, P 6-4, P 9-4, P 9-8 and P 8-9). The 2 wet irradiation channels were added in 2 positions of core periphery (P 1-4 and P 13-2). After reloading the working configuration of reactor core consisted of 104 FAs (98 HEU FAs and 6 new LEU FAs). We had first 8 spent HEU FAs. Figure 2 and 3 show reloading schema of DNRR and working

configuration of DNRR. The value of 0.68 \$ was increased to the reactor excess reactivity after reloading operation. Figure 4 and 5 show measured neutron spectrum at neutron trap and measured neutron flux distribution at neutron trap. Table 1 presents measured thermal and fast neutron flux at irradiation positions.

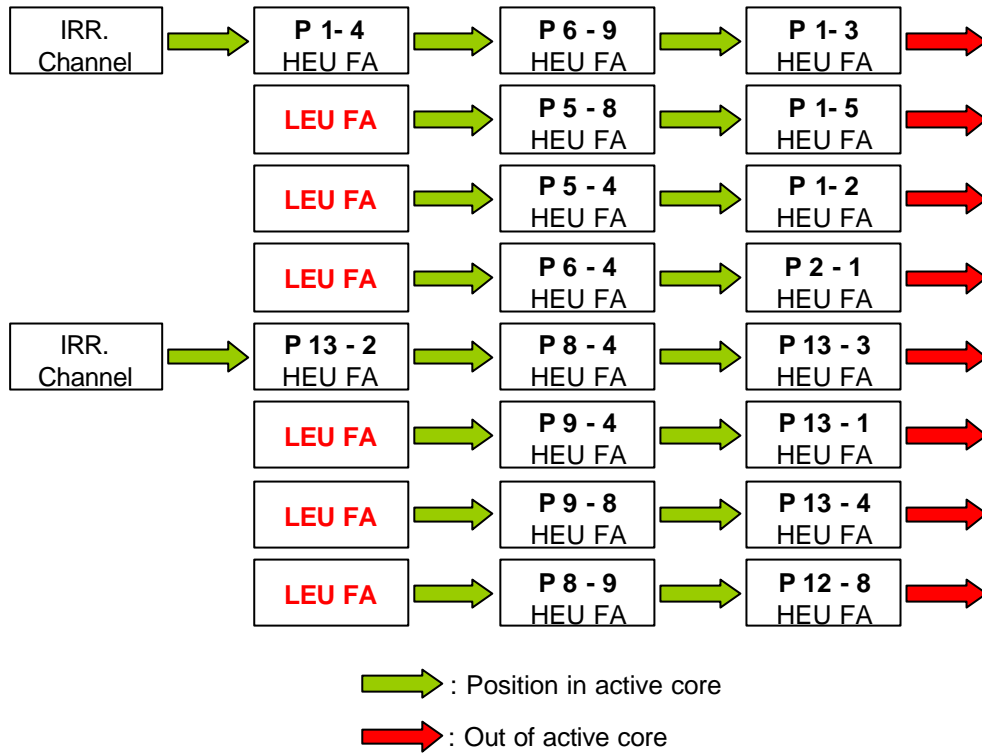


Fig 2. Reloading schema of DNRR

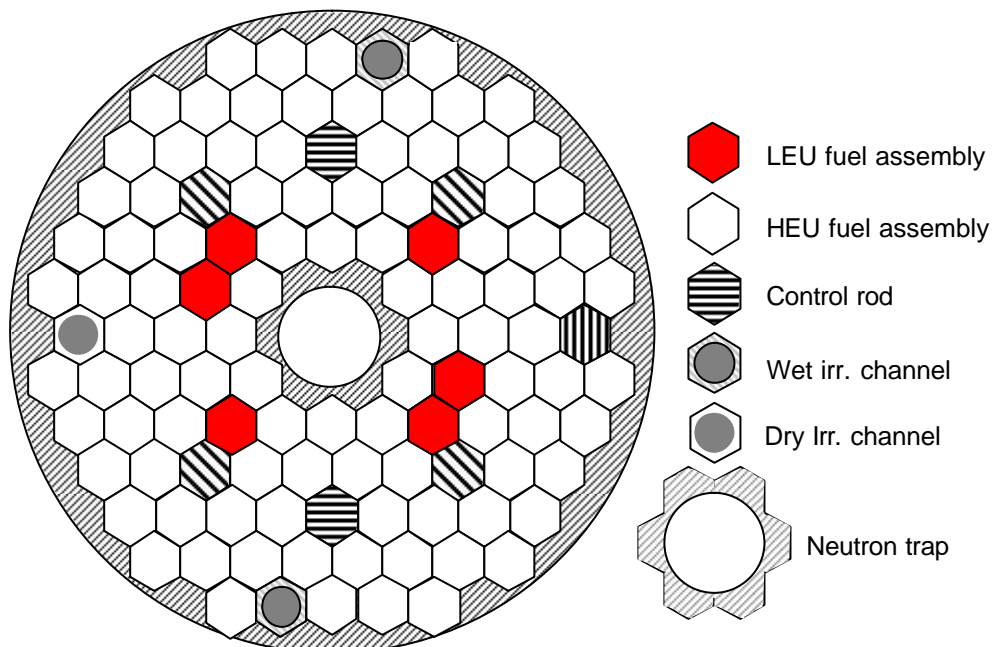


Fig 3. Working configuration of DNRR

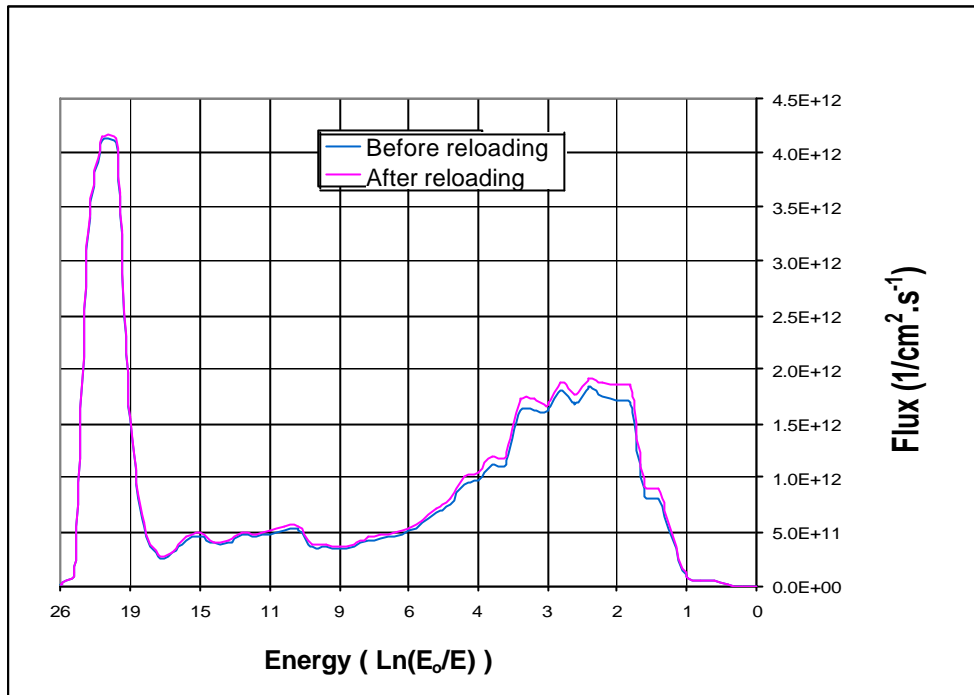


Fig 4. Measured neutron spectrum at neutron trap

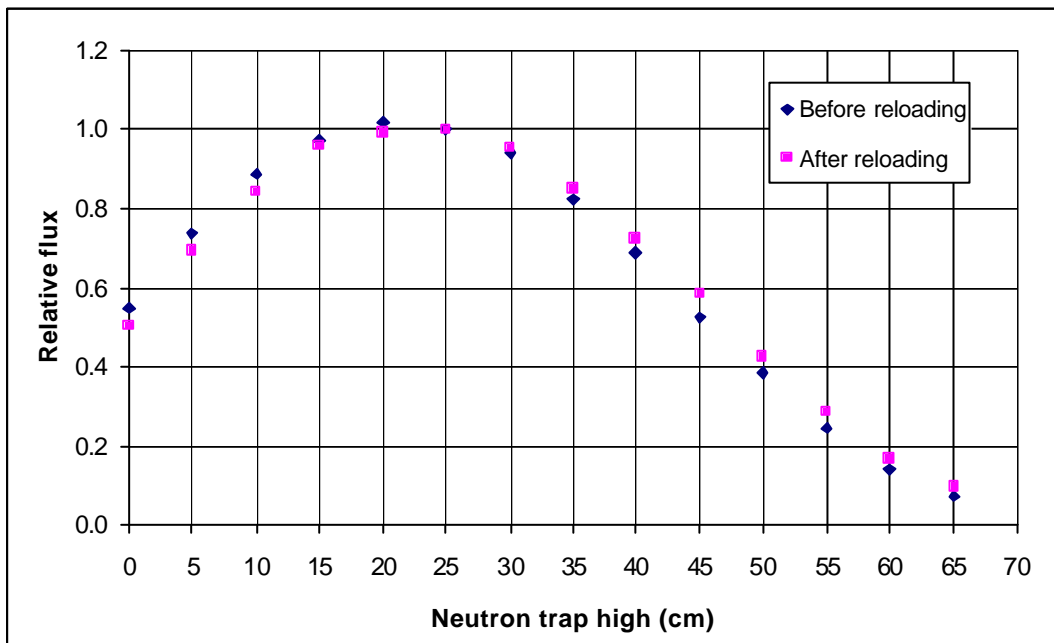


Fig 5. Measured neutron flux distribution at neutron trap

We carried out measurement of maximum fuel cladding temperature after reloading. In fact we measured fuel cladding temperature of instrumented FA. Because of instrumented FA has very low burnup compare to replaced FA then measured fuel cladding temperature of instrumented FA higher than value of replaced FA. Table 2 presents measured maximum fuel cladding temperature of instrumented FA placed at hottest position (P 9-6) near neutron trap. From table 2 we note that measured maximum fuel cladding temperature of instrumented FA with reactor power of 500 kW and inlet coolant temperature of 32 °C is less than 94 °C. This value is less than designed value of 107 °C.

Position	Before reloading		After reloading	
	$\phi_{th}^{(*)}$	$\phi^{(**)}$	$\phi_{th}^{(*)}$	$\phi^{(**)}$
Neutron Trap	$1,99 \times 10^{13}$	$4,45 \times 10^{12}$	$1,98 \times 10^{13}$	$4,61 \times 10^{12}$
Wet channel 13-2	-	-	$4,61 \times 10^{12}$	-
Rotary specimen rack	$4,28 \times 10^{12}$	-	$4,67 \times 10^{12}$	-

(*) Thermal neutron flux, $n.cm^{-2}.s^{-1}$.

(**) Fast neutron flux, $n.cm^{-2}.s^{-1}$

Tab 1: Measured thermal and fast neutron flux at irradiation positions

P (kW)	T_{in} (°C)	$T_{c,max}$ (°C)
2,5	20,3	21,9
250	20,8	61,2
400	22,0	79,0
500	23,1	90,2
	32,0	93,7

P: Reactor power

T_{in} : Inlet coolant temperature

$T_{c,max}$: Maximum fuel cladding temperature

Tab 2: Measured maximum fuel cladding temperature after reloading

3. Conclusions

We have fulfilled project to replace the reactor control system by new one in 2007. Licence for use of new control system has been issued on 3 October 2007. The contracts for reactor core conversion between Russia, Vietnam, USA and the International Atomic Energy Agency for Nuclear fuel manufacture and supply for DNRR and Return of Russian-origin non-irradiated highly enriched uranium fuel to the Russian Federation have been realized. The 35 fresh HEU FAs were sent back to Russian Federation. We have received 36 new LEU FAs. Fuel reloading has been executed by using LEU FAs. Now DNRR mixed core consists of 98 HEU FAs and 6 LEU FAs. We have first 8 spent HEU FAs. The DNRR is continuously operated safely after replacement of reactor control system and reactor core conversion.

4. References

- [1] Pham Van Lam et al., "The Dalat Nuclear Research Reactor Operation and Conversion Status", the RRFM & IGORR 2007, Lyon, France, March 2007.

- [2] V. V. Le, T. N. Huynh, B. V. Luong, V. L. Pham, J. Liaw, and J. Matos, "Comparative Analyse for Loading LEU Instead of HEU Fuel Assemblies in the Dalat Nuclear Research Reactor", International RERTR Meeting, Boston, US, 5-10/11/2005.
- [3] The sixth Fuel Reloading for the Dalat Nuclear Research Reactor", Dalat, 2007 (in Vietnamese).

SPENT FUEL ASSEMBLIES MANAGEMENT AT IEA-R1 RESEARCH REACTOR

R. FRAJNDLICH

*Nuclear and Energetic Research Institute
Av. Prof. Lineu Prestes, 2242, 05508-000 – Brazil*

ABSTRACT

The Brazilian RR IEA-R1 at ipen, São Paulo was the first reactor to operate in Southern Hemisphere and it is at the present time one of the oldest reactor still operating in the world. Since the reactor start-up on September 16, 1957 to December 2007, 234 core configurations have been implemented and around 200 fuel assemblies have been used. Actually, the spent fuel reactor storage is ipen major concern, because, according to the proposed operation schedule for the reactor, unless an action is taken, by the year 2009 there will be no more racks available to store its spent fuel. This paper gives a brief description of the type and amount of fuel elements utilized in the reactor and a short discussion about the fundamental importance for Brazilian researches to understand the problems related to the storage of spent fuel, and make a clear definition about the most suitable alternatives for interim storage of the spent fuel in the next future. The paper describes also the spent fuel transportation to the United States that occurred in 1999 and 2007.

1. Introduction

1.1 The IEA-R1 RR and the fuel assemblies /2/

The IEA-R1 reactor is pool type, light water moderated and beryllium and graphite reflected research reactor located at the Nuclear and Energetic Research Institute (IPEN), settled in the city of São Paulo, Brazil. The reactor was designed and built by Babcock & Wilcox Co. in accordance with specification furnished by the Brazilian Nuclear Energy Commission, and financed by the U.S “Atoms for Peace” Program.

The first start-up was on September 16th, 1957, being the first criticality achieved in the Southern hemisphere. Although designed to operate at 5 MW, this reactor had been operating until 1997 at a power level of 2 MW mainly for basic and applied research, as well as in experimental production of radioisotopes for medicine, industry and life sciences applications. Due to the growth of radioisotope demand in Brazil in the eighteens for medical diagnosis and therapies, IPEN had decided since that time to increase the reactor power level to 5 MW and to operate the reactor continuously.

Since startup to present time (2007), 234 core configurations have been installed and around 200 fuel element assemblies used. Concerning fuel utilization it is possible to analyze the reactor history in four cycles as shown in Table 1:

the first cycle corresponds to the first core of the reactor. It was composed of U-Al alloy fuel with 20wt% enrichment, having 19 curved fuel plates produced by B&W. These fuel assemblies failed at the earlier stages of the reactor operation, due to pitting corrosion caused by brazing flux used to fix the fuel plates to the support plates. These fuels were replaced, in 1958, by new ones, also produced by B&W. They were identical to the earlier ones (U-Al alloy, 20wt% enrichment, 19 curved fuel plates) but brazing was not used for assembling. The

fuel plates were fixed mechanically to the support plates. These fuels operated with good performance up to the discharge burn up used at that time.

The second cycle corresponds to a complete substitution of the core. Fuel made with U-Al alloy, 93 wt% enrichment, having 18 flat fuel plates were bought from UNC (USA). At this time the core was converted from LEU to HEU. In the middle of this cycle the control rod mechanical concept was also changed from rod type to fork type (plate type). The control fuel element assemblies were fabricated by CERCA (France), using U-Al alloy, 93 wt% enrichment, and flat plates.

Characteristics		First Cycle		Second Cycle		Third Cycle	Fourth Cycle
		1 st core	2 nd core	original	modified		
First Year in Reactor		1957	1959	1968	1972	1981	1985/2007
Stand		34	33	33		5	60
Contr.		5	4	6	4		14
Partial		1	2				2
Original Enrichment		20%	20%	93%	93%	20%	20%
Manufacturer		B&W (USA)	B&W (USA)	UNC (USA)	CERCA (France)	NUKEM (Germany)	IPEN (Brazil)
Fuel Type		U-Al alloy	U-Al alloy	U-Al alloy	U-Al alloy	UAl _x -Al	U ₃ O ₈ -Al U ₃ Si ₂ Al
Number of plates per F.A	Standard	19	19	18		18	18
	Control	9	9	9	12		12
	Partial	10	9 / 10				2 / 10
Type of Fuel Plate		curved	curved	flat	flat	flat	flat

Tab 1: Fuel Element Assemblies of IEA-R1 Research Reactor

The third cycle was characterized by the restriction of HEU fuel supply. IPEN bought, from NUKEM (Germany), 5 fuel element assemblies of UAl_x-Al dispersion type, with 20wt% enrichment and having 18 flat fuel plates per fuel element assembly. The amount of ²³⁵U in the LEU fuel plate was almost the same as the HEU fuel plate and the geometry of the fuel element assembly was the same. With this partial LEU core load, the HEU fuels that stayed in core began to have higher burn up and the numbers of fuel element assemblies used in the reactor core had to be increased due to reactivity needs.

The fourth cycle has began with IPEN decision of fabricating its own fuel and to replace, gradually, the high burn up HEU fuels in the core. IPEN had already, at that time, good knowledge and experience in core engineering, fuel engineering and fuel fabrication, so the decision to produce MTR fuel to the IEA-R1 was a natural way to maintain the reactor in operation. The IPEN fuel are of U₃O₈-Al and U₃Si₂Al dispersion type, with 20wt% enrichment and geometrically identical to LEU fuel from the third cycle.

1.2 The storage racks capacity

The reactor pool is divided in two different compartments. The first one where core and irradiation facilities are located, is used for reactor operation,. The second is the storage

compartment, where spent fuel storage racks are laid. In this compartment there are seven (7) stainless steel structural members bolted together and suspended on the pool walls at a depth sufficient to provide adequate shielding, two (2) stainless steel racks settled in the bottom of the pool and four (4) racks, aluminum made, located also on the bottom of the pool. The racks have a total capacity of 156 positions. In 2000, aluminum boxes were placed inside the racks made of stainless steel in order to avoid galvanic corrosion on fuel outer plates.

2. Characterization of Spent Fuel

2.1 Burn up calculation and measurement

The burn up calculation methodology used for IEA-R1 reactor is based on LEOPARD and HAMMER-TECHNION programs for cross section generation, 2DB program for the core and burn up calculation in a two-dimensional geometry and CITATION program for a three-dimensional analysis to obtain effective multiplication factor, neutron flux and power density distributions, integral and differential control rod worth, reactivity coefficients and kinetic parameters. For fuel burn up measurements, an experimental arrangement has been developed to measure the MTR fuel type burn up using the non destructive methodology based on gamma spectroscopy. The methodology considers the use of fission product ^{137}Cs for fuel elements with cooling time longer than 2 years, and the ratio $^{144}\text{Ce}/^{144}\text{Pr}$ for elements with cooling time shorter. This system was developed in 2000, and can be used whenever it is necessary.

2.2 Visual Inspection

IEA-R1 irradiated fuel assemblies have been routinely inspected using an underwater radiation resistant video camera, operated from the top of the reactor pool. The system, shown in figure 1, allows only the visualization of the surface conditions of the two external fuel plates. The system has been extensively used during the last years, to inspect reflectors, fuel assemblies and control rods.

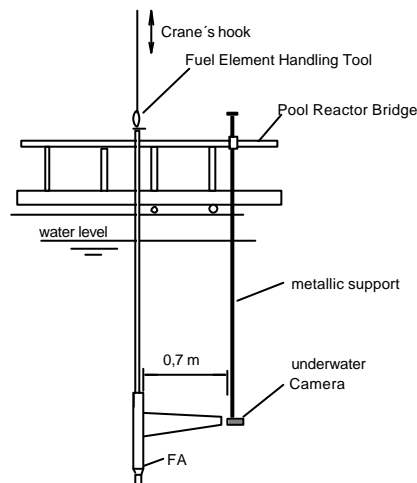


Fig. 1 - fuel element assemblies inspection system

2.3 Sipping Test /3/

Sipping tests are performed to detect and quantify failures in fuel elements. In order to perform the sipping test, the irradiated fuel assembly is withdrawn from the storage rack, having a rigid plastic pipe connected to its bottom nozzle, and placed inside an aluminum sipping tube (120 mm of diameter, 3 m length, ~ 33 l of volume), as shown in Figure 2. This first part of the

procedure is always done with the fuel assembly positioned, approximately, 2 meters of depth inside the pool water and monitored continuously by the radiological protection staff. Before the test, the sipping tube is washed with demineralized water to reduce as much as possible any kind of residual contamination of radionuclide (mainly ^{24}Na). The sipping tube with the fuel assembly inside is then lifted up and the top nozzle of the tube put above the surface of the water. It is then fixed to the pool bridge by a nylon rope. A total of 150 liters of demineralized water is then injected through the plastic pipe and flushed through the fuel assembly in order to wash it. After that, a background sample of the tube water is collected in a small plastic bottle (100 ml) and submitted to gamma -ray spectrometry analysis. The fuel assembly is then left at rest inside the sipping tube during a time interval of at least four hours. Once finished the resting time, compressed air is injected through the plastic pipe and flushed through the fuel assembly, during two minutes, in order to homogenize the solution that might contain fission products released by the leaking fuel assembly. A sample of this solution is collected in a small plastic bottle (100 ml) and submitted to gamma-ray spectrometry analysis.

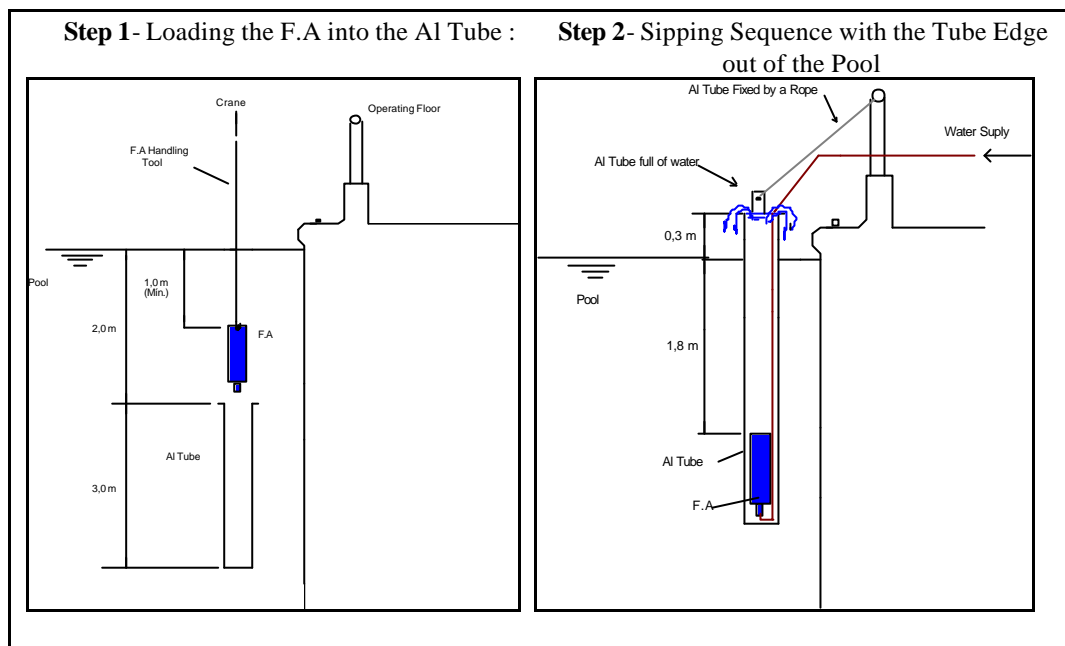


Fig. 2 - Scheme of Sipping

3. Spent fuel assemblies transportation to the United States

3.1 Spent Fuel transportation to the United States

Along 40 years of the reactor operation, 127 SFA's from the first, second and third operational cycles had been stored at the facility, 40 in a dry storage and 87 inside the reactor pool. The contract among the Nuclear Energy National Commission (CNEN/Brazil) and the Department of Energy (DOE/USA) was signed in 1998. Edlow International Co. and a Germany Consortium formed by Nuclear Cargo + Services (NCS) and Gesellschaft fur Nuklear-Service (GNS) were hired to perform the transport. The German Consortium provided 4 transport casks (two GNS-11 and two GNS-16), a transfer cask, equipment and experts to handle their equipment. IPEN/CNEN-SP performed the work necessary to accomplish Brazilian

legislation as export license, a detailed Transport and Security Plan, safeguards documents, Appendix A and so on, as well as operational and radiological protection support to the entire operation.

In 2007, thirty three (33) other fuel assemblies were identified that met eligibility requirements and were therefore eligible for shipment. Current fuel located at IPEN was effectively identical to some of the fuel returned in the 1999 shipment. NAC INTERNATIONAL provided the NAC-LWT cask for the spent fuel assemblies' transportation.

4. Plans for the future

In 2000, IAEA approved the project RLA4-18 for the biennium 2001-2002, with participation of Argentina, Brazil, Chile, Mexico and Peru to define a regional strategy for the management of the spent fuel from all RR of the region, based on the economic and technological realities of each participant country and two specific objectives to define the conditions for operational and interim storage of the SFA's for each specific reactor and to establish forms of regional cooperation for final disposal of the SFA's or its sub-products. For the success of the project, a fuel characterization was performed, and the storage options, public communication, regulation and safety were discussed. During the period of 2001-2002 IPEN-CNEN/SP started an internal discussion regarding the necessity of an interim storage facility to be built before 2009, when all positions on the fuel storage pool of the reactor will be loaded. Two possibilities were defined. The first one considers the possibility of using an installation close to the reactor building and adapts it to a dry interim storage facility. The second option considered is to store the spent fuel within a dual purpose cask which is being developed as part of the regional project. A final decision, including the emission of the safety related documents for approval of the regulatory authority, is expected to be done by the next future.

5. References

- [1] Frajndlich, Roberto; Maiorino, J. R; Perrotta, J. A; Soares, A.J. "Experience of IEA-R1 Research Reactor Spent Fuel Transportation back to United States" - IPEN/CNEN-SP Internal Report, 1997.
- [2] Soares, A.J.; Silva, J.E.R.; "Management of Spent Fuel from Research Reactors – Brazilian Progress Report (within the framework of Regional Project IAEA-RLA-4/018)" - IPEN/CNEN-SP
- [3] Perrotta, J.A; Terremoto, L.A.A; Zeitune, C.A. "Experience on Wet Storage Spent Fuel Shipping at IEA-R1 Brazilian Research Reactor" - IPEN/CNEN-SP 1996

Russian academy of sciences
SPb nuclear physics institute

**TOPICS ON CONTROL OF THE COMPOUND METAL
AND CONCRETE PROTECTION QUALITY**

Gatchina

2008

TOPICS ON GAMMA-RAY CONTROL OF THE COMPOUND METAL AND CONCRETE PROTECTION QUALITY (NUCLEAR FUEL TRAFFICKING CASK)

N.D.Shchigolev, O.M.Golubev

INTRODUCTION

In compliance with the requirements of national standards and regulations which are valid in nuclear engineering and also IAEA recommendations [1] transportation packing modules (TPM) for long-term storage and shipment of the spent nuclear fuel (SNF) have to ensure rated protection against ionizing radiation and withstand emergency impacts while preserving integrity of tightness system and radiation protection.

Special Mechanical Engineering Design Office has developed and some of JSC manufacture such a module on the basis of metal and concrete cask (TPM MCC) for SNF of RBMK-1000 reactors, nuclear-powered submarines and fleet etc. In general the structure of MCC may be presented as three coaxial steel shells the space between them being filled with superheavy concrete of high ductility and reinforced with composite grid of bars, clamps and rings.

Authors have developed a procedure to control radiation protection (RP) of this cask and RP integrity checks after dynamic testing which simulate emergency situation during transportation. Test bench of gamma-control [2,3] was designed and constructed as a technical decision of such a task (Fig. 1).

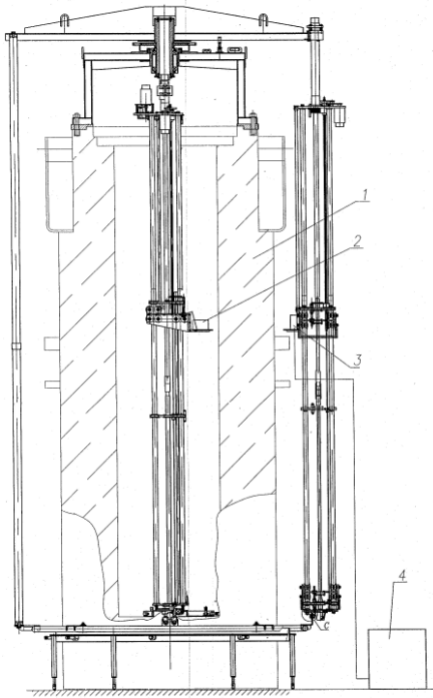


Fig.1. Test bench

- 1-Cask
- 2-Gamma source
- 3- Detector
- 4- Control unit

PROCEDURE. RESULTS ANALYSES

Technique is based on item containment wall radiography from point γ -source with successive scanning of the whole wall by pair of radioactive source – scintidetector. So one effects the determination of local values for intensity of γ -radiation (pulse counting) point by point at the item surface. Source – cobalt-60. Control of MCC corps radiation shielding is carried out with the use of the cask wall sample (WS) for minimum mass thickness.

For better visual understanding and easy processing of test results, measurement of pulse counts on the cask surface have been completed with visualization of all current information on PC display and further recording on HDD in the form of text files by a number of covered horizontal (“azimuth”) tracks during perimeters scanning. Display provides enough information: it plots a bar graph of current azimuth track - diagram in coordinates pulse count / angle of measurement (Fig. 2, 3), the track number is also displayed as well as actual time, count rates and kinematics movement, time to cycle start etc. The key purpose of bar chart is to reflect

detected defect inside concrete intermediate layer (cavity, air pocket, slot) in the form of peak value, or other count excess over average level. Defect length by perimeter may be assessed by a length of generated peak value basis (X-axis); defect height is enough precisely determined by a number of tracks where such peak or "spike" is repeated.

In the course of review and processing of data on MCC gamma-control authors have used a gradient method for treatment of results: comparison of recorded values of pulse counts for neighboring, adjacent or vertically remote azimuth tracks during scanning of cask surface.

In case of the MCC structure inequalities absence and in assumption of zero errors of measurement (statistical and systematic) the following ratio for registered values of count intensity $N_i(\mathbf{q})$ and $N_j(\mathbf{q})$ on tracks i, j at angle \mathbf{q} must be available on sundry azimuth tracks

$$\frac{N_i(\mathbf{q})}{N_j(\mathbf{q})} = 1. \quad (1)$$

Owing to difference in average values of count intensity on different tracks (e.g. due to availability of horizontal rebars) as well as probable difference in the number of registered points on various tracks (at different rate of pair S-D movement on compared tracks) ratio (1) must be replaced by

$$\Lambda = \frac{N_i(\mathbf{q}_l)}{k \cdot N_j(\mathbf{q}_m)} \approx 1, \quad (2)$$

where $k = \frac{\bar{N}_i}{\bar{N}_j}$ (\bar{N}_i, \bar{N}_j - average values of intensity on tracks i, j respectively);

$\mathbf{q}_l, \mathbf{q}_m$ - maximum close azimuth angles for registered values of intensity on different tracks.

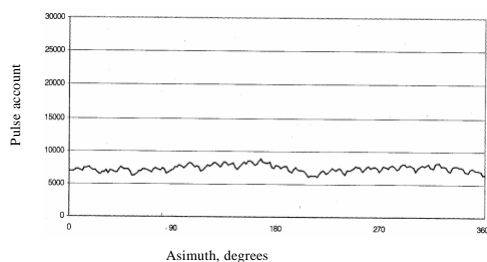


Fig.2. Exposure rate at MCC surface

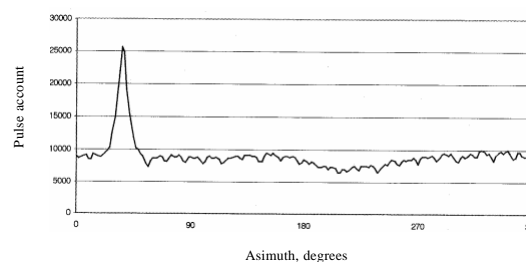


Fig 3. The same with defect

Analysis of distribution (2) obtained in the course of numerous gamma-control cycles on MCC shells demonstrates:

- gradient Λ deviations from the unit during comparison of neighbouring or enough close tracks, as a rule, shall be 15 % maximum (Fig. 4);
- difference ? from 1 for close tracks above 15% may be explained with features of corps structure or concrete filler defect;
- comparison of sufficiently remote tracks by height of MCC shell depicts presence of monotony deviations of distribution Λ from the unit associated with changing of shell shape.

Fig. 5 depicts display of filler defect by means of two tracks comparison – through the defect and out of it.

Since any defect of concrete filler leads to an increase of value Λ during comparison of count intensity in area of defect with such value on tracks without defect, in future the following assumption is taken as a criterion for defect identification in concrete filler (for maximum value of gradient due to presence of defect Λ_{def}):

$$\Lambda_{\text{def}} \geq 1,3 \quad (3).$$

This assumption is enough conservative, however it allows to exclude false identification of defect completely due to uncontrolled changes of cask shape, irregularity of S-D movement etc.

We speak also about maximum allowed area of single defect or total length of several defects by height or perimeter. Any revealed defects are reduced to equivalent area defect. Equivalency of area defect to registered defect in concrete filler is accepted here as an equality of maximum value λ for such defects.

We make also attempts analysis of available information on signal calibration to define depth of area defect.

Using of gamma-control data for MCC shell allows to introduce such a enough simple semi-empirical ratio to assess growth of signal intensity due to reduction of metal and concrete obstacle mass thickness in location of area defect in concrete filler by value $X_{def} = \mathbf{r} \times h$ (\mathbf{r} - concrete density, h - defect depth):

$$N_{max} = N_o \exp\left(\frac{X_{def}}{I}\right). \quad (4)$$

Here N_{max} - maximum intensity of count in defect location, N_o - count intensity without defect, λ - constant value defined by results of calculation and theoretical as well experimental investigations.

Very representative data for us were ones on gamma-control on the same MCC obtained during two cycles at a time interval 133 days. Activity of source ^{60}Co during above interval was dropped 0.953 between cycles vs initial activity. In case of "ideal" matching of mutual placement for a pair source - detector, and absence of statistical error it should produce the same value of average value ratio on the same tracks. Ratio of average values here is 0.93, i.e. error of measurements is 3 % maximum. Comparison is also interesting for maximum count values recorded on these tracks, since exactly this value is used to control mass thickness, therefore, MCC shell RP. These values for above track in the first and successive cycles were 8243 and 7503 pulse/s respectively, or ratio of maximum count intensity 0.91.

This ratio is exactly taken to assess error during control of MCC shell mass thickness. Above data are confirmed by comparison results for other tracks, besides evaluated error for reproduction of mutual placement for the source and detector during installation and assembly of test bench is 5 % maximum.

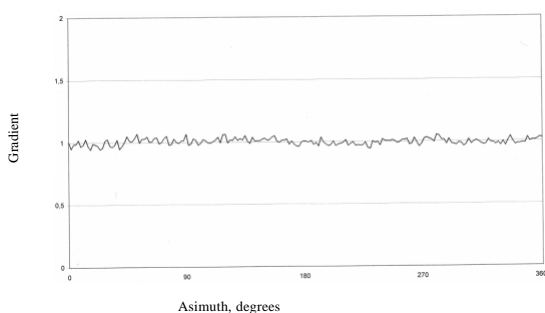


Fig.4.

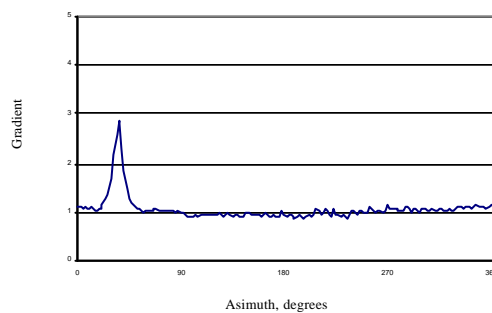


Fig.5.

RESULTS. CONCLUSIONS

Assessment on the method sensitivity of minimum defected imperfection size approaches to 20 mm.

To reveal defects the special results processing code SCAN 2D was developed. It allows to indicate flaw coordinates and linear dimensions. It's ready also to let out a conclusion about completed test.

By testing, display and processing of check results in PC the buildup of multicolor resultant chart-scanning of ER values on the whole cask surface is accumulating. It shows reliable and weak sites of protection, technological elements, bars etc. (color scale 24 hues; Fig. 6).

Selected method of the γ -control and results analysis had showed their applicability, reliability and representation during investigation of variety samples of metal and concrete casks for SNF. Durable operation of test bench as it's practical solution an accurateness of estimated design, technological and program decisions had confirmed for a hundred fretworks.

In passing it may be used for the iron casks also.

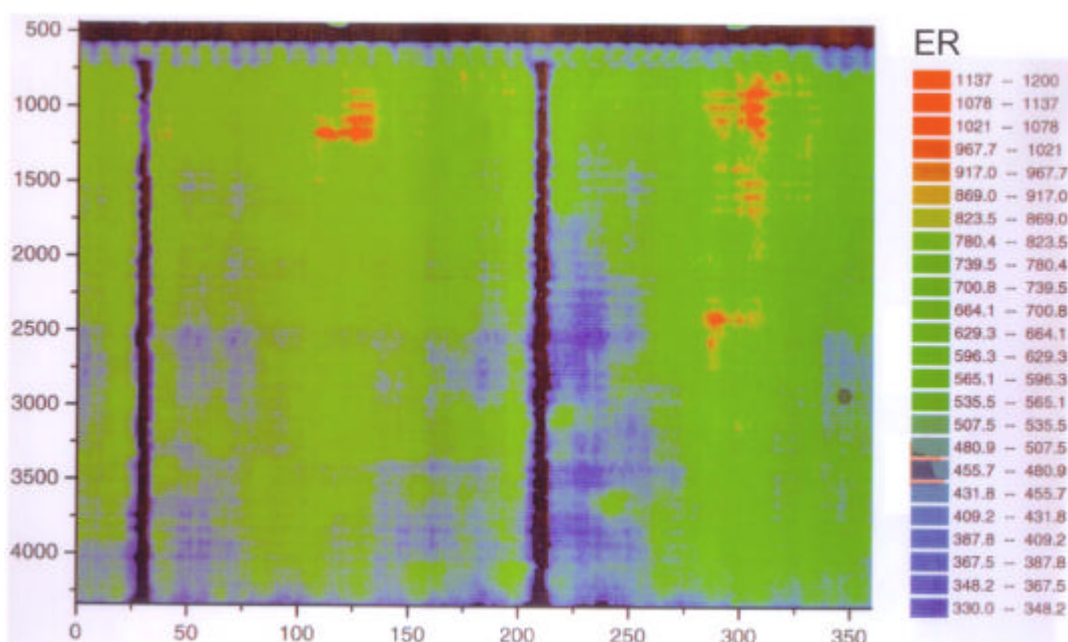


Fig.6.

REFERENCE

1. Safety regulations of the radioactive material transport ??-053-04. Radioactive substances safe transporting standards ST-1. IAEA, 1996.
2. N.D.Schigolev, Y.S.Blinnikov et al. Issue on control of radiation protection quality during manufacturing of metal and concrete casks. VII All-Russia scientific conference "Protection against ionizing radiation of nuclear engineering plants". Obninsk, 1998.
3. N.D.Shchigolev et al. The γ -ray control of metal and concrete cask corps protection. International Conference on Storage of Spent Fuel from Power Reactors. IAEA-CN-102-67P, Vienna 2003.

RESEARCH REACTOR DAMAGED SPENT FUEL MANAGEMENT

?. BARINKOV, ?. IVASHCHENKO, B. KANASHOV, S.??M?ROV

*Sosny, R&D Company
Slavsky Street, 433506, Dimitrovgrad, Russian Federation*

ABSTRACT

In the course of implementing projects on shipment of spent fuel assemblies (SFA) from research reactors (RR) the operating and shipping companies deal with problems to handle damaged SFA. The above problems concern mainly the fuel from the Russian reactors built in the fifties of the last century. This paper presents results of analysis of Russian and international experience in preparation of the damaged SFA to be stored and shipped. It demonstrates that method of preparing the damaged SFA depends on the further purposes, and type of the fuel composition is to be considered, first of all, when justifying the safe transport for reprocessing or storage.

1. Introduction

Now handling of the damaged spent fuel is an urgent problem due to expiration of lifetime of research reactors built in the fifties of the 20th century and designed by the Russian developers. No matter when the fuel damage arisen (during operation or storage), SFA are to be prepared for shipment to the reprocessing or long-term storage facilities.

Appropriate methods of preparing the damaged SFA are selected according to the further purpose (reprocessing or long-term storage). Here handling of SFA means to preserve or optimize their state so as to be appropriate for the further storage at the specified facilities, shipment to the reprocessing or long-term storage facilities.

SFA are considered to be damaged if they do not conform to the applicable standards for SFA state (e.g. ?S?-95 for SFA from the Russian research reactors) [1]. In case of absence of the standards, a special document "Technical requirements of SFA delivery" is to be developed. In any case, conformance of the SFA state to requirements of the above documents as well as safety shipment standards is evaluated [2, 3]. In the present context SFA are considered to be damaged if they contain fuel rods with leaky claddings.

2. Evaluation of RR SFA state after a long-term storage

Claddings of nearly all Russian RR SFA are made of aluminium alloy. The Russian alloy SAV-1 is sufficiently resistant to corrosion at the typical temperatures for spent fuel storage (in the range of 30-50^{??}); however even this alloy is exposed to uniform and point corrosion after a wet storage during 30 years at the nominal parameters (water electrical conductivity is no less than 5 $\mu\text{Sm}/\text{m}$, content of chloride anions is less than 1 $\mu\text{g}/\text{kg}$). When the Al-cladding is 1 mm thick, a storage time of 43 ± 3 years is critical [4]. I.e. the most SFA claddings unloaded from cores in the fifties-sixties of the last century are damaged due to corrosion. Problem is that it is easier to change storage type for all "old" RR SFA based on aluminium than to separate them as leaky or leak-tight ones (which in 3-5 years will be failed too) in case of the absence of proper criteria.



3. Features of handling of leaky SFA with different fuel types

All other things being equal, the corrosion damage level of fuel rod claddings depends on cladding material. But consequences of their leakage and safety of the further RR SFA handling are directly relate to the type of fuel composition.

At first, metal uranium was the main fuel material for RR operation. Due to its low safety, metal uranium is no longer used but a lot of nuclear fuel containing metal uranium is stored at the RR sites. E.g. such fuel was delivered in the fifties to the heavy water reactor of the “Vinca” Institute (former Yugoslavia). Due to its high corrosion rate, hydrogen release, hydrogenation susceptibility and, as a result, explosion hazard of SNF containing metal uranium, it is required to make such SFA safe as soon as possible.

Handling of SFA based on UAl_3 intermetallide alloy or its dispersion in Al matrix is safer, as the Al matrix acts as an additional barrier to fission product release. Such fuel was delivered by the Russian suppliers for the VVR, ITR and MR reactors. But in view of high corrosivity of uranium alloys, special measures are to be taken to provide a required level for the safe storage.

Since the seventies of the last century a fuel composition based on uranium dioxide microparticles dispersed in metal (mainly Al) matrix was widely used. Two safety barriers (cladding and matrix) with high corrosion resistance of uranium dioxide allow considering this fuel to be the safest one for the handling. An exception is a fuel composition based on magnesium matrix; enhanced safety measures are required for this fuel fabricated at the early stages of RR SFA operation (e.g. the EK-10 fuel rods) due to the high chemical activity of magnesium.

Table 1 shows stability rating of the main fuel compositions applied for manufacture of the RR fuel assemblies [5,6].

Table 1.

Stability of different fuel compositions under wet storage conditions

	Metal U	U alloy	UO ₂ in metal matrix
Corrosion resistance under the “good” water conditions (no electrochemical corrosion)	Low (about 200 $\mu\text{m}/\text{year}$)	Good (about 5 $\mu\text{m}/\text{year}$ for UAl alloy)	High: corrosion rate of the matrix (Al – less than 1 $\mu\text{m}/\text{year}$), UO ₂ – stable.
Corrosion resistance under the “bad” water conditions (indicated by electrochemical corrosion)	Low (complete fuel failure in the salt water during one year storage is possible).	Satisfactory for Al- and Mo-alloys.	Good.
Explosion safety	Hydrogen, metal uranium and its hydride released during corrosion are explosive.	Safe	Safe
Ability to contain fission products (FP)	Complete release of water soluble FP during corrosion	Release of 1-10% of water soluble FP (depending on alloy).	The most FP are contained in uranium dioxide and corrosion products

The international experience in SNF handling based on features of different fuel compositions. E.g. French strategy of SNF handling depends on fuel type [7]: the “old” SFA with metal uranium are stored in the CASCAD dry storage in Cadarache and SFA based on uranium dioxide are placed in the water pools. The American program “Return of Spent Nuclear Fuel from Foreign Research Reactors to the United States” considers fuel composition type to be most important criteria for selection of any further activities concerning SNF [8].



Authors of the present paper dealt with the above problem in the course of preparation of SNF from the RA reactor (the “Vinca” Institute, Serbia). Two types of fuel elements – metal uranium fuel and UO_2 dispersed in Al matrix – were stored at the reactor-site storage facility under water with very improper characteristics (electrical conduction was in the range of 50-500 $\mu S/m$, chloride content - up to 70 mg/l) for a long time (48-25 years). Fuel elements were loaded in sets of 10-12 pcs. into the special stainless canisters, initially filled with deionized water; this water was not renewed later on. Water volumetric activity (Cs-137 activity in water) was measured in 200 canisters containing fuel elements of the first or second type; 50 canisters contained fuel elements of both types. Measurement results [9] showed that the water volumetric activity did not exceed 100 Bq/ml in the canisters with UO_2 , while the water activity in the canisters containing metal uranium was higher than 1000 Bq/ml.

Distribution of canisters according to Cs-137 release from SFA with metal uranium fuel and fuel dispersed in Al matrix is showed in Fig.1. Data on canisters with both fuel types are given too: number of such canisters takes an intermediate position.

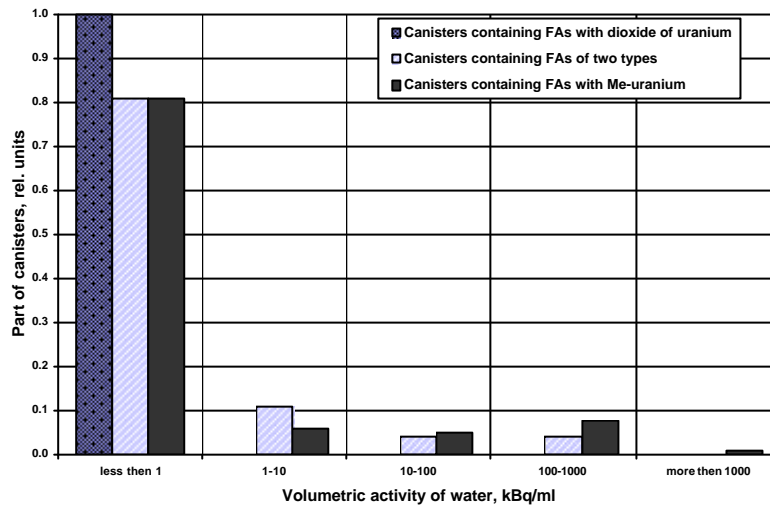


Fig. 1. Distribution of canisters according to volumetric activity of water.

It is proved by the results of water activity analysis that material of fuel composition is the most important criterion for strategy of leaky SFA handling.

4. Storage of RR SFA

Method and time of SFA storage in the reactor-site pools and at storage facilities are justified by a developer of the specified FA type. Requirements for SFA storage conditions are stated in the FA operating rules.

All SFA from the Soviet RR were intended for the wet storage after their irradiation (just as SFA from the most foreign RR). At the time of development of the Soviet RR, SFA were supposed to be shipped to a reprocessing facility a short time after a minimum cooling time; therefore the specified (and justified) storage time for the RR SFA did not exceed 8 years and issues of a long-term storage were not duly taken into account.

At the post-Soviet time, SFA are usually stored for a long time. As a result, storage of SFA with leaky fuel rods is an urgent problem now. Research facilities follow the strategy of a delayed shipment of SFA (in expectation of the better days) or extension of storage time in order to decrease shipment frequency.

A radical enhancement of water quality using chemical water treatment is usually applied to extend the wet storage time. But this method is efficient only for the leak-tight fuel.



As a rule, with the approach of critical storage time, a decision on changing a storage technology is made.

In Czech Republic [10] the wet storage was changed to the dry one using concrete unsealed containers with the purpose to extend storage time of the leak-tight SFA. The leak-tight SFA in Hungary [11] and Poland [12] were also prepared (dried) for storage and loaded into sealed capsules; now these capsules are stored under water.

Change to the dry storage is efficient for the leak-tight SFA, but it is a very expensive approach as to the leaky SFA because of the strict requirements for drying technology and difficulties for justification of storage safety [13]. There are no easy solutions of storage methods applied to the leaky SFA at present time.

5. Preparation to shipment of the damaged SFA

In the course of planning of SFA handling in the reactor-site pools and at storage facilities, the operating companies can choose any technology but their choice is restricted by approval by their regulatory authorities. When SFA are shipped to an another facility, the following requirements for packages with SFA should be added – national normative requirements for shipment conditions, international normative requirements for shipment conditions, general regulation of SNF handling on the territory of the consignor and consignee as well as technical requirements of a company which accepts SNF.

If a fuel is classified as damaged, the stage “Preparation to shipment” is obligatory – only work scope is variable. Besides, the accepting company (storage or reprocessing facility) specifies its additional requirements for the SFA state. Thus, to perform shipment of the leaky SFA, the safe handling of SFA should be justified both by the consignor and consignee as well as technical specifications for delivery are developed for the specified fuel type.

One of the methods to preserve the safe state of SFA is capsulation. A capsulation technique and capsule design depend on the further purpose of SNF handling:

- o Temporary (but sufficiently long-term) storage on the territory of an operation company,
- o Shipment to a reprocessing facility,
- o Shipment to a facility for a long-term SNF storage (dry or wet),
- o Shipment to a facility for the final disposal of the leaky SNF.

Capsulation, including SNF drying, filling of a canister with rare gas and sealing, is a difficult and labour-intensive process. Residual water (free or hydrogenated) causes a sealed canister to be explosive due to hydrogen accumulation. The normative documents do not require complete sealing of the canisters, they just specify limits for fission product release to the environment. A safe shipment is provided by characteristics of the modern containers.

Therefore, if the further purposes of SNF handling allow applying unsealed canisters, it is necessary to consider such possibility. Features of fuel composition, corrosion state of fuel claddings and SNF damage level make it possible to justify safe design of the unsealed canisters for achievement of the specified above purposes.

6. Conclusions

Shipment of SNF to a reprocessing or long-term storage facility is an optimal solution as to the safe handling of the damaged SNF. In the course of SFA preparation to their shipment, it is important to fulfill both requirements for the safe shipment and conditions of the good acceptance by a reprocessing or storage facility. Preparation to shipment of the damaged SFA is obligatory.

Due to ability to contain fission products by the fuel composition as well as to handle leaky SFA by the reprocessing facilities, it is possible to transport leaky RR SFA to be reprocessed using unsealed capsules.

7. References



1. Industry Standard. «Spent fuel assemblies of nuclear research reactors. General requirements to delivery (OST 95 10297-95)».
2. «Safety rules at radioactive material shipment (NP-053-04)», Rostekhnadzor, 2005.
3. International Atomic Energy Agency, «Regulations for the Safe Transport of Radioactive Materials», TS-R-1, 2005.
4. S. Efarov, B. Kanashov, S. Komarov at al. "Safety Aspects of Spent Nuclear Fuel Shipment from "Vinca" Institute, The Fifth International Conference (YUNSG2004) of the Yugoslav Nuclear Society September 27-30, 2004, Belgrade, Serbia & Montenegro.
5. Bruce A. Hilton. «Review of Oxidation Rates of DOE Spent Nuclear Fuel». Nuclear Technology Division, Argon National Laboratory, November 2000.
6. Martin G. Plys, D. R. Dunkan: «Uranium Pyrophoricity Phenomena and Prediction», SNF Division, Fluor Hanford, October 2000.
7. J. Chenais "General Policy and Strategy for French Naval Spent Fuel Management", in book "Scientific and Technical Issues in the Management of Spent Fuel of Decommissioned Nuclear Submarines", Springer Netherlands, 2006.
8. O. Keener Earle. A Perspective on U.S. Spent Nuclear Fuel Policy, in book "Scientific and Technical Issues in the Management of Spent Fuel of Decommissioned Nuclear Submarines", Springer Netherlands, 2006.
9. Institute of Nuclear Sciences "Vinca" Centre for Nuclear Technologies and Research, "NTI": «Verification of Stainless Steel Containers in The Spent Fuel Storage», Final Report on the IAEA Service Contract SCG4003-89087A, Vinca – NTI – 140, Vinca, February 2007.
10. «Czech National Report on the Safety of Spent Fuel Management and on the Safety of Radioactive Waste Management», February 2003.
11. S. Tozsér, «Spent Fuel Management: Semi-dry storage». KFKI Atomic Energy Research Institute, Budapest, Hungary, IAEA Scientific Forum, 21-22 September 2004, Vienna, Austria.
12. «National report of poland on compliance with the obligations of the joint convention on the safety of spent fuel management and on the safety of radioactive waste management», October 2005.
13. «Issues of preparation of failed research reactor spent nuclear fuel for shipment to the reprocessing facility», O. Barinkov, B. Kanashov, S. Komarov, A. Smirnov, "Sosny" Company, Moscow.



PREPARATION AND ORGANIZATION EXPERIENCE OF SFA TRANSPORTATION FROM LVR-15 RESEARCH REACTOR (NRI, REZ, CZECH REPUBLIC) TO THE RUSSIAN FEDERATION

?. DOROFEEV, S.V. KOMAROV, S.N. KOMAROV, ?. SMIRNOV
R&D S0SNY
Derbenevskaya naberejnaya, 115114 Moscow – Russian Federation

F. PAZDERA, F. SVITAK, J. KYSELA
NRI Rez
Husinec-Rež 130, 250 68 Rež – Czech Republic

ABSTRACT

Experience of preparation and arrangement of transportation of LVR-15 SFAs to the Russian Federation with the purpose of their interim technological storage, reprocessing and handling with reprocessing products is stated in present report. Main stages to provide realization of SFAs transportation are summarized and described: type of used package, its adaptation and certification, peculiarities of SFAs preparation for transportation, stages and peculiarities of development of permissible documentation necessary to provide transit and import of SFAs to the Russian Federation, specifics of handling with LVR-15 SFAs and their reprocessing products at FSUE "PA "Mayak" radiochemical plant.

1. Introduction

In the frame of international agreement between the RF and USA signed on May 2004, the work on import of spent nuclear fuel (SNF) of research reactors (RR) constructed with the assistance of USSR at different countries of Europe, Asia and Africa (RRRFR program) to the Russian Federation.

Today two projects are successfully performed – import of spent fuel assemblies (SFA) from Uzbekistan (2005) and Czech Republic (2007), preparation of SFA import from other four countries in 2008 is conducted (Latvia, Bulgaria, Hungary, Kazakhstan).

2. General description of LVR-15 research reactor SFAs

Nuclear Research Institute was established in 1955 (city of Rez near Prague). In 1957 was put into operation VVR-S reactor (nowadays LVR-15) with power 2 MWatt (nowadays 15 MWatt), which still operate up to present days.

Evolution of nuclear fuel used at reactor:

Fuel assemblies (FAs) of EK-10 type (10% enrichment by U-235); IRT-2M type FA (80% enrichment by U-235); IRT-2M type FA (36% enrichment by U-235).

In accordance with foreign trade contract Czech party declared for removal to the Russian Federation IRT-2M type SFAs – 343 pieces, EK-10 type SFAs – 184 pieces, irradiated fuel elements of EK-10 type – 657 pieces.

3. SFA preparation for removal to the Russian Federation

EK-10 type SFAs and EK-10 type fuel elements were long time stored into special containers. Specialists of NRI according to the agreement with FSUE "PA "Mayak" have made a decision to place EK-10 type SFAs and EK-10 type fuel elements before shipment into special transport canisters made from stainless steel and which is a part of SKODA VPVR/M Packaging. Canister designs were agreed with FSUE "PA "Mayak".

IRT-2M type SFAs underwent leakage testing before loading into casks. Two IRT-2M type SFAs were considered non-tight (condition – gas looseness) during performance of sipping tests. These 2 SFAs together with 5 IRT-2M type SFAs, which considered non-tight during operation in the reactor, also were placed into transport canisters according to the decision of NRI specialists.

Extraction of SFAs and EK-10 type fuel elements from storage containers and packing them and 7 IRT-2M type SFAs into transport canisters were performed in special hot cell. SFA and fuel elements are placed in 549 cells of 16 SKODA VPVR/M packaging.

4. SKODA VPVR/M cask preparation

SKODA VPVR/M casks was developed and manufactured to transport SFAs by the request of NRI at Skoda JS a.s. SKODA VPVR/M cask is passed the certification in Czech Republic with issuance of certificate for package design CZ/048/B(U)F-96(Rev.1) with validity until July 1, 2011. In Russia cask is passed full examination considering requirements of "Safety regulations for transportation of radioactive materials" (NP-053-04) with issuance of certificate for package design RUS/3065/B(U)F-96 with validity until January 23, 2009. Czech certificate is also endorsed in Slovakia and Ukraine.

Use of foreign cask in the program of Russian-origin research reactor fuel repatriation to the RF was for the first time. In order to prepare for acceptance of SKODA VPVR/M cask at FSUE "PA "Mayak" the following works were performed:

designed and manufactured the auxiliary equipment, purchased the standard equipment which allow SKODA VPVR/M cask handling in accordance with transport and technological scheme of radiochemical plant;

developed technological documentation determining handling order with SKODA VPVR/M cask;

performed theoretical and practical training of personnel maintaining SKODA VPVR/M cask;

performed full-scale testing of head prototype of SKODA VPVR/M cask at radiochemical plant.

The conclusion regarding readiness of FSUE "PA "Mayak" to accept NRI SFAs into SKODA VPVR/M cask was made in accordance with testing results.

FSUE "PA "Mayak" has experience on reprocessing of SFAs of IRT-2M and EK-10 (IRT-1000) type, therefore present technology of radiochemical plant allows successful reprocessing of this fuel. Stated type of fuel is introduced to the radiochemical plant regulations. FSUE "PA "Mayak" has all necessary licenses to handle SFAs and their reprocessing products.

Separate certificate RUS/3065/B(U)F-96? was developed to transport SFAs into SKODA VPVR/M cask on the territory of the Russian Federation with validity until 23.03.2010.

5. Development of permissible documentation to provide import of SFAs to Russia

Development of permissible documentation to provide import of SFAs to Russia is extremely difficult problem especially in the part of preparation of necessary documentation in Russia. This is stipulated by peculiarities of Russian legislation demanding development of Unified project of SFA import. Unified project is a set of documents consisting of the following: draft of foreign trade contract, special ecological program financing at a part of costs funding to handle and reprocess SFA; justification of radiation risk mitigation and enhancement of ecological safety level as a result of Unified project implementation; environmental impact assessment; meeting minutes of public hearings of the Unified project with civilians and public organizations and etc. Unified project documents should undergo state ecological expertise review in specially authorized RF regulating body – Rostekhnadzor. Only at positive outcome Rostekhnadzor commission on Unified project documents signing of foreign trade contract is possible.

Realization of Czech project was additionally complicated by necessity to agree equivalent activity criterions of SFAs imported with reprocessing purpose and activity of returned RW. In this connection development and agreement of special methods determining quantity, inventory, composition, package type of returned radioactive waste to Czech Republic generated during reprocessing NRI SFAs. Such methods in connection with NRI SFA were developed by R&D Sosny Company specialists involving FSUE “PA “Mayak” specialists, agreed with specialists of NRI, Rostekhnadzor, Rosatom.

Preparation, agreement, state ecological expertise of Unified project of SFA import from Czech Republic to Russia is required cooperation of more than forty Russian organizations including public ones. Total time of Unified project documents development is 13 months.

Preparation of international documents to provide SFA transit on the territory of Slovakia and Ukraine is based on the Agreement between RF Government, Slovakia Government, Cabinet of Ministers of Ukraine, Czech Republic Government about cooperation in the field of nuclear materials shipment between the Russian Federation and Czech Republic through the territory of Slovakia and Ukraine of 14.03.1998. Conditions of arrangement and implementation of special goods shipment from Czech Republic to the Russian Federation by transit through the territory of Slovakia and Ukraine were specially developed and agreed by competent authorities of Czech Republic, Slovakia, Ukraine and Russia in the development of this Agreement.

Transit approvals through the territory of Slovakia and Ukraine were obtained after submission of necessary documents including foreign trade contract between NRI and JSC “Tenex”, Czech license for SFA export, Russian license for SFA import to the competent authorities of these countries.

Over thirty international agreements, licenses and permissions should be prepared and concurred for SFAs import implementation. Over 12 months are required for this.

6. Shipment arrangement of packages with SFAs from Czech Republic to Russian Federation

Interested parties of Czech Republic, Russian Federation, Slovakia and Ukraine after developmental work on several transport scheme options of SFA shipment from Czech Republic to Russia are reached the following agreements:

Empty special warranty train for special goods shipment is formed with its full complement at FSUE “PA “Mayak” and directed through the territory of Ukraine to the Slovakia station at Slovakian-Ukrainian border. NRI is provided shipment and arrival of transport completed by

JSC "Czech Railway" with special goods by agreed date to the same station. Then reloading of ISO-containers with SKODA VPVR/M cask from Czech special warranty train to the Russian train was performed.

After the reloading of ISO-containers, special warranty train with special goods went to the Russian Federation by transit through the territory of Ukraine.

Responsibility for all risks concerned with SFA shipment in accordance with foreign trade contract conditions is rested on NRI until the moment of SFA transfer at Ukrainian – Russian border. Further responsibility for the risks rests at FSUE "PA "Mayak".

7. Conclusion

RRRFR program realization in the part of RR SFAs return to the Russian Federation in contrast to return of non-irradiated nuclear fuel, which import is practically finished, is on the initial stage. Moreover, import of SFAs to the Russian Federation is combined with the necessity of solution of much more serious tasks: legal, economic, technical, and organizational, and needs close cooperation between all organizations involved to the project. In this connection, experience of arrangement of SFA import from Czech Republic to the Russian Federation is demonstrative and extremely important. It is necessary to use deep and high-quality analysis of existing work experience for successful realization the program in whole.

CALCULATION OF NEUTRON FLUX TRANSIENTS

F. REISCH

*Nuclear Power Safety, KTH, Royal Institute of Technology
Alba Nova, Roslagstullsbacken 21, S-106 91 Stockholm – Sweden*

ABSTRACT

When withdrawing or inserting control rods in the core of a research reactor generally only the end values of the resulting neutron flux is calculated. This code offers a possibility to - in advance - depicture the whole course of changes of the neutron flux. This computer program was developed first of all for application at research reactors by students. However there is no research reactor in Sweden anymore. Therefore the code verification was made from an earlier start-up sequence of a Swedish Pressurized Water Reactor. The purpose of this presentation is to convince Research Reactor Operators to test the validity of the code and if it is successful, apply it in the training of nuclear engineering students

1. Introduction

The classical reactor kinetic equations with six groups of delayed neutrons (point kinetics) are not solved analytically. In the presented program the fuel and the moderator thermal dynamic equations are coupled to the reactor kinetic equations. The equation system is solved numerically. This short program is suitable to be used by nuclear engineering students when practicing at research reactors. The parameters to be used are depending on the reactor design of course. As there is no research reactor in Sweden the program was verified with data from the start up phase of a Pressurised Water Reactor. The result of the calculations and the measured data are in reasonable agreement. The measured values and the results of the calculations are presented graphically. Mr. Fredrik Winge reactor physics specialist at the Ringhals Nuclear Power Plant supplied the chart with the measured data and was a valuable discussion partner.

2. The simplified neutron kinetics equations

are
$$\frac{dN}{dt} = \frac{dk - \beta}{l} N + \sum_{i=1}^6 \lambda_i c_i \quad \frac{dc_i}{dt} = \frac{\beta_i}{l} N - \lambda_i c_i$$

Here

t time (sec)

N neutron flux (proportional to the reactor power)

dk change of the effective neutron multiplication factor (k_{eff})

β sum of the delayed neutron fractions (here 0.006502)

β_i the i:th delayed neutron fraction

l neutron mean lifetime (here 0.001 sec)

λ_i i:th decay constant (sec^{-1})

c_i concentration of the i:th fraction of the delayed neutrons' precursors,

At steady state, when time is zero $t=0$ all time derivatives are equal to zero, all $d/dt=0$ and the initial value of the relative power equals unity $N(0)=1$, and also no reactivity perturbation is present $dk=0$

$$N(0)=1 \quad \frac{dN}{dt}=0 \quad dk=0 \quad \sum_{i=1}^6 \lambda_i c_i = \frac{\beta}{l} \quad \frac{dc_i}{dt}=0 \quad c_i(0) = \frac{\beta_i}{l \lambda_i}$$

Table 1: Delayed neutron data for thermal fission in U^{235} is used

Group	1	2	3	4	5	6
Fraction β_i	0.000215	0.001424	0.001274	0.002568	0.000748	0.000273
Decay constant λ_i	0.0124	0.0305	0.111	0.301	1.14	3.01

Table 2: The initial values of the delayed neutrons' precursors are;

i	1	2	3	4	5	6
$c_i(0)$	17.3387	46.6885	11.4775	8.5316	0.6561	0.0907

Using the MATLAB notations; $x(1)=N$ $x(2)=c_1$ $x(7)=c_6$

3. Fuel

The fuel temperature change (T_{Fuel}) follows after the power with a time delay (t_{Fuel})

$$T_{Fuel} = \frac{c_{NF} N}{1 + p t_{Fuel}}$$

T_{Fuel} Fuel temperature change

N Relative neutron flux proportional to the relative power

c_{NF} fuel temperature proportionality constant to relative power

p Laplace operator d/dt , 1/sec

t_{Fuel} thermal time constant of the fuel, here 5 sec

t time, sec

The differential equation form is

$$T_{Fuel} + t_{Fuel} \frac{dT_{Fuel}}{dt} = c_{NF} N ; \quad \frac{dT_{Fuel}}{dt} = \frac{c_{NF}}{t_{Fuel}} N - \frac{1}{t_{Fuel}} T_{Fuel}$$

At steady state (equilibrium) $d/dt=0$ $N(0)=1$

Suppose that at zero power the fuel temperature changes by 0.001 °C when $N=1$ and thereby $c_{NF}=0.001$

$$\text{Suppose } t_{Fuel} = 5 \text{ sec} \quad \frac{1}{t_{Fuel}} = 0.2 \quad \frac{c_{NF}}{t_{Fuel}} = 0.0002 \text{ °C/sec}$$

With the MATLAB notation $x(8) = T_{Fuel}$

and the neutron kinetics equations can be expanded to include the fuel dynamics
 $0.0002 \cdot x(1) - 0.2 \cdot x(8)$

3.1 The Doppler reactivity of the fuel is

$$dk_{Fuel} = k_{Fuel} (T_{Fuel} - T_{Fuel}(0))$$

Here

dk_{Fuel} the reactivity contribution of the fuel temperature change, at the initial phase ($t=0$), at steady state (equilibrium) is zero $dk(0)_{Fuel} = 0$

k_{Fuel} Fuel temperature coefficient (Doppler coefficient) here is $-3.1 \text{ pcm}/^\circ\text{C}$

The reactivity of the Fuel's Doppler effect is

$$dk_{Fuel} = k_{Fuel} \cdot (T_{Fuel} - T(0)_{Fuel}) = -3.1 \cdot 10^{-5} \cdot (T_{Fuel} - 0.001)$$

with MATLAB notation; $\Delta k_{fuel} = -3.1 \cdot 10^{-5} \cdot x(8) + 0.0031 \cdot 10^{-5}$

4. Moderator

The differential equation for the moderator is similar to that of the fuel, when the moderator thermal time constant is much bigger then the fuel thermal time constant $t_{Moderator} \gg t$:

$$T_{Moderator} + t_{Moderator} \frac{dT_{Moderator}}{dt} = c_{NM} N$$

$$\frac{dT_{Moderator}}{dt} = \frac{c_{NM}}{t_{Moderator}} N - \frac{1}{t_{Moderator}} T_{Moderator}$$

$T_{Moderator}$ Moderator temperature change

$t_{Moderator}$ Moderator thermal time constant, here 100 sec

c_{NM} Moderator temperature proportionality constant to the relative power, suppose that at zero power operation the moderator temperature change is only $0.0005 \text{ }^\circ\text{C}$ when the relative power $N=1$. Then $c_{NM}=0.0005$

Suppose $t_{Moderator} = 100 \text{ sec}$ $\frac{1}{t_{Moderator}} = 0.01/\text{sec}$ $\frac{c_{NM}}{t_{Moderator}} = 0.0005 \cdot 0.01 \text{ }^\circ\text{C}/\text{sec} = 0.000005$

With the MATLAB notation $x(9) = T_{Moderator}$; and the neutron kinetics equations can be expanded to include the moderator dynamics too; $0.000005 \cdot x(1) - 0.01 \cdot x(9)$

4.1 Moderator reactivity contribution from temperature change

$$dk_{Moderator} = k_{Moderator}(T_{Moderator} - T(0)_{Moderator})$$

Here

$dk_{Moderator}$ the reactivity contribution of the moderator temperature change at the initial phase (t=0), at steady state (equilibrium) is zero $dk(0)_{Moderator} = 0$

$k_{Moderator}$ Moderator temperature coefficient here is - 0.6pcm/°C

The reactivity contribution from the changing moderator temperature is

$$dk_{Moderator} = k_{Moderator} \cdot (T_{Moderator} - T(0)_{Moderator}) = -0.6 \cdot 10^{-5} \cdot (T_{Moderator} - 0.0005)$$

with MATLAB notation; DeltaKmoderator=-0.6*10⁻⁵.x(9)+0.0003*10⁻⁵

5. Control Rods




dk_{CR} the reactivity contribution of the control rods' movement, here with the maximum value is 50 pcm (~8 cent, 1\$~650 pcm)
The movements of the rods and the corresponding reactivity changes are given in the 1st and 3rd chart

5.1 The reactivity balance with the control rods, the fuel's Doppler effect and the moderator's temperature effect

$$dk = dk_{CR} + dk_{Fuel} + dk_{Moderator}$$

The reactivity balance with MATLAB notation;
DeltaK = DeltaKcr + DeltaKfuel + DeltaKmoderator

6. Comparison with Measured Data

In the **1st chart** there are the measured data,
the neutron flux is the light blue curve 
the control rod reactivity is the yellow curve 
and the dark blue dots  are indicating the control rod steps.

In the **2nd chart** the calculated relative neutron flux is displayed, the curve is pretty much in agreement with the measured data

In the **3rd chart** there is the schematic of the control rod reactivity used in the calculations

In the **4th chart** there are the characteristics of the fuel and moderator temperature increase. The values are very small as here the calculations are performed for the zero power operation when practically no power is generated in the fuel and transferred into the moderator. However

the curves clearly demonstrate that the fuel's thermal time constant is much smaller than that of the moderator's

Figure 1: 1st chart, measured data

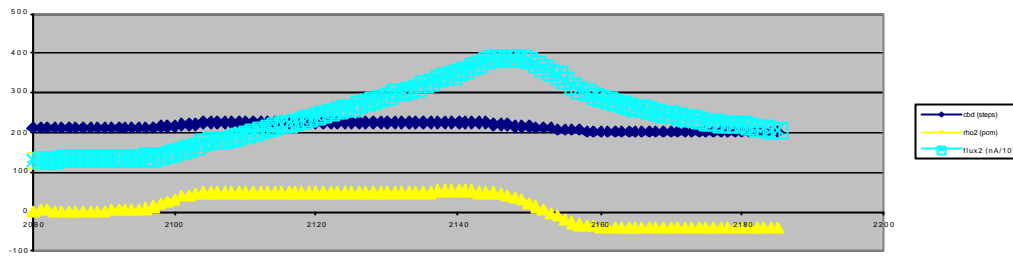


Figure 2; 2nd chart, calculated relative neutron flux

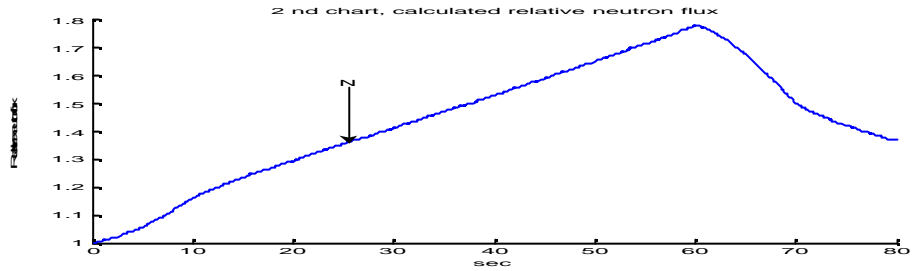


Figure 3; 3rd chart, schematic of the control rod reactivity

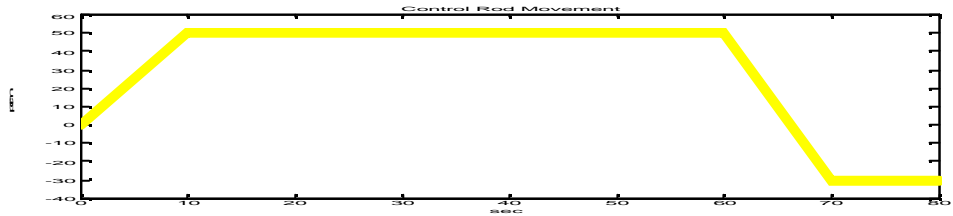
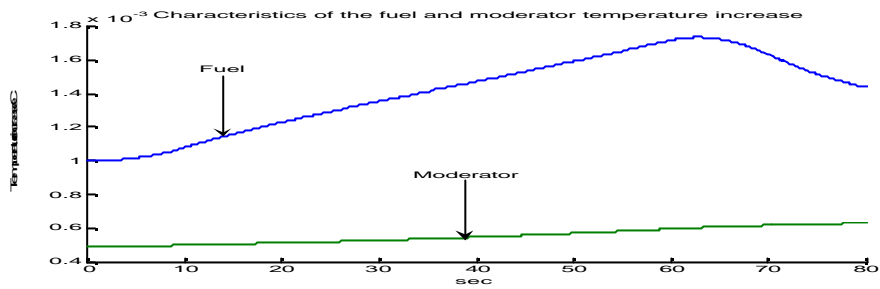


Figure 4; 4th chart, characteristics of the fuel and moderator temperature increase



7. The Code

contains two parts

Part one

%Save as xprim9FM.m

```
function xprim = xprim9FM(t,x,i)
```

```
DeltaKcr=i*10^5;
```

```
DeltaKfuel=-3.1*10^5*x(8)+0.0031*10^5;
```

```
if t>=0 & t<10
```

```
    DeltaKcr=((i*10^5)/10)*t;
```

```
end
```

```
if t>60 & t<70
```

```
DeltaKcr=(10^5)*(i-8*(t-60));
```

```
end
```

```
if t>70
```

```
    DeltaKcr=-30*(10^5);
```

```
end
```

```
DeltaKmoderator=-0.6*10^5*x(9)+0.0003*10^5;
```

```
DeltaK=DeltaKcr+DeltaKfuel+DeltaKmoderator;
```

```
xprim=[(DeltaK/0.001-
```

```
6.502)*x(1)+0.0124*x(2)+0.0305*x(3)+0.111*x(4)+0.301*x(5)+1.14*x(6)+3.01*x(7);
```

```
0.21500*x(1)-0.0124*x(2);
```

```
1.424000*x(1)-0.0305*x(3);
```

```
1.274000*x(1)-0.1110*x(4);
```

```
2.568000*x(1)-0.3010*x(5);
```

```
0.748000*x(1)-1.1400*x(6);
```

```
0.273000*x(1)-3.0100*x(7);
```

```
0.000200*x(1)-0.2000*x(8);
```

```
0.000005*x(1)-0.0100*x(9)];
```

Part two


```
%Save as ReaktorKinFM.m
```

```
figure  
hold on  
for i=50 %i is the max Control Rod reactivity i pcm  
[t,x]=ode45(@xprim9FM,[0 80],[1; 17.3387; 46.6885; 11.4775; 8.5316; 0.6561; 0.0907;0.001;  
0.0005],[],i);  
plot(t,x(:,1:1))  
end  
hold off
```

8. References

University text books on nuclear engineering and control engineering contain the applied equations and text books on information technology and numerical analyses contain the applied method used to solve the differential equations.

USING MONTE CARLO INSTRUMENTATIONS CODES FOR THE OPTIMIZATION OF HIGH FLUX RESEARCH REACTORS

M. ENGLERT and W. LIEBERT

*Interdisciplinary Research Group in Science, Technology and Security (IANUS)
Darmstadt University of Technology, Hochschulstr.4a, 64289 Darmstadt, Germany*

ABSTRACT

Optimizing a neutron source one has to take into account that the performance of the system is not only dependent on the maximum flux, but is a function of available beam time per year, number and efficiency of neutron guides and instruments and available flux at the experiment. Of course to design or redesign a research reactor the first and inevitable steps of the optimization procedure are neutron simulation calculations of the reactor core. To assess the performance of the complete system it would be well-advised to expand the model beyond the moderator tank and address the experimental devices as well, right from the beginning of the optimization process. To that end it is possible today to simulate virtually a complete experiment using a variety of Monte Carlo codes which track the propagation of neutrons through the neutron guides to the instrument. So far, we have used MATHEMATICA as a tool for our simulation routines addressing the reactor core optimization of Research Reactors, which have to be converted. Now, we implemented also a linkage routine between MCNPX and the neutron ray-tracing code MCSTAS within MATHEMATICA. This code system is capable of assessing and quantifying changes in performance of a high flux research reactor from core to experiment. The tools might prove useful to assess overall strategies for design or conversion cases, by making the various trade-offs between neutron flux, neutron quality, costs of design or conversion measures and neutron usage at experiments more transparent.

1. Introduction

From year to year, the global threat from nuclear weapons usable material becomes more imminent in a rapidly changing world with nations seeking to acquire nuclear weapons and with the risks of nuclear terrorism. A policy of non-proliferation and programs for the reduction of risks associated with nuclear weapon usable materials get the more and more important therefore. In the case of civilian use of Highly Enriched Uranium (HEU) the only way to make technologies more proliferation resistant and to avoid the intrinsic dual-use capability, is a conversion of existing technologies and machines and the design of future technologies for the use of LEU only. Thus it might be possible to find technical solutions to abstain from HEU usage completely in the future. However, especially in the case of HEU usage, there has still a lot to be done [1] and it is evident that a global effort is necessary to reach the goal. Each case, which may be an exemption from such a global effort, either out of physical, historical or other reasons, will weaken the overall effort considerably.

Usually an operator either for a facility to be converted or to be build, will base his decision of using HEU or LEU on technical, scientific and economic arguments, but also organisational (e.g. fuel supply) or political rationales have to be considered. It would be necessary and helpful to study in more detail some historical conversion cases and construction decisions, and to investigate why a specific path was chosen and what where the arguments [3].

Especially for the conversion of existing HEU machines, in each case the question must be answered, if a conversion is technically feasible and what are the gains or losses for the operator and users of such a facility. Indeed it is clear, that in terms of flux performance usually a loss will occur. Arguments of proponents and opponents of a conversion usually concern what defines an acceptable or so called "marginal"[2] loss. But the successful conversion of 48 relevant cases of research reactors and the aggressive goal of the global threat reduction initiative (GTRI) to convert a targeted number of about 100 remaining HEU reactors worldwide to LEU fuel by the year 2014 and about 130 by the year 2018 shows, that there can be incentives for an operator to consider conversion.

In the following we will concentrate on a subgroup of research reactors specialized for neutron research. The main purpose of these facilities is to provide neutrons for scientific research including usually the use of a variety of neutron scattering instruments.

2. System Performance

In most of the conversion cases and similarly for the design of a new reactor a first approach is a neutronic simulation of the reactor core with LEU fuel. Due to the exponential increase of computing power in the last decades it is nowadays feasible to optimize the neutronics of complete three dimensional models of a reactor core with Monte Carlo codes like MCNPX [4]. Thus it is possible to execute vast parameter studies in detail and to calculate the important parameters of a reactor like cycle length, reactivity, flux etc. for different design or conversion options. Thus one can optimize or re-optimize a reactor for an optimum performance with LEU usage (see [5,6,7,8,9,10] as an example for conversion calculations done by our group).

First approaches to quantitatively assess the performance of neutron sources were made e.g. by [11][6]. In the case of research reactors for neutron research and especially for high flux research reactors one significant parameter in such an optimization procedure is the maximal flux of the facility. The authors of [11] propose an overall facility weight factor $W=2^{\log(\Phi)}$, with Φ in units of 10^{13} n/cm²s to compare different facilities. Thus a 10^{14} n/cm²s facility would have a weight factor of 2 and a high flux source with about 10^{15} n/cm²s a weight factor of 4 in comparison to a 10^{13} n/cm²s facility. It is also clear that the more instruments can be hosted at a facility the higher is its figure of merit $M=W*N$ (N =Number of instruments). This emphasizes the usage of one or more cold sources at a neutron scattering facility, which allows the usage of long neutron guides and therefore a larger number of instruments, which increases the figure of merit therefore.

But assessing the system as a whole it is useful to assess the performance of such a reactor in greater detail. This would include the identification of the actual available flux per year at the instrument (sample), the quality of the neutron beam for the investigated scientific problem as well as the quality of the instruments.

The available flux at the sample for example is determined by the flux at the beam tube nose in the reactor, the quality of the neutron guides and other optical components like collimators, monochromators and choppers. Especially for the quality of neutron guides considerable progress could be achieved in the last 10 years and neutron guides get sophisticated geometries and materials specified for a specific instrumental setup. The continuing research and development of supermirror coatings for neutron guides to increase the critical angle from $m=1$ with natural nickel coating to $m=4$ with bilayered Ni-Ti supermirror coatings allowed a variety of neutron research facilities a remarkable gain in performance exceeding possible profits due to flux increase. The most prominent example is the millennium program at ILL [12].

Although the obstacle for supermirror coatings today is that supermirror coatings beyond $m=2$ usually suffer from a loss in reflectivity due to an increasing number of bilayers and overall coating thickness, one has to trade off the loss in reflectivity with the gains of a larger critical angle. But in addition to the material developments the invention of ballistic guides [13] and the use of new guide geometries (elliptic, parabolic) [14] or focusing elements can increase the flux at the sample further. (An overview of possible gain factors due to supermirror coatings and guide geometries gives [15])

So it seems to be reasonable that nowadays the neutron flux per unit power for a research reactor designed with LEU or to be converted to LEU counts not so much anymore than the possible gains due to better neutron optics at the position where it truly counts - at the experiment.

3. Optimizing from Core to Experiment

To optimize a research reactor to be designed or a to be converted and to assess its performance it would be vital therefore to not only address the reactor core with simulations, but to expand a model beyond the moderator tank to include the instruments. Today, a variety of neutron ray-tracing codes are available to simulate the guide section and the instruments and detectors (McStas [16], ResTrax [17], Vitess [18], NISP [19], IDEAS [20]). These tools offer the possibility of making virtual experiments and the possibility of optimizing the optical components, especially the neutron guides, of a reactor [21].

To that end it is necessary to couple the reactor neutronic codes like MCNPX to the instrumentation code. So far this was done by running a reactor simulation using e.g. MCNPX and tally the neutron flux over a certain area e.g. the beam tube nose. The MCNP flux was then usually parameterized and a source probability distribution was fitted to the tallied fluxes. This distribution was used in a subsequent virtual neutron simulation experiment to sample neutrons entering the neutron guide. However, testing this kind of coupled simulation against the measurement showed bad agreement with an overestimation of cold neutron flux [22]. Besides other possibilities, one reason for this discrepancy given by [22], could be the approximation of the neutron distribution at the interface between MCNP and MCSTAS. It is also possible that the MCNPX transport models of cold neutrons through a complex geometry like a beam tube are not correctly working as is discussed in [23]. Although in this case occurred an underestimation of the cold neutron flux in the simulation possibly because of reflection of neutrons on the side walls of the beam tube. This reflections due to the high Ni content of the stainless steel beam tubes are not simulated correctly in MCNPX. It was concluded that a first step to enhance the simulation would be to directly couple MCNPX and neutron ray-tracing codes. However up to now neutron ray-tracing codes do not allow to consider real material mixtures in the simulation but assume ideal materials.

Besides fitting a source distribution to couple MCNPX to MCSTAS, another possibility is available via the `virtual_mcnp_input` component since Version 1.10 of MCSTAS (Dec. 2006) [24]. By starting a reactor simulation with MCNP it is possible to write a particle track (PTRAC) file to store the tracks of certain neutrons. In the PTRAC file the location, direction and energy of selected neutrons is stored. The choice of neutrons to be stored can be adjusted within MCNP. It is possible to store only those neutrons, which cross e.g. a predefined area like the beam tube nose, but other choices are possible as well (starting in a certain volume, having certain energy etc.).

With the `virtual_mcnp_input` component the neutron track informations can be read into MCSTAS and in a following MCSTAS simulation neutrons are statistically sampled according to the track informations. With this coupling of MCSTAS and MCNPX via the `virtual_mcnp_input` component it might be possible to overcome some of the problems mentioned above.

However in an optimization process of a research reactor it is useful to automatize the procedures necessary to use the `virtual_mcnp_input` component feature between MCNPX and MCSTAS. To that end we use Mathematica as a linkage tool between the codes and automatised the process of starting the codes, changing geometries and transferring and changing source file information. With the implementation of the MCSTAS linkage routine it is now possible to assess performance changes at the instrument more adequately and to take these changes into account when optimizing a reactor design or during conversion.

It is also possible to integrate genetic algorithms into the framework of the system to find global optima's for the reactor performance. We work on the full implementation of a search algorithm (genetic algorithm) for all variables, especially the implementation of a radially (or even axially) shaped meat thickness to optimize flux and power distribution in the core. We also improve our reactor model to assess the axial flux in greater detail. This implies mainly the integration of the control rod movement into the code. With these features and the linkage to MCSTAS it will be possible to adequately calculate the integrated flux over the cycle length at the experiment, which is one of the important parameters to assess performance losses or gains for a reactor conversion or of course for the design of a new reactor.

5. Conclusion and Outlook

In an effort to phase out civilian HEU usage a lot of research reactors still have to be converted to LEU usage. To trade of losses in terms of flux per unit power it is necessary to re-optimize the complete system as a whole, especially in the case of research reactors for neutron science. To that end the simulation models of the core and moderator should be extended to include the neutron optics and instrument as well.

With the new available MCSTAS component `mcnp_virtual_input` it is possible to directly link the reactor simulation code MCNPX with the neutron instrument ray-tracing code MCSTAS. This linkage offers new possibilities for the process of optimizing the overall performance of a research-reactor. We integrate this linkage component into the existing Mathematica reactor optimization code system.

A first validation of the system is under way and will be tested with published measurements at the cold source of FRM-II. With this system it should be possible to adequately assess the performance of research reactors by taking into account the integrated flux at relevant experimental positions.

References:

- [1] Glaser, A.; Hippel, Frank von: Global Cleanout: Reducing the Threat of HEU-Fueled Nuclear Terrorism. *Arms Control Today*, 1, 2006.
- [2] "Report of INFCE Working Group 8: Advanced Fuel Cycle and Reactor Concepts," Vienna, 1980, p. 18.
- [3] See the RERTR conference proceedings <http://www.rertr.anl.gov/> for more details of historical conversions.
- [4] Pelowitz, D.B. (ed.): MCNPX User's Manual, Version 2.5.0, April 2005, LA-CP-05-0369.
- [5] Glaser, A.: "Monolithic Fuel and High-Flux Reactor Conversion", In: *Proceedings of the 26th RERTR Meeting*, Vienna International Centre, Vienna, Austria, November 7–12, 2004.
- [6] Glaser, A.: Neutronics Calculations Relevant to the Conversion of Research Reactors to Low-Enriched Fuel, Dissertation, Department of Physics, Darmstadt University of Technology, 2005.
- [7] Englert, M.E.W.; Glaser, A.; Liebert, W.: Optimization Calculations for Use of Monolithic UMo Fuel in High Flux Research Reactors, *Transactions of the 10th RRFM Meeting*, April 30–3 May, 2006, Sofia, Bulgaria, pp. 235–239.
- [8] Englert, M.; Liebert, W.: Investigating the Potential of Monolithic UMo for the Conversion of FRM-II, *Proceedings of the 28th RERTR Meeting*, Cape Town, South Africa, October 29 - November 2, 2006.
- [9] Englert, M.; Glaser, A.; Liebert, W.: Untersuchungen zu technischen Potenzialen für die Umrüstung des Forschungsreaktors München II (Analysis of the technical potentials for the conversion of the FRM-II), final report to the German Ministry of Science and Education (BMBF), July 2006
- [10] Englert, M.E.W.; A.; Liebert, W.: Neutronic Calculations for Conversion of One-Element Cores from HEU to LEU Using Monolithic UMo Fuel, *Transactions of the 11th RRFM Meeting*, March 11-15, 2007, Lyon, France.
- [11] Richter, D; Springer, T.: A twenty years forward look at neutron scattering facilities in the OECD Countries and Russia, OECD, 1998.
- [12] See Proceedings of the ILL Millenium Symposium & European User Meeting, Grenoble, 2001, and the website of the ILL Millenium Symposium and European User Meeting 2006. http://www.ill.eu/fileadmin/users_files/Other_Sites/symposium/IIISymposium2006.html
- [13] Mezei, F: The Raison d'Etre of Long Pulse Spallation Sources, *Journal of Neutron Research*, 6, 1997, p. 6-33.
- [14] Schanzer, C.; Böni, P.; Filges, U.; Hils, T.: Advanced geometries for ballistic neutron guides, *Nuclear Instruments and Methods A* 529, 2004, p. 63-68.
- [15] Glaser, A.: Neutron Use Optimization with Virtual Experiments to Facilitate Research-Reactor Conversion to Low Enriched Fuel, *Proceedings of the 29th RERTR Meeting*, Prague, Czech Republic, September 23 - 27, 2006.
- [16] K. Lefmann and K. Nielsen. *Neutron News*, 10, 20–23, 1999.
- [17] Saroun, J.; Kulda, J.: *Physica B*, 234, 1102, 1997.
- [18] D. Wechsler, G. Zsigmond, F. Stre? er, and F. Mezei. *Neutron News*, 25, 11, 2000.
- [19] P. A. Seeger, L. L. Daemen, T. G. Thelliez, and R. P. Hjelm. *Physica B*, 283, 433, 2000.
- [20] W.-T. Lee and X.-L. Wang. *Neutron News*, 13, 30, 2002.
- [21] Farhi, E., Hansen, T., Wildes, A., Ghosh, R. Lefmann, K.: Designing New Guides and Instruments Using MCSTAS, *Applied Physics A*, 74, p. 1471-1473, 2002.
- [22] Zeitelhack, K.; Schanzer, C. Kastenmüller, A. Röhrmoser, A. Daniel, C. Franke, J. Gutmiedl, E.; Kdryashov, V. Páthie, D. Petry, W. Schöffel, T. Schreckenbach, K. Urban, A. Wildgruber, U.: Measurement of Neutron Flux and Beam Divergence at the Cold Neutron Guide System of the New Munich Research Reactor FRM-II, *Nuclear Instruments and Methods in Physics Research A*, 560, 2006, p. 444-453.
- [23] Nuenighoff, K.; Pohl, C.; Bollini, V.; Bubak, A.; Conrad, H.; Filges, D.; Glueckler, H.; Goldenbaum, F.; Hansen, G.; Lensing, B.; Neef, R.D.; Paul, N.; Pysz, K.; Schaal, H.; Soltner, H.; Stelzer, H.; TietzeJaensch, H.; Ninaus, W.; Wolmuther, M.; Ferguson, P.; Gallmeier, F.; Iverson, E.; Koulikov, S.; Smirnov, A.: Investigations of the Neutron Performance of a Methane Hydrate Moderator, *Nuclear Instruments and Methods in Physics Research A* 562, 2006, p. 565-568.
- [24] MCSTAS like most of the neutron ray tracing codes uses component files, which can be added together before this compilation of components is compiled into a final setup. Components can be various neutron optic elements like neutron guides, monochromators, detectors etc. and sources. The virtual-mcnp-input and virtual-mcnp-output components are contributed components to MCSTAS from E. Farhi and C. Hennane from ILL.



European Nuclear Society

Rue de la Loi 57
1040 Brussels, Belgium
Telephone +32 2 505 30 54
Fax + 32 2 502 39 02
rrfm2008@euronuclear.org
www.euronuclear.org